O. M. Rygh[1,2,4]
J. Cappelen[1]
T. Selbekk[3,4]
F. Lindseth[3,4]
T. A. N. Hernes[2,3,4]
G. Unsgaard[1,2,4]

Endoscopy Guided by an Intraoperative 3D Ultrasound-Based Neuronavigation System

Abstract

Objective: We have investigated the feasibility of using 3D ultrasound-based neuronavigation for guiding neuroendoscopy. **Methods:** A neuronavigation system with an integrated ultrasound scanner was used for acquiring the 3D ultrasound image data. The endoscope with a tracking frame attached was calibrated to the navigation system. The endoscope was guided based on intraoperative 3D ultrasound data in 9 operations. In 5 of the operations, ultrasound angiography data were also obtained. Updated image data (e.g., more than one 3D ultrasound dataset) were obtained in 6 of the operations. **Results:** We found that the image quality of 3D ultrasound was sufficient for image guidance of the endoscope. Planning of the entry point and trajectory as well as finding optimal sites for fenestration were successfully performed. Blood vessels were visualized by 3D ultrasound angiography. In one procedure of third ventriculostomy, the basilar artery was visualized. Updated image data were quickly obtained, and in two of the cases, a reduction of the size of cysts was demonstrated. **Conclusions:** 3D ultrasound gives accurate images of sufficiently high quality for image guidance of neuroendoscopy. Updated 3D ultrasound datasets can easily be acquired and may adjust for brain shift. Ultrasound angiography image data are also available with this technology and can visualize vessels of importance.

Key words

Ultrasound · three-dimensional ultrasound · neuronavigation · neuroendoscopy

Introduction

Advances in endoscope technology have resulted in more frequent use of neuroendoscopy. A number of different indications for using this technology exist, such as third ventriculostomy [1–3], colloid cysts [4,5], septum pellucidum cysts [6,7], intraventricular tumors [8,9], and pituitary tumors [10] among others. However, even with advances in neuroendoscopy, certain limitations still exist, such as orientation of the endoscope in abnormal anatomy, inserting the endoscope into small narrow ventricles, visualization in opaque fluids and finding small subependymal tumor masses [11].

Several methods for solving these limitations are reported. Intraoperative imaging with MRI [12,13] and ultrasound [14–19] has been used to give improved anatomical orientation in neuroendoscopic procedures. Real-time 2D ultrasound has been used to guide neuroendoscopic procedures since the 1980s and has been reported to give satisfactory images for guiding such procedures [16–19]. However, other authors find ultrasound less suitable for guiding neuroendoscopic procedures [11]. Stereotaxy has been used for finding the optimal entry point and trajectory for endoscopic procedures in the ventricular system and for third ventriculostomy [9,20,21], but still this method has its practical limitations.

Neuronavigation integrated with an endoscope seems to be a natural evolution of neuroendoscopy and is reported to give improved anatomical orientation, and to facilitate the selection of

Affiliation
[1] Department of Neurosurgery, St. Olav University Hospital, Trondheim, Norway
[2] The Norwegian University of Science and Technology, Trondheim, Norway
[3] SINTEF Health Research, Trondheim, Norway
[4] National Centre for 3D Ultrasound in Surgery, St. Olav University Hospital, Trondheim, Norway

Correspondence
Ola M. Rygh, M. D. · Department of Neurosurgery · St. Olav University Hospital Trondheim · Olav Kyrres gate 17 · 7005 Trondheim · Norway · Tel.: +47/9284/9775 · Fax: +47/7386/7977 · E-mail: ola.rygh@ntnu.no

Bibliography
Minim Invas Neurosurg 2006; 49: 1–9 © Georg Thieme Verlag KG Stuttgart · New York
DOI 10.1055/s-2005-919164
ISSN 0946-7211

Table **1** Summary of the patients treated by endoscopic procedures with neuronavigation based on 3D ultrasound

Patient	*Sex/age*	*Diagnosis*	*Procedure*	*No. of 3D ultrasound acquisitions*	*US angiography used*	*Preoperative 3D MRI used in neuronavigation*
1	F/63 years	Unilateral hydrocephalus, post-SAH	Fenestration of septum pellucidum	2	No	No
2	F/67 years	Intracerebral cysts	Fenestration of cysts	2	Yes	No
3	F/73 years	Colloid cyst, hydrocephalus	Extirpation of cyst, septostomy	1	Yes	No
4	M/19 years	Septum pellucidum cyst	Fenestration of cyst	2	Yes	No
5	M/11 years	Interhemispheric cyst	Fenestration of cyst	3	No	Yes
6	M/3 months	Multiloculated hydrocephalus	Fenestration of cysts	1	No	No
	2 years	Multiloculated hydrocephalus	Fenestration of cysts	2	Yes	No
7	M/25 years	Septum pellucidum cyst	Fenestration of cyst	1	No	No
8	M/33 years	Hydrocephalus, aqueduct stenosis	Third ventriculostomy	2	Yes	Yes

the optimal entry point and trajectory for an endoscopic procedure [7,11,20,22,23]. However, neuronavigation systems based on preoperative images in general may suffer from inaccuracy due to registration errors and brain shift [24–28].

Ultrasound image quality has improved considerably in the last decades due to technological development and application adaptation [29,30]. The combination of 2D ultrasound and tracking technology enables freehand 3D ultrasound reconstruction. This gives a 3D ultrasound dataset that can be used in a similar manner as 3D MRI datasets are used in a conventional neuronavigation system [29,30]. In addition, with 3D ultrasound, the inaccuracy caused by patient registration is avoided and updated intraoperative images can be acquired whenever needed during surgery. This technology has been reported to solve some of the challenges of navigated tumor surgery and vascular neurosurgery [29–31]. In the present study, we have investigated the feasibility of using intraoperative 3D ultrasound for image guidance in neuroendoscopy. We here report our experience with this technology in 9 procedures.

Patients and Methods

Patients

Between January 2003 and February 2005, 9 procedures in 8 patients were performed using the described system. (Two procedures were performed on patient 6 in Table **1**, at ages 3 months and 2 years). There were 3 female patients. The age of the patients ranged from 3 months to 72 years. The patients are summarized in Table **1**.

Endoscopic equipment

We used a rigid operating endoscope (Aesculap, Tuttlingen, Germany) of 6 mm outer diameter and one working channel, one irrigation channel, one overflow channel as well as the optic channel. A single chip video camera was mounted on the eyepiece for visualization and connected to a monitor.

An optical tracking frame (Mison, Trondheim, Norway), usually used with the CUSA, was used for tracking the endoscope. The tracking frame was attached to the fixation adapter for the trocar. A custom-made insert (see Fig. **3C**) for the fixation adapter was used to make the plane of the tracking frame and the endoscope parallel, necessary for correct calibration for neuronavigation. Fixation of the endoscope was accomplished with a single-arm fixation device (Aesculap, Tuttlingen, Germany).

Ultrasound and neuronavigation system

An ultrasound-based intraoperative imaging and neuronavigation system (SonoWand®, Mison, Trondheim, Norway) was used. This system may be used as an ultrasound scanner, a conventional neuronavigation system, or an integrated, ultrasound-based neuronavigation system that uses the features of both technologies [30]. The system is based on optical tracking technology, and comes with a 4–8 MHz flat phased array ultrasound probe, precalibrated for image data acquisition and optimized for neurosurgery and with optimal resolution at depths of 3–6 cm [32]. A patient reference frame is attached to the head-holder (Mayfield frame). In one case the patient reference frame was attached to the operating table, because the young age of the patient (3 months) prohibited the use of a head-holder. For tracking of the ultrasound probe, a tracking frame is attached to the probe. Neuronavigation can be performed with a tracked pointer device, or any surgical instrument with an attached tracking frame after calibration. The trajectory and position of the pointer or surgical tool tip is displayed as a line with crosshairs or a dot (depending on the version of the neuronavigation software) in the corresponding images. The pointer and surgical tool can be virtually elongated using an offset feature. The ultrasound probe is tilted or translated over the area of interest by free hand movement and the 2D ultrasound images acquired are reconstructed, making a 3D ultrasound dataset ready for navigation (Fig. **1B**). The procedure takes about one minute. The ultrasound probe is not in the operating field after the acquisition of a 3D ultrasound volume, unless additional 3D ultrasound datasets are acquired or real-time 2D imaging is needed. The workflow of this procedure and set-up of equipment are summarized in Fig. **1**.

Navigation based on 3D ultrasound can be performed directly without any patient registration with fiducials, since the images are acquired in the same coordinate system as navigation is performed. Therefore, no patient or image registration error will affect the overall accuracy of the system when navigation based on

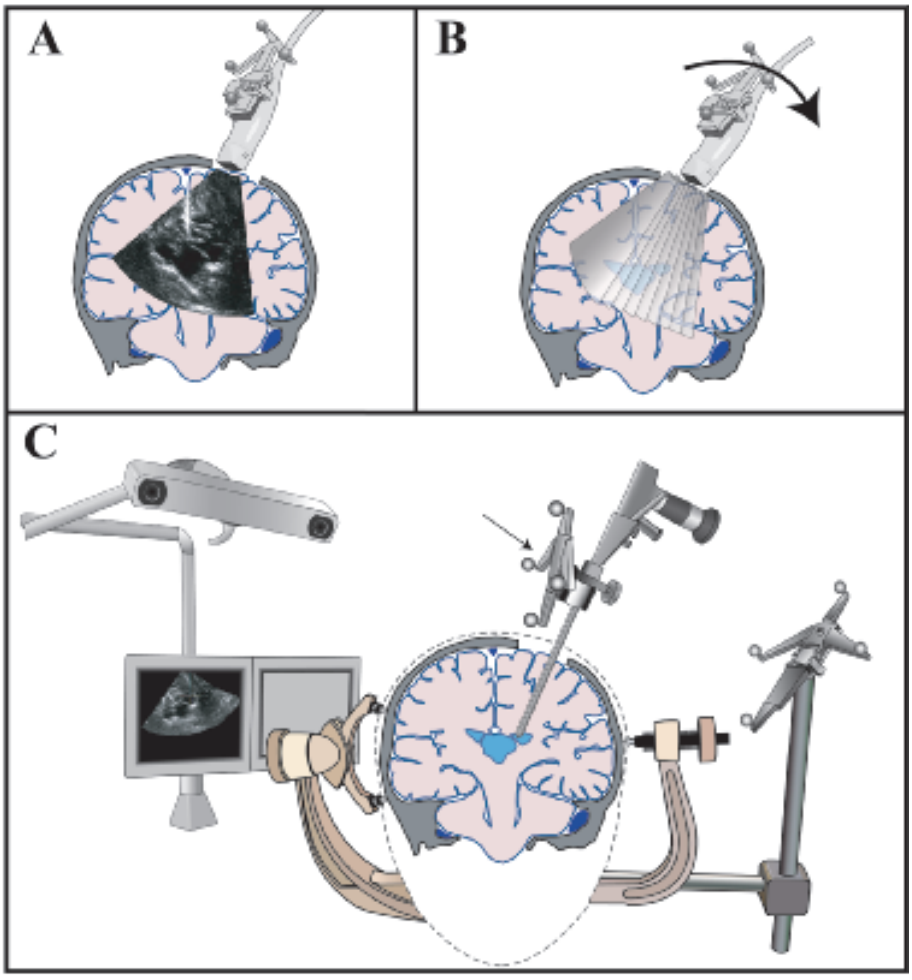

Fig. **1** Neuroendoscopy guided by 3D ultrasound. **A** The probe is placed on the dura. The anatomy and pathology are visualized by real-time 2D ultrasound. **B** During image acquisition, the probe with tracking frame is tilted or translated over the area of interest. A 3D ultrasound dataset is reconstructed from a stack of 2D images. **C** The calibrated endoscope with the tracking frame (arrow) is tracked by the navigation system and the tip position and trajectory of the endoscope are displayed on the neuronavigation screen. The patient reference frame is attached to the head-holder.

3D ultrasound is performed [24]. If neuronavigation based on preoperative MRI also is desired, patient registration of course will be necessary.

The display modalities available are: 1) Orthogonal slicing: three 2D slices are oriented as axial, sagittal and coronal slices (Fig. **2A**). 2) Anyplane slicing: One slice defined by the axis and rotation of the pointer or custom calibrated tool (for example, the endoscope) (Fig. **2B**). A plane perpendicular to the anyplane can also be added (dual anyplane) (Fig. **2C**). With a tracking frame attached, the endoscope tip and trajectory defines the slicing of the image volume (Fig. **2D**).

The overall accuracy of 3D ultrasound-based navigation using the SonoWand® system in a clinical setting may be as good as 2 mm [24].

Operative technique

All the operations were performed with neuronavigation based on 3D ultrasound. In two of the operations, preoperative MRI also was available for navigation.

The position of a small craniotomy (diameter approximately 4 cm) was chosen based on preoperative CT or MR images (but not neuronavigation) (Fig. **3A**). After cleaning the dura for blood and bone debris, sterile ultrasound gel was applied on the dura, and 3D ultrasound data were acquired (Fig. **3B**). If required, also 3D ultrasound angiography image data were acquired. The tracking frame was attached to the fixation adapter for the trocar, using the custom-made insert (Fig. **3C**). The endoscope was then calibrated to the navigation system by directing the tip of the endoscope at a small hole in the centre of the reference frame (Fig. **3D**). Based on the ultrasound images, and using the offset feature to display the trajectory of the endoscope, the best entry point and trajectory for the endoscope were decided, and a small opening in the dura was made. The endoscope was then inserted with image guidance (Fig. **3E**). The surgical procedure planned, for example, fenestration of a cyst, was then performed with the live video images from the endoscope, as well as image guidance. If updated images were required, additional 3D ultrasound datasets were obtained during the procedure. In one operation, real-time ultrasound was also used as a method for confirming the flow of CSF through the fenestration, using power Doppler.

Results

Nine procedures were performed on 8 patients during this study (Table **1**). We found the image quality of ultrasound to be satisfactory for image guidance in all cases. The ventricles as well as pathological cysts were clearly outlined and we found that the ultrasound images gave sufficient information for: 1) deciding the optimal entry point and trajectory for inserting the endoscope, especially in cases with small narrow ventricles; 2) anato-

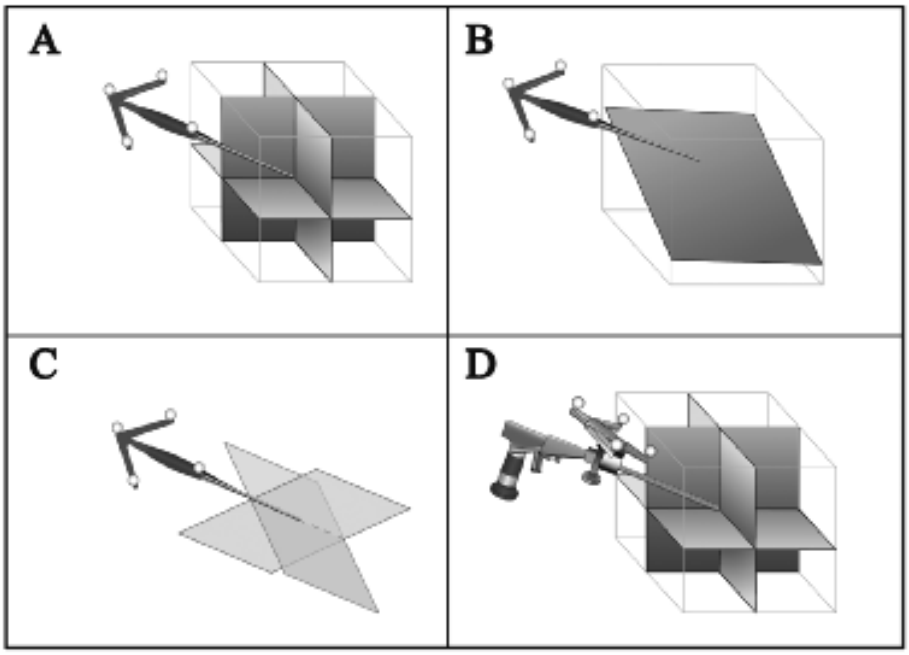

Fig. **2** Display techniques. **A** Orthogonal slices: Three orthogonal 2D slices from each 3D volume oriented as axial, sagittal and coronal slices. **B** Anyplane slices: Anyplane slices are defined by the trajectory and rotation of the pointer or surgical tool. **C** Dual anyplane slices: In dual anyplane mode an additional plane perpendicular to the first plane is added. **D** The endoscope or any surgical tool with a tracking frame, when calibrated, works as a pointer, for example, with orthogonal slices.

mical orientation during endoscopy, thus facilitating the choice of sites for fenestration of cysts; 3) quality control at the end of the procedure, excluding bleeding and in two cases verifying the reduction of size of cysts (patients 2 and 4 in Table **1**).

Even though we did not measure the clinical accuracy systematically, the general impression was that the accuracy was satisfactory. This could be confirmed by approaching a recognizable structure (for example, the foramen of Monro) with the endoscope and by comparing with the position of the endoscope tip displayed on the navigation screen.

In five of the operations ultrasound angiography also was acquired. We found that blood vessels were clearly visualized in all these cases. This was found to give particularly useful information in two cases: In patient 6, vessels in septa of multiloculated hydrocephalus were visualized (see Fig. **6B**), while in patient 8 the basilar artery could be visualized (see Fig. **6A**).

In six operations updated 3D ultrasound image data were obtained, and in two cases (cases 2 and 4), the updated ultrasound images could demonstrate the reduction of the size of a cyst. Updated ultrasound image data were acquired quickly; it typically took about a minute.

Seven of the operations were performed with only 3D ultrasound data for navigation. In two procedures we had preoperative 3D MRI with fiducials available in addition to the 3D ultrasound data (patients 5 and 8 in Table **1**).

All procedures were successful, e. g., the goal of the procedure, such as fenestration of a cyst, was reached. One patient (patient 1 in Table **1**) had postoperative meningitis, but recovered from this. We did not record any other complications at 1 – 2 months follow-up. The patients are summarized in the Table **1**. Two illustrative cases (patients 4 and 5 in Table **1**) are presented in detail.

Illustrative Cases

Patient 4

A man aged 19 years at the time of the operation, had episodes of loss of consciousness. A septum pellucidum cyst was found on CT and MRI investigations (Fig. **4A**). An endoscopic fenestration of the cyst to the ventricular system using navigated 3D ultrasound was planned. We did not have preoperative 3D MR images for this procedure, so only 3D ultrasound images were used for navigational guidance of the endoscope. 3D ultrasound images were acquired after making a mini-craniotomy. The ultrasound images were of sufficient quality for inserting the endoscope with navigation guidance into a narrow right ventricle (Fig. **4C**). The fenestration was done using conventional technique. The foramen of Monro was observed to be occluded by the cyst wall. Updated 3D ultrasound acquired after removing the endoscope demonstrated that the septum pellucidum cyst already was reduced somewhat in size (Fig. **4D**). It also showed the canal after removal of the endoscope, with no signs of bleeding. A postoperative CT taken the following day showed that the cyst was reduced in size (Fig. **4B**). The postoperative recovery was uneventful, and at 2 months follow-up, the patient had not had any new episodes of syncope.

Patient 5

This boy of 11 years of age at the time of the operation had been investigated because of tics in his face and arms. An interhemispheric cyst was found on investigations with CT and MRI, as well as an agenesis of the corpus callosum (Fig. **5A** and Fig. **5B**). An endoscopic fenestration of the cyst using navigated 3D ultrasound was planned. Preoperative 3D MRI with fiducials was available; consequently patient registration was done in this case. Ultrasound images were acquired through a mini-craniotomy before opening the dura and showed the interhemispheric cyst and the small ventricles clearly, in our opinion just as good as the MR images in the navigation system (Fig. **5D** and Fig. **5E**). We chose to display both the ultrasound and the MR images on

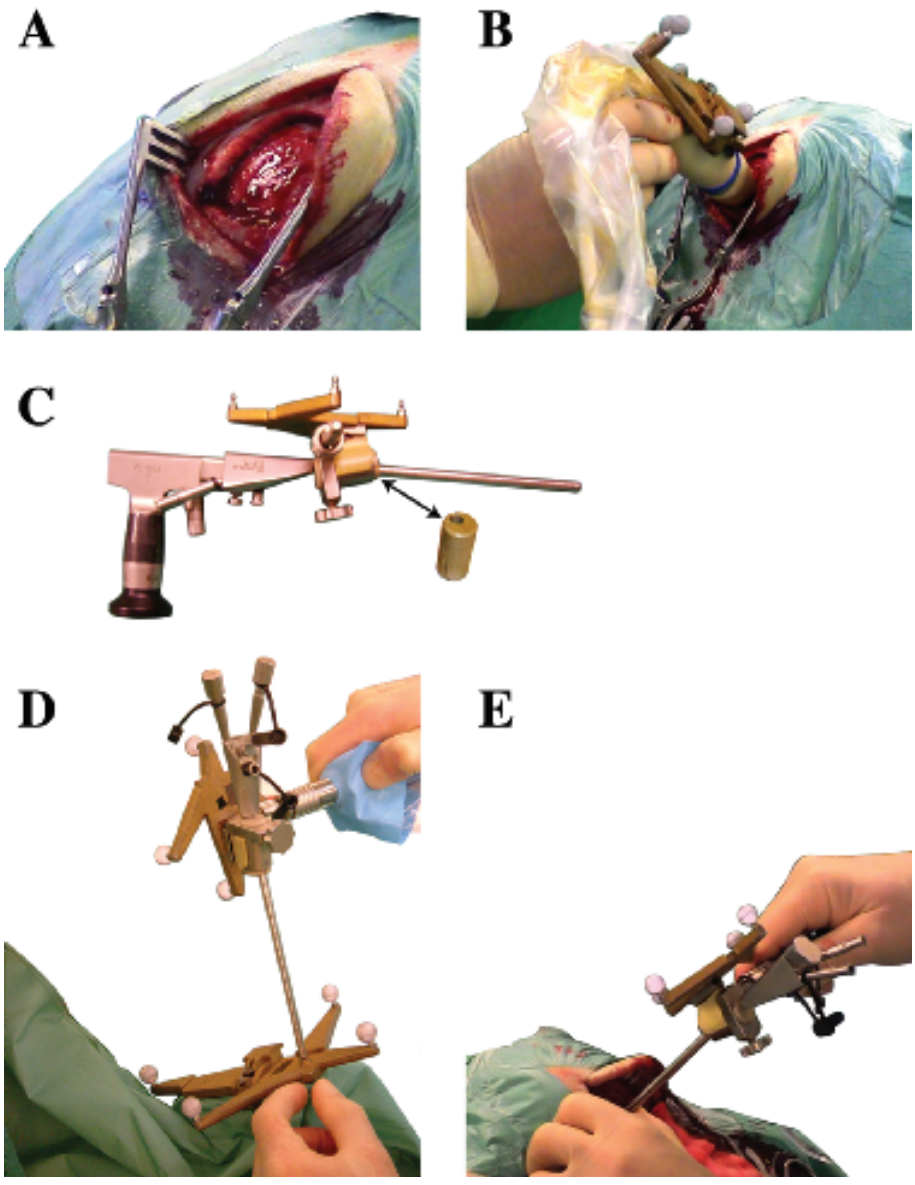

Fig. **3** Operative technique.
A A mini-craniotomy, about 4 cm in diameter is made. **B** The ultrasound probe with a tracking frame is placed on the dura for imaging. **C** A tracking frame (in this case without marker spheres) is attached to the fixation adapter for the endoscope trocar. A custom-made insert (arrows) ensures that the plane of the tracking frame and the endoscope are parallel. **D** The neuroendoscope with the tracking frame attached is calibrated by directing the tip of the endoscope at a small hole in the centre of the reference frame. **E** With the tracking frame attached, the neuroendoscope is inserted with image guidance, based on the 3D ultrasound image data.

the navigation screen during the procedure. However, we based the operation on intraoperative 3D ultrasound knowing that these volumes were not affected by registration errors, and also that the inaccuracy due to brain shift was minimal since the 3D ultrasound was acquired just before the procedure. Neuronavigation was used to guide the endoscope into the small right lateral ventricle (Fig. **5D**). We noticed a small difference (approximately 4 mm) between the position of the endoscope tip displayed on the MRI and the ultrasound images on the navigation screen (Fig. **5E**). This difference we assumed to be caused by brain shift or registration error of the MR images. A fenestration of the cyst to the ventricle was done, as well as a fenestration from the cyst to the basal cistern. The postoperative recovery was uneventful, and a postoperative CT demonstrated that the cyst was reduced in size (Fig. **5C**). On follow-up after two months the patient's symptoms had improved considerably and he was performing better in school.

Discussion

Several ultrasound solutions have been proposed in neuroendoscopy. Real-time ultrasound has been used as an adjunct to neuroendoscopic procedures [15 – 18], but it has not gained popularity. This is probably due to old experiences of low image quality, as well as the fact that the probe has to be kept in the operation field for acquiring real-time images, a somewhat inconvenient concept.

More modern ultrasound solutions have also been explored. Resch et al. [16,17] developed a technique where a small sono catheter (originally developed for intravascular use) is inserted into the working canal of an endoscope, giving a 360-degree axial (to the endoscope) real-time view of the anatomy, like a "mini-CT". The solution gives good images of the anatomy in a plane axial to the endoscope, but no image ahead of the endoscope. 3D ultrasound datasets acquired on pediatric patients have been used for simulating virtual neuroendoscopies pre-

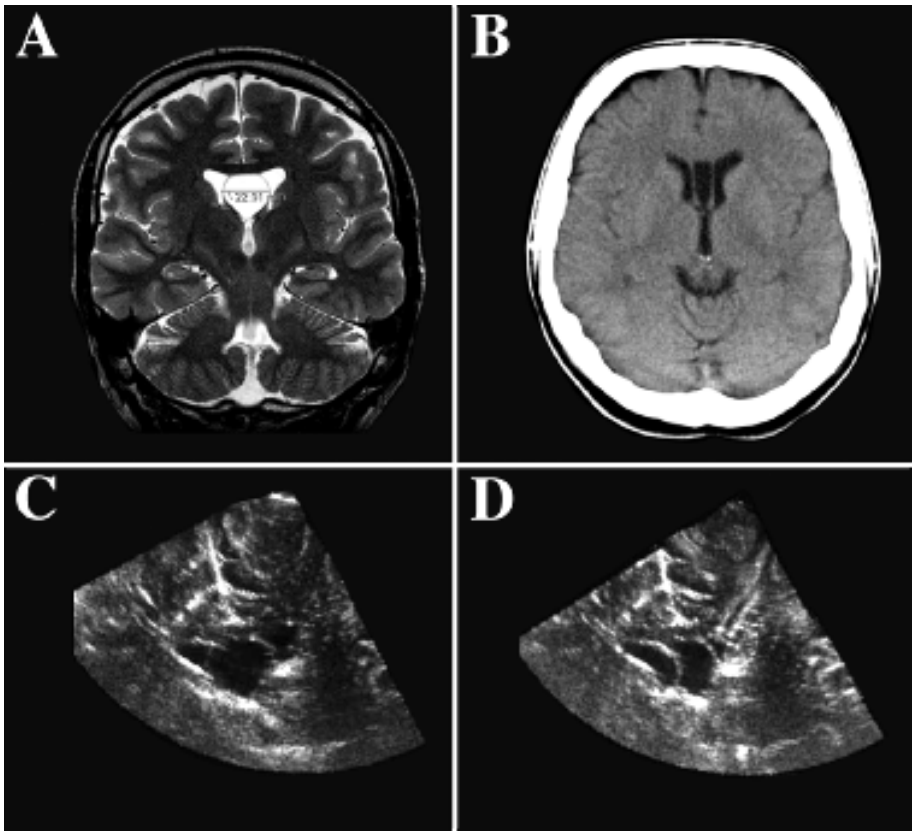

Fig. **4** Patient 4: **A** Preoperative T_2-weighted MRI, showing a septum pellucidum cyst, 22 mm in diameter, the walls of the cyst bulging into the lateral ventricles. **B** Postoperative CT, showing the septum pellucidum cyst reduced in size. **C** Ultrasound image before the procedure, clearly depicting the ventricles and the septum pellucidum cyst with its bulging walls. **D** Ultrasound image after the procedure of fenestration of the cyst. The cyst is already a little reduced in size. The channel after removal of the endoscope is also displayed, showing no signs of hematomas.

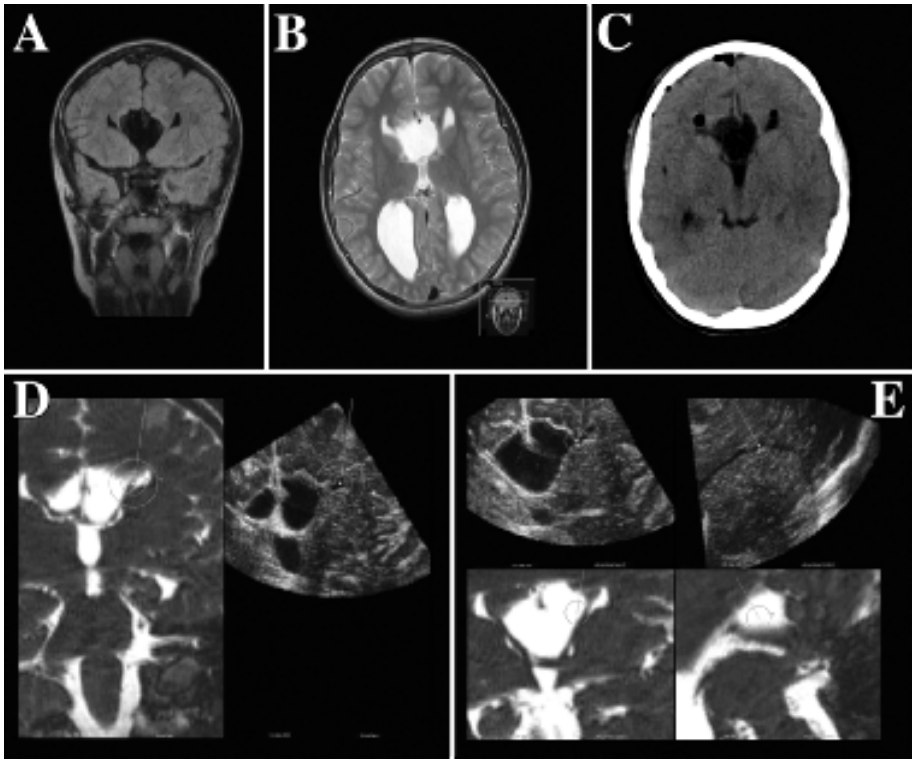

Fig. **5** Patient 5: **A** Preoperative T_1-weighted MRI showing the interhemispheric cyst and the lateral ventricles on each side. **B** Preoperative T_2-weighted MRI. **C** Postoperative CT. **D** Screenshot from the navigation system during insertion of the endoscope into the lateral ventricle. The line represents the trajectory of the endoscope, and the dot at the end of the line represents the tip of the endoscope. The two concentric rings mark the radii of 5 and 10 mm from the centre of the dot. **E** Another screenshot from the navigation system. Notice the small difference between the demonstrated position of the endoscope on the MR and the ultrasound images, about 4 mm. This difference we assumed to be caused by brain shift or registration inaccuracy.

operatively, enhancing the perception of pathoanatomy in cases of complicated anatomy [33]

Recent advances in neuronavigation technology based on preoperative CT and MRI have made neuronavigation integrated with the neuroendoscope a natural evolution in the field of neuroendoscopy. It is reported by several groups to be helpful in planning and performing endoscopic procedures [11,20,22,23, 34–38].

However, ultrasound technology has also evolved and ultrasound images can be reconstructed into a 3D dataset and used

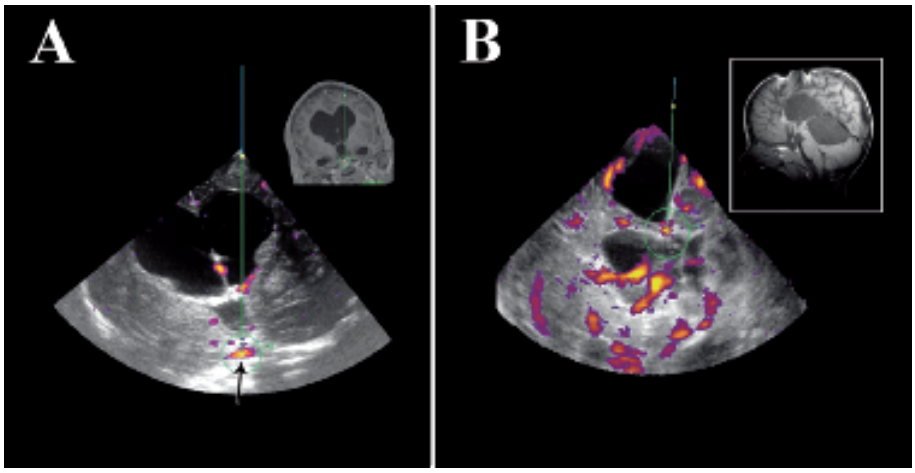

Fig. **6** Ultrasound angiography. **A** Image from patient 8 in Table **1**. Corresponding MRI is inserted in the top right corner. The vessels are highlighted in red. The yellow dot indicates the tip of the neuroendoscope, while the green line and the cross represents a virtual elongation of the neuroendoscope, "offset", useful for planning the trajectory of the endoscope. In this case the basilar artery (arrow) is depicted on ultrasound angiography. **B** Ultrasound angiography image from patient 6 in Table **1** (second operation). Preoperative MRI in the top right corner. There are numerous vessels depicted in this case of multiloculated hydrocephalus.

the same way as conventional navigation systems use preoperative image data [30]. Our experience with navigated 3D ultrasound is that it gives images of high quality and good detail, depicting the anatomy in a manner that gives good anatomical overview and orientation. We found that this was particularly useful in cases where the ventricles were small and narrow, and where the anatomy was abnormal (as in multiloculated hydrocephalus). In two cases (patients 2 and 5) this technology was considered essential for the success of the procedure, in both cases because of small narrow ventricles. The two illustrative cases presented here serve to highlight these benefits of navigated 3D ultrasound for endoscope guidance.

In our opinion, neuronavigation based on 3D ultrasound is comparable in image quality to navigation by preoperative MRI. In addition, it has a couple of advantages. When navigation of the neuroendoscope is based on 3D ultrasound images alone, the system does not require preoperative CT or MR images. This simplifies logistics, as in most cases of CT- or MRI-based neuronavigation one would require an extra set of CT or MR images for navigation purposes, both for imaging with fiducial markers and also to have as updated images as possible with good resolution and 3D protocol. When only 3D ultrasound is used for navigation, patient registration is not required, as the ultrasound images are acquired in the coordinate system of the navigation system. This means that patient registration error, otherwise one source of inaccuracy, is avoided. A small amount of time is also saved. However, as the 3D ultrasound only depicts parts of the anatomy and not the whole brain, preoperative CT or MRI can be a useful supplement for orientation, for example, in cases of large cysts where it can be a technical challenge to make an ultrasound scan which covers all of the pathology of interest.

Another benefit of this system is the possibility of doing several 3D ultrasound image acquisitions during the operation. Brain shift is a known source of inaccuracy in neuronavigation [24–28], and the inevitable loss of CSF during procedures such as those discussed here means that some brain shift is likely to occur. Some authors find that brain shift is not a problem as the live video image from the endoscope after having reached the cyst or ventricular system gives the necessary information for performing the surgery [39]. However, if the surgeon suspects that brain shift has occurred, he will of course not trust the navigation system. To have updated images increases the accuracy of the navigation and the surgeon's confidence in the technology. Often, the amount of time for acquiring updated 3D images is about one minute. To acquire new 3D ultrasound datasets, the endoscope has to be removed during image acquisition and reinserted afterwards. This may be considered a disadvantage, as removing and reinserting an endoscope might theoretically increase the risk of complications for the patient. However, this must be weighed against the risk of navigating with inaccurate image data. At the end of the procedure, a final ultrasound scan may detect bleeding, and demonstrate reduced size of fenestrated cysts as it did in two cases (patients 2 and 4 in Table **1**).

Ultrasound technology also includes Doppler technology, in our case power Doppler imaging. Thus ultrasound angiography data can be acquired and used with the navigation system. We obtained power Doppler image data during five of the operations. Power Doppler shows the blood vessels highlighted in shades of red in addition to the tissue image, according to the intensity of the Doppler (shift) signal (Fig. **6**). We found that this gave useful information as well as, for example, visualizing the position of the basilar artery in patient 8 (Fig. **6A**). In patient 6, ultrasound angiography showed blood vessels in the walls and septa of the multiple cysts (Fig. **6B**). The visualization of important vessels by ultrasound angiography may improve the safety of neuroendoscopic procedures.

In one case (patient 2 in Table **1**) we tried power Doppler for visualizing CSF flow through a fenestration using real-time 2D ultrasound, and found that this indeed was possible. Other groups have also reported that Doppler technology is able to show CSF flow [40].

Some aspects of the technique presented here might be considered disadvantages. Using ultrasound for guidance of endoscopic procedures means that one has to make a small craniotomy instead of a burr hole. We do not think that this contradicts the philosophy of minimally invasive neurosurgery, as the channel in the normal brain tissue required for the endoscope is the same as it would be with a burr hole. The larger skin incision and opening in the bone is mainly of cosmetic concern, but need not be much different than the cosmetic problems of a burr hole procedure.

A disadvantage of using only ultrasound images for neuronavigation is that surgical planning cannot be done before the craniotomy. We did not find this a restraint, as the area of the craniotomy was large enough to fine-tune the choice of position for the entry point.

We found that the tracking frame attached to the endoscope in some instances limited movement of the endoscope when it was in the deepest areas of the brain. This did not restrain the procedure in any of the operations we performed, but it is an issue that needs to be improved. In future solutions a reference frame specially designed for the endoscope must be developed.

We have not investigated 3D ultrasound navigation guidance of neuroendoscopy in pituitary surgery or other skull base approaches where the endoscope is used. Other groups have reported the use of neuronavigation integrated with endoscopy in recurrent pituitary adenomas [34]. Our own experience with modern ultrasound imaging of tumors on the skull base is that ultrasound also can depict both tumors and the normal anatomy close to the skull base in a satisfactory way. Other groups also have found ultrasound imaging to be helpful for depicting tumors near the skull base [41].

Conclusion

In summary, we found that 3D ultrasound gave satisfactory image quality for image guidance of the neuroendoscope. Neuronavigation based on 3D ultrasound improved the anatomic orientation. When using only 3D ultrasound for neuronavigation, no patient registration is necessary, thus inaccuracy due to patient registration is avoided, and logistics are simplified. Updated 3D ultrasound datasets are acquired quickly, and may adjust for brain shift. Furthermore, 3D ultrasound angiographic imaging is also available, and may improve safety as important vessels can be visualized. Based on this preliminary study, we believe that ultrasound technology will have a place in future neuroendoscopy.

Acknowledgements

The Norwegian Research Council and the Ministry of Health and Social Affairs in Norway supported this work.

References

[1] Kelly PJ. Stereotactic third ventriculostomy in patients with nontumoral adolescent/adult onset aqueductal stenosis and symptomatic hydrocephalus. J Neurosurg 1991; 75: 865 – 873
[2] Jones RF, Kwok BC, Stening WA, Vonau M. Neuroendoscopic third ventriculostomy. A practical alternative to extracranial shunts in noncommunicating hydrocephalus. Acta Neurochir (Suppl) 1994; 61: 79 – 83
[3] Kunz U, Goldmann A, Bader C, Waldbaur H, Oldenkott P. Endoscopic fenestration of the 3rd ventricular floor in aqueductal stenosis. Minim Invas Neurosurg 1994; 37: 42 – 47
[4] Hopf NJ, Perneczky A. Endoscopic neurosurgery and endoscope-assisted microneurosurgery for the treatment of intracranial cysts. Neurosurgery 1998; 43: 1330 – 1336; discussion: 1336 – 1337
[5] Schroeder HW, Gaab MR. Endoscopic resection of colloid cysts. Neurosurgery 2002; 51: 1441 – 1444; discussion: 1444 – 1445
[6] Lancon JA, Haines DE, Lewis AI, Parent AD. Endoscopic treatment of symptomatic septum pellucidum cysts: with some preliminary observations on the ultrastructure of the cyst wall: two technical case reports. Neurosurgery 1999; 45: 1251 – 1257
[7] Fratzoglou M, Grunert P, Leite dos Santos A, Hwang P, Fries G. Symptomatic cysts of the cavum septi pellucidi and cavum vergae: the role of endoscopic neurosurgery in the treatment of four consecutive cases. Minim Invas Neurosurg 2003; 46: 243 – 249
[8] Gaab MR, Schroeder HW. Neuroendoscopic approach to intraventricular lesions. J Neurosurg 1998; 88: 496 – 505
[9] Grunert P, Perneczky A, Resch K. Endoscopic procedures through the foramen interventriculare of Monro under stereotactical conditions. Minim Invas Neurosurg 1994; 37: 2 – 8
[10] Cappabianca P, Cavallo LM, Esposito F, de Divitiis E. Endoscopic endonasal transsphenoidal surgery: procedure, endoscopic equipment and instrumentation. Childs Nerv Syst 2004; 20: 796 – 801
[11] Dorward NL, Alberti O, Zhao J, Dijkstra A, Buurman J, Palmer JD, Hawkes D, Thomas DG. Interactive image-guided neuroendoscopy: development and early clinical experience. Minim Invas Neurosurg 1998; 41: 31 – 34
[12] Balmer B, Bernays RL, Kollias SS, Yonekawa Y. Interventional MR-guided neuroendoscopy: A new therapeutic option for children. J Pediatr Surg 2002; 37: 668 – 672
[13] Scholz M, Deli M, Wildforster U, Wentz K, Recknagel A, Preuschoft H, Harders A. MRI-guided endoscopy in the brain: a feasibility study. Minim Invas Neurosurg 1996; 39: 33 – 37
[14] Auer LM. Ultrasound stereotaxic endoscopy in neurosurgery. Acta Neurochir Suppl (Wien) 1992; 54: 34 – 41
[15] Auer LM. Intraoperative ultrasound as guide for neurosurgical endoscopic procedures. Acta Radiol (Supp) 1986; 369: 164 – 166
[16] Resch KD, Perneczky A, Schwarz M, Voth D. Endo-neuro-sonography: principles of 3-D technique. Childs Nerv Syst 1997; 13: 616 – 621
[17] Resch KD. Endo-neuro-sonography: first clinical series (52 cases). Childs Nerv Syst 2003; 19: 137 – 144
[18] Yamakawa K, Kondo T, Yoshioka M, Takakura K. Ultrasound guided endoscopic neurosurgery - new surgical instrument and technique. Acta Neurochir (Suppl) 1994; 61: 46 – 48
[19] Rieger A, Rainov NG, Sanchin L, Schopp G, Burkert W. Ultrasound-guided endoscopic fenestration of the third ventricular floor for non-communicating hydrocephalus. Minim Invas Neurosurg 1996; 39: 17 – 20
[20] Grunert P, Hopf N, Perneczky A. Frame-based and frameless endoscopic procedures in the third ventricle. Stereotact Funct Neurosurg 1997; 68: 80 – 89
[21] Kelly PJ, Goerss S, Kall BA, Kispert DB. Computed tomography-based stereotactic third ventriculostomy: technical note. Neurosurgery 1986; 18: 791 – 794
[22] Muacevic A, Muller A. Image-guided endoscopic ventriculostomy with a new frameless armless neuronavigation system. Comput Aided Surg 1999; 4: 87 – 92
[23] Broggi G, Dones I, Ferroli P, Franzini A, Servello D, Duca S. Image guided neuroendoscopy for third ventriculostomy. Acta Neurochir (Wien) 2000; 142: 893 – 898; discussion: 898 – 899
[24] Lindseth F, Lango T, Bang J, Nagelhus Hernes TA. Accuracy evaluation of a 3D ultrasound-based neuronavigation system. Comput Aided Surg 2002; 7: 197 – 222
[25] Trantakis C, Tittgemeyer M, Schneider JP, Lindner D, Winkler D, Strauss G, Meixensberger J. Investigation of time-dependency of intracranial brain shift and its relation to the extent of tumor removal using intra-operative MRI. Neurolog Res 2003; 25: 9 – 12
[26] Nabavi A, Black PM, Gering DT, Westin CF, Mehta V, Pergolizzi Jr RS, Ferrant M, Warfield SK, Hata N, Schwartz RB, Wells 3rd WM, Kikinis R, Jolesz FA. Serial intraoperative magnetic resonance imaging of brain shift. Neurosurgery 2001; 48: 787 – 797; discussion: 788 – 797
[27] Dorward NL, Alberti O, Velani B, Gerritsen FA, Harkness WF, Kitchen ND, Thomas DG. Postimaging brain distortion: magnitude, correlates, and impact on neuronavigation. J Neurosurg 1998; 88: 656 – 662
[28] Hill DL, Maurer Jr CR, Maciunas RJ, Barwise JA, Fitzpatrick JM, Wang MY. Measurement of intraoperative brain surface deformation under a craniotomy. Neurosurgery 1998; 43: 514 – 526; discussion: 527 – 518
[29] Gronningsaeter A, Kleven A, Ommedal S, Aarseth TE, Lie T, Lindseth F, Lango T, Unsgard G. SonoWand, an ultrasound-based neuronavigation system. Neurosurgery 2000; 47: 1373 – 1379; discussion: 1379 – 1380
[30] Unsgaard G, Ommedal S, Muller T, Gronningsaeter A, Nagelhus Hernes TA. Neuronavigation by intraoperative three-dimensional ultrasound:

initial experience during brain tumor resection. Neurosurgery 2002; 50: 804 – 812; discussion: 812
[31] Hernes TA, Ommedal S, Lie T, Lindseth F, Lango T, Unsgaard G. Stereoscopic navigation-controlled display of preoperative MRI and intraoperative 3D ultrasound in planning and guidance of neurosurgery: new technology for minimally invasive image-guided surgery approaches. Minim Invas Neurosurg 2003; 46: 129 – 137
[32] Grønningsæter Å, Kleven A, Ommedal S, Årseth TE, Lie T, Lindseth F, Langø T, Unsgård G. SonoWand, an Ultrasound-based Neuronavigation System. Neurosurgery 2000; 47: 1373 – 1380
[33] Jodicke A, Accomazzi V, Reiss I, Boker DK. Virtual endoscopy of the cerebral ventricles based on 3-D ultrasonography. Ultrasound Med Biol 2003; 29: 339 – 345
[34] Lasio G, Ferroli P, Felisati G, Broggi G. Image-guided endoscopic transnasal removal of recurrent pituitary adenomas. Neurosurgery 2002; 51: 132 – 136; discussion: 136 – 137
[35] Gumprecht H, Trost HA, Lumenta CB. Neuroendoscopy combined with frameless neuronavigation. Br J Neurosurg 2000; 14: 129 – 131
[36] Hopf NJ, Grunert P, Darabi K, Busert C, Bettag M. Frameless neuronavigation applied to endoscopic neurosurgery. Minim Invas Neurosurg 1999; 42: 187 – 193
[37] Rhoten RL, Luciano MG, Barnett GH. Computer-assisted endoscopy for neurosurgical procedures: technical note. Neurosurgery 1997; 40: 632 – 637; discussion 638
[38] Schroeder HW, Wagner W, Tschiltschke W, Gaab MR. Frameless neuronavigation in intracranial endoscopic neurosurgery. J Neurosurg 2001; 94: 72 – 79
[39] Burtscher J, Sweeney R, Bale R, Eisner W, Twerdy K. Neuroendoscopy based on computer assisted adjustment of the endoscope holder in the laboratory. Minim Invas Neurosurg 2003; 46: 208 – 214
[40] Milhorat TH, Bolognese PA. Tailored operative technique for Chiari type I malformation using intraoperative color Doppler ultrasonography. Neurosurgery 2003; 53: 899 – 905; discussion: 905 – 906
[41] Watson JC, Shawker TH, Nieman LK, DeVroom HL, Doppman JL, Oldfield EH. Localization of pituitary adenomas by using intraoperative ultrasound in patients with Cushing's disease and no demonstrable pituitary tumor on magnetic resonance imaging. J Neurosurg 1998; 89: 927 – 932

Endoscopic Transsphenoidal Treatment in Recurrent and Residual Pituitary Adenomas – First Experience

A. Rudnik[1]
T. Zawadzki[1]
B. Gałuszka-Ignasiak[1]
P. Bażowski[1]
I. Duda[2]
M. Wojtacha[1]
A. I. Rudnik[1]
I. Krawczyk[1]

Abstract

Aim of the Study: The aim of the study has been the assessment of the endoscopic method in the surgical management of recurrent and residual pituitary adenomas, as concerns treatment efficiency, substantial complications, and its possible advantages for the operating surgeon and patient. **Material and Methods**: In Department of Neurosurgery, Silesian University School of Medicine in Katowice, between October 2001 and June 2004, 125 patients underwent endoscopic surgery due to pituitary adenoma. The analysis comprised 20 patients, who were operated on due to recurrent adenomas or residual tumour not completely removed during the first surgical procedure. The group of patients was composed of 9 women and 11 men. The youngest patient was 32 years of age, the oldest 79. The average age was 53.9 years. The analysed group had 14 non-functioning adenomas, 4 GH-secreting adenomas, 1 PRL-secreting adenoma and 1 ACTH-secreting adenoma. 19 of them were macroadenomas while 1 was a microadenoma. 11 of the 20 adenomas infiltrated the cavernous sinuses. The surgical procedures were performed by a stable team, composed of 2 neurosurgeons, a laryngologist and an anaesthesiologist. The surgery method was based upon the technique developed by Jho and Carrau, with own modifications of the operators. A rigid neuroendoscope having the diameter of 4 mm with 0 and 30 optics by Storz was used. The follow-up period after surgery was between 12 and 42 months, 24.2 months on average. **Results:** Of the 20 cases, complete recovery was achieved in 40% of patients undergoing secondary surgical procedures. In the group of 11 patients with adenomas not infiltrating the cavernous sinuses, recovery was reported for 8 of them, that is 73%. No fatalities occurred. 7 cases of liquorrhoea occurred during operation, requiring reconstruction and sealing of the sella by means of tissue glue and artificial dura or freeze-dried human dura. In 1 case, despite the application of post-operative lumbar drainage, rhinorrhoea occurred one month after the procedure, which required endoscopic reconstructive treatment. In the same patient, a pneumoencephalocele was observed. The average time of the repeat surgical procedure using endoscopic techniques was shorter by 18 minutes than the repeat procedure using microscopic techniques. **Conclusions:** The endoscopic method is a safe, hardly invasive and efficient surgical technique in the treatment of recurrent and residual pituitary adenomas. Advantages which add to its attractiveness are also reduction of the procedure duration, very good visualisation of the operative field, absence of serious complications, less pain experienced after the surgery.

Key words

Recurrent adenoma · secondary surgery · endoscopic method · transsphenoidal approach

Introduction

Pituitary adenomas make up 10 to 12% of primary intracranial tumours. In a vast majority of cases they are benign neoplasms, characterised by slow growth. Malignant adenomas or adenocarcinomas are extremely rare.

Surgical treatment of adenomas is not easy, however, and depends upon many diverse factors which, among others, include

Affiliation
[1] Department of Neurosurgery, Silesian University School of Medicine, Katowice, Poland
[2] Department of Anaesthesiology, Silesian University School of Medicine, Katowice, Poland

Correspondence
Adam Rudnik, M. D. · Department of Neurosurgery · Centralny Szpital Kliniczny · ul. Medyków 14 · 40–736 Katowice · Poland · Tel.: +32/7894/503 · Fax: +32/2525/812 · E-mail: adamrudnik@wp.pl

Bibliography
Minim Invas Neurosurg 2006; 49: 10–14 © Georg Thieme Verlag KG Stuttgart · New York
DOI 10.1055/s-2006-932126
ISSN 0946-7211

hormonal changes, size of the tumour, suprasellar penetration of the tumour and, above all, the relation of the adenoma to the cavernous sinuses adjacent to sella turcica. In addition, it appears difficult to reconcile in the surgical procedure, on the one hand, the need to make the procedure radical and, on the other hand, to fulfil the demand to be selective in the adenoma removal.

The treatment of choice in the case of pituitary adenomas, with the exception of prolactinomas, is surgery. In the pituitary gland surgery, the transsphenoidal microsurgical approach is a contemporary and recognised standard in the treatment of adenomas [1]. Despite the continuous progress made in diagnosis and treatment, the percentage of recurrent pituitary adenomas remains high and, according to literature data, ranges between 7% and even 33% [2–5]. In the mid 1990s a new, endoscopic surgical technique appeared for the treatment of sella turcica pathologies [6]. As time went by, reports began to appear concerning large groups of patients operated on using the new surgical method [7,8]. Among those patients, there were also patients with recurrent pituitary adenomas [9].

The aim of the present study is to assess the endoscopic method in the treatment of recurrent and residual pituitary adenomas, as regards treatment efficiency, substantial complications, and its possible advantages for the operating surgeon and the patient.

Material and Methods

In the Department of Neurosurgery, Silesian University School of Medicine in Katowice since 2001, the one and only method applied in surgeries of sella turcica pathologies has been the transsphenoidal endoscopic technique, based on the experiences of Jho and Carrau, with our own modifications [6]. Between October 2001 and June 2004, 157 transsphenoidal endoscopic explorations of the sella turcica were performed, in 125 cases the patients underwent endoscopic surgery due to pituitary adenoma. The analysis comprised 20 patients who were operated on due to recurrent adenomas or residual tumour not completely removed during the first surgical procedure. The group of patients was composed of 9 women and 11 men. The youngest patient was 32 years of age, the oldest 79. The average age was 53.9 years. 16 patients had been previously treated using traditional transseptal transsphenoidal approach and 4 had been previously treated using the transnasal endoscopic method. In the first group, the time that elapsed between the last procedure and repeat operation was 3 years on average (between 2 and 9 years), in the second group 6.5 months on average (between 4 and 11 months). Before the surgical procedure, patients underwent MR of the pituitary gland, as well as ophthalmological and endocrinological examinations.

The analysed group had 14 non-functioning adenomas, 4 GH-secreting adenomas, 1 prolactinoma and 1 ACTH-secreting adenoma. 19 of them were macroadenomas while 1 was a microadenoma. 11 of the 20 adenomas infiltrated the cavernous sinuses. In case of non-functioning adenomas, 9 typical recurrences of tumour were observed, whereas in 5 cases of incomplete adenoma removal this was obvious after the first procedure, on the basis of the observations during the surgical procedure, when the part located in a highly suprasellar position could not be got within reach of the surgical instruments. The MR check-up in those patients revealed residues of the adenoma, surgically available. In case of 6 hormonally active adenomas, a typical recurrence was diagnosed in 2 patients, while in 4 more the decision to operate upon the adenoma residues was taken after a thorough analysis of the situation, in the absence of reaction of the tumour to pharmacological treatment, and postponement of the decision about radiosurgery. All tumours of the GH-secreting adenoma type were macroadenomas and had infiltrated the cavernous sinuses (III and IV on Knosp's scale), a prolactinoma was a macroadenoma included as II on Knosp's scale, whereas a corticotropinoma was a microadenoma (0 on Knosp's scale). All non-functioning adenomas were macroadenomas. 5 of them infiltrated unilaterally or bilaterally the cavernous sinuses, while 9 were classified as I and II on Knosp's scale.

The surgical procedures were performed by a stable team, composed of 2 neurosurgeons, a laryngologist and an anaesthesiologist. Details of the surgical procedure have been presented in one of earlier papers [10]. A rigid neuroendoscope having a diameter of 4 mm with 0 and 30 optics by Storz was used. The approach to the sphenoid sinus was through the right nasal cavity. Repeat anterior sphenoidotomy was performed, most often widening it to a diameter of 20–25 mm. No nasal retractor was used. For the reconstruction of the sella, tissue glue was used, as well as non-absorbable artificial dura or freeze-dried allogenic dura. No post-operative nasal packing was applied. After the procedure, initially, all patients received antibiotic cover obligatorily. Later on, antibiotic therapy was applied only in case of patients with liquorrhoea during the procedure. During the first day after operation, particular attention was paid to fluid balance, electrolytic disturbances, and the occurrence of post-operative liquorrhoea. On the day following the surgical procedure, patients were mobilised and completely self-sufficient, they could breathe freely through the nose. Hospitalisation after operation continued for 3 to 7 days. At 3 and 12 months after the surgical procedure, the patients underwent MR examinations of the pituitary gland, they also underwent endocrinological and ophthalmic examinations. The follow-up period after surgery was between 12 and 42 months, 24.2 months on the average. On the basis of protocols and surgery registers, the average duration of the endoscopic surgical procedure not being a repeat procedure has been calculated, as well as the average duration of the repeat procedure. The results were compared with the average duration of surgical procedures with the use of a microscope, treated in the years 2000 and 2001. Each patient objectively assessed the possibility of breathing through the nose after the procedure, and subjectively compared the pain sensations after the transsphenoidal transseptal procedure and after the endoscopic procedure.

Results

The characteristics of the surgically treated adenomas, based upon the Knosp's scale as well as the results of treatment are presented in Table **1**. Complete recovery was obtained in 40% of surgically treated adenomas. Of the 16 patients with non-functioning adenomas, the tumour was radically removed in 6 patients, that is 42.8% of the cases (Figs. **1** and **2**). None of the 4 patients

after repeated surgical procedure for GH-secreting adenomas met the criteria of recovery of acromegaly (IGF-I < 450 μg/L, GH in OGTT < 1 μg/L). Presently, one of these patients has been undergoing stereotactic radiotherapy, the remaining three are treated by means of analogues of somatotropin release inhibiting factor. The case of a prolactinoma that underwent a repeat surgical procedure ended with complete removal, while the control PRL levels did not exceed 20 μg/L. In case of the patient with Cushing's disease, the microadenoma was removed completely, meeting the biochemical criteria of recovery.

Among the 20 patients who underwent repeat surgical procedures by means of the endoscopic technique, 7 cases of liquorrhoea were observed during the procedure (Table **2**). In one patient who underwent total resection of a recurrent non-functioning adenoma, with liquorrhoea during the procedure, lumbar drainage was applied. In the same patient, a pneumoencephalocele was noted, while a month after the procedure rhinorrhoea appeared, requiring endoscopic reconstructive treatment. In the observed series of patients, no laryngological or infectious complications were noted. New postoperative manifestations of insufficiency of the anterior lobe of the pituitary gland appeared in 3 patients. Table **3** presents the average duration of endoscopic surgical procedures performed so far in case of pituitary adenomas, as well as their comparison with the results of duration calculations for transseptal surgical procedures with the use of microscope, in 44 patients. The analysis of these calculations is presented later on in this study. All patients (16 cases) who had been previously operated on using the transsphenoidal, transseptal method, cherished most the possibility to breathe freely through the nose almost immediately after the procedure. They also assessed the pain sensations experienced after endoscopic surgery as being less profound.

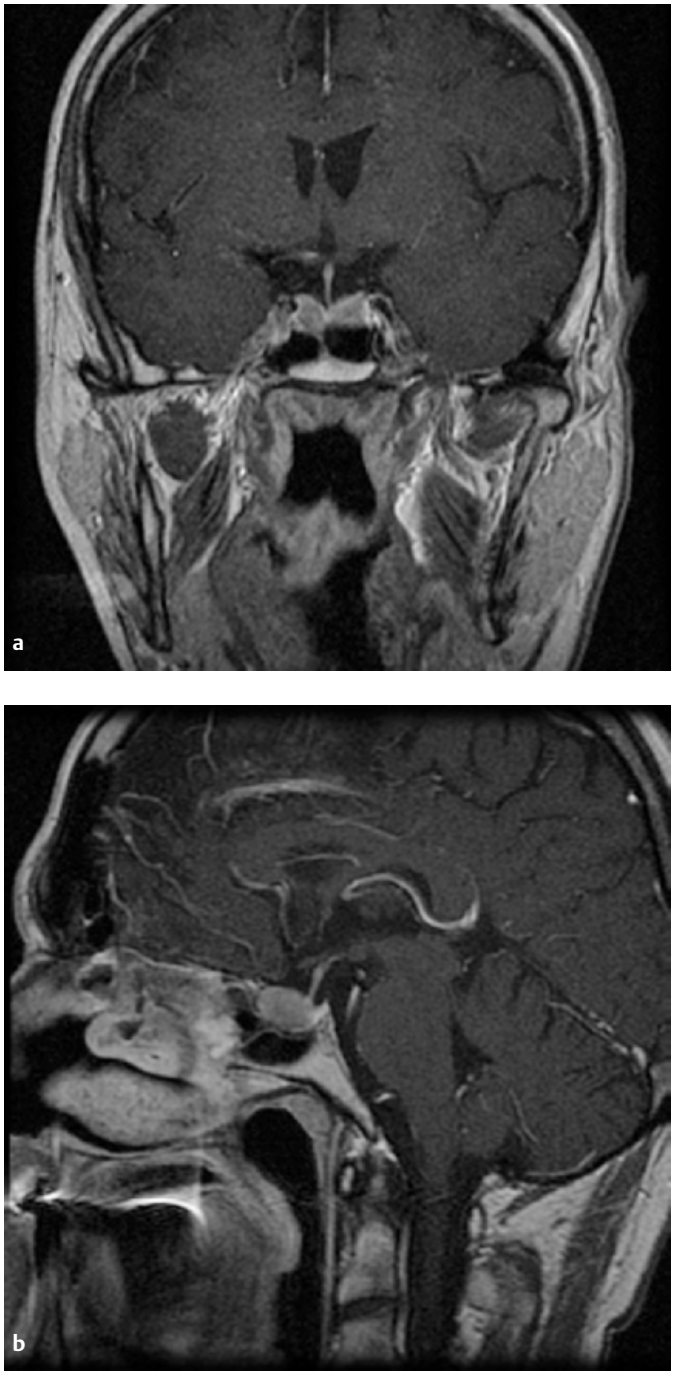

Fig. **1** Non-functioning recurrent macroadenoma before operation. Coronal (**a**) and sagittal (**b**) T_1-weighted MRI scan.

Table **1** Characteristics of the surgically treated adenomas and results of treatment

Adenoma hormonal type	*Size of the adenoma*	*Type of growth*	*Knosp scale ( )*	*No. of patients*	*No. of recovery*	*% of recovery*
non-functioning adenoma	> 10 mm	Intrasellar	I	2	2	100
		Intrasellar and suprasellar	II	7	4	57
		Intrasellar + cavernous sinus	III	1	0	0
		Intrasellar + suprasellar + cavernous sinus	IV	4	0	0
GH-secreting adenoma	> 10 mm	Intrasellar + cavernous sinus	III IV	2 2	0 0	0 0
PRL-secreting adenoma	> 10 mm	Intrasellar + suprasellar	II	1	1	100
ACTH-secreting adenoma	< 10 mm	Intrasellar	0	1	1	100
total				20	8	40

Table **2** Complications in the group of 20 surgically treated patients

Type of complication	*Number of patients*	*% of patients*
liquorrhoea during surgery	7	35
liquorrhoea after surgery	1	5
pneumoencephalocele	1	5
diabetes insipidus	0	0
hypofunction of the anterior lobe	3	15

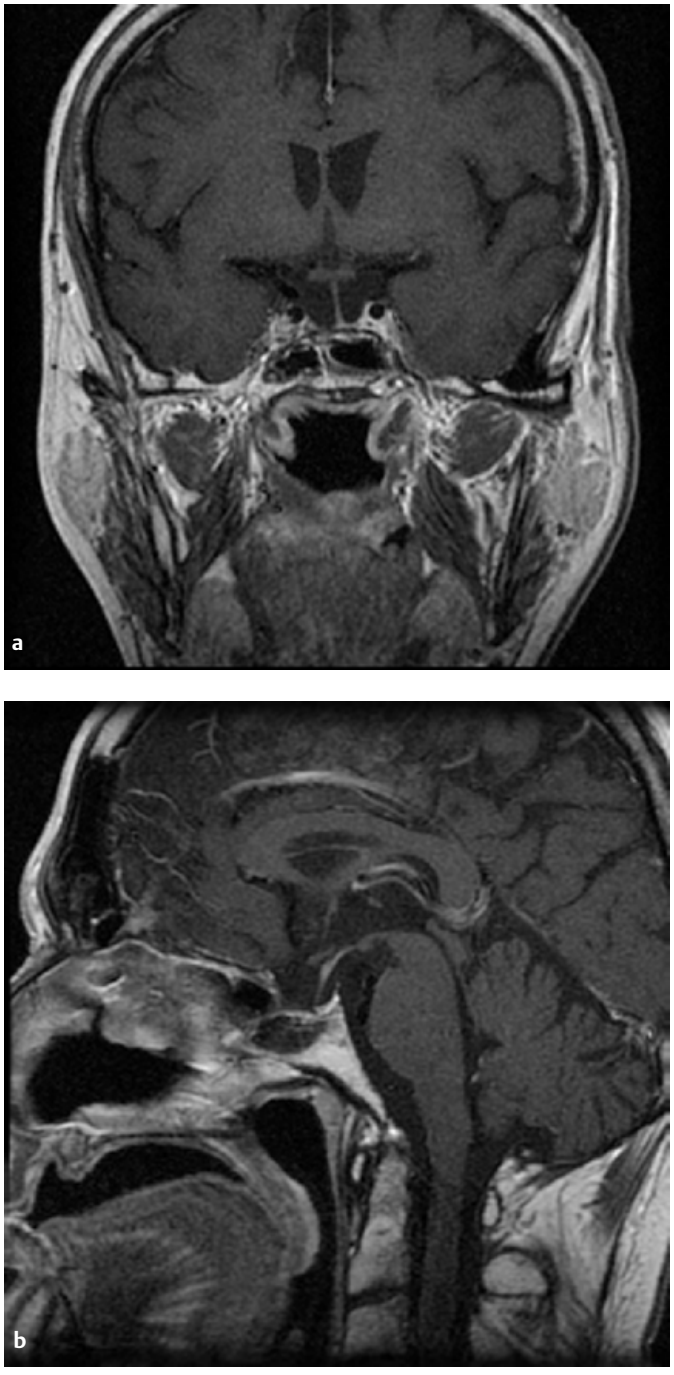

Fig. **2** Non-functioning recurrent macroadenoma in the same case after operation. Coronal (**a**) and sagittal (**b**) T_1-weighted MRI scan.

Discussion

Repeated transsphenoidal treatment of recurrent pituitary adenomas is not easy. Microscopic reoperations of sella pathologies following previous transsphenoidal interventions appear to be difficult, first of all at the stage of approaching the sphenoid sinus. The absence of the bony part of nasal septum, as well as adhesions of soft tissues make surgical access more difficult, extend the duration of procedure, and expose the patient to laryngological complications. For that reason Landolt [11], in transsphenoidal repeated surgical procedures, makes use of the so-called direct transnasal approach, described by Griffith and Veerapen [12] and Cooke and Jones [13].

Table **3** Type of surgical procedure and duration of surgery

Type of surgical procedure	*Average duration of surgery [min]*
endoscopic surgery	98
microscopic surgery	106
endoscopic repeat surgery	107
microscopic repeat surgery	129

Making use of a similar, direct approach to the sphenoid sinus in the endoscopic method, omitting the construction of a submucosal channel along the nasal septum, makes the technique also particularly attractive in the treatment of recurrent pituitary adenomas. The advantages of transsphenoidal endoscopy, namely perfect visualisation, giving up the use of a stiff nasal retractor, freedom of use for surgical tools, and possibilities of applying additional angular optics make the orientation and moving about in the secondary surgery operative field easier and safer [9]. Access to the sphenoid sinus, its opening and exposing the sella turcica posed no problem in any of the 20 patients in whom we performed the repeat surgical procedure. In most procedures, it was also easy to find the previous opening of the sella turcica. Only in 4 patients did we encounter total bony closure of the re-operated sella. In the remaining cases, after preparation of the bony margins of the "old" opening, most often we noticed that it was still available for widening, making the access to the adenoma after opening of the dura wide and free. However, most of the adenomas operated upon were hard, and not easy to apply suction to. The border with regular pituitary gland was blurred, while numerous adhesions existed between the tumour wall and cavernous sinuses as well as the arachnoidea. Altered anatomic conditions demanded patience and conscientiousness from the surgeon.

The results of treatment of recurrent pituitary adenomas are not satisfactory. Visot [14], in a group of 50 patients with non-functioning recurrent adenomas, obtained total or subtotal recovery in 60% surgically treated patients. In case of our group of 14 patients with non-functioning adenomas, total resection of the tumour was achieved in 42.8% of the surgically treated patients. Also in 4 cases of partial removal of GH-secreting adenomas, we failed to cure patients of acromegaly. It should be remembered, however, that all our patients developed adenomas infiltrating the cavernous sinuses. In the studies by Abe and Kurosaki [15,16] concerning the surgical treatment of recurrent somatotropinoma with the possibility to monitor the level of GH during the surgical procedure, no patient with a tumour infiltrating the cavernous sinuses was cured. The results of treatment of adenomas infiltrating the cavernous sinuses are poor. Perhaps in future surgical procedures applying an endoscopic technique may improve the results of treatment of these aggressive, disadvantageously located tumours. Attempts at a transnasal endoscopic approach to the cavernous sinus made on cadavers, as well as first clinical reports appear to be encouraging at least [17,18].

In our group of patients, complications were not serious. No diabetes insipidus, inflammatory or laryngological complications were observed. In 1 case, despite the application of postoperative

lumbar drainage, rhinorrhoea occurred, which required endoscopic reconstructive treatment. In the same patient, a complication in the form of a transient pneumoencephalocele was observed.

In reports by numerous authors dealing with endoscopic surgery of the pituitary gland, shortening the duration of the procedure is stressed as an advantage of the method [7,8,19]. The issue of the duration of the repeat endoscopic surgical procedure in the treatment of recurrent pituitary adenomas appeared of interest for us. The average duration of 125 consecutive endoscopic surgical procedures on pituitary adenomas was 98 minutes, whereas the average time of 44 consecutive surgical procedures using the microscope in the years 2000 and 2001, just before the introduction of endoscopic technique to surgical practice, was 106 minutes. The difference is relatively small, it should be remembered, however, that the series of endoscopic procedures initiated the application of a new technique, while the series of transseptal procedures using microscope was based upon a 10-year long experience. The average time of repeat procedures using the endoscope was 107 minutes, and was much shorter than the average time of repeat surgery of pituitary adenoma with the use of the microscope, the latter amounting to 129 minutes. As was stressed above, in the endoscopic transsphenoidal technique of pituitary adenoma surgery, the transseptal route is omitted, and the sphenoid sinus is approached directly. It seems that it is this stage that allows us to save most of the time, and the comparisons made above very much testify about that.

Reports of patients, who had been previously operated upon using the transseptal technique with the microscope, that pain sensations were much alleviated and possibilities of "normal" breathing through the nose were much enhanced after endoscopic surgery, have to appear very credible and are an undisputed proof for the superiority of the latter method in that respect.

In summary, omission of the transseptal stage in the transsphenoidal repeat surgical procedure, which is offered by the endoscopic method, is one of its advantages. This manoeuvre reduces the duration of the procedure, as well as allows us to avoid numerous complications of rhinological nature. Another advantage of the endoscopic technique is the possibility of making use of the good visualisation of the operative field, not only when looking straight, but also thanks to the angular optics, to the sides, towards the cavernous sinuses, and upwards, to the suprasellar region. Magnificent visualisation, angular optics, and the possibility of making full use of surgical instruments, not limited by a stiff retractor, make anatomic orientation and precise preparatory procedures simpler, which in consequence allows us to enhance the security and radical character of treatment in case of patients with recurrent pituitary adenomas.

Conclusions

1. The endoscopic method is a safe, minimally invasive and efficient surgical technique in the treatment of recurrent and residual pituitary adenomas.
2. Reduction of the procedure's duration, very good visualisation of the operative field, absence of serious complications, and less pain experienced after the surgery are advantages which recommend the endoscopic method for surgical treatment of recurrent pituitary adenomas.
3. Continuous development of endoscopic technique opens new perspectives in the treatment of pathologies of the sella turcica and parasellar structures.

References

[1] Hardy J. Transsphenoidal approach to the pituitary gland. In: Wilkins RH, Rengachary SS (eds). Neurosurgery. New York: McGraw-Hill Book Co, 1983: 889 – 898
[2] Ciric I, Mikhael M, Stafford T, Lawson L, Garces R. Transsphenoidal microsurgery of pituitary macroadenomas with long-term follow-up results. J Neurosurg 1983; 59: 395 – 401
[3] Ciccarelli E, Ghigo E, Miola C, Gandini G, Muller EE, Camanni F. Long-term follow-up of "cured" prolactinoma patients after successful adenomectomy. Clin Endocrinol 1990; 32: 583 – 592
[4] Friedman RB, Oldfield EH, Nieman LK, Chrousos GP, Doppman JL, Cutler Jr GB, Loriaux DL. Repeat transsphenoidal surgery for Cushing's disease. J Neurosurg 1989; 71: 520 – 527
[5] Abosch A, Tyrrell JB, Lamborn KR, Hannegan LT, Applebury CB, Wilson CB. Transsphenoidal microsurgery for growth hormone-secreting pituitary adenomas: initial outcome and long-term results. J Clin Endocrinol Metab 1998; 83: 3411 – 3418
[6] Jho HD, Carrau RL. Endoscopic endonasal transsphenoidal surgery: Experience with 50 patients. J Neurosurg 1997; 87: 44 – 51
[7] Jho HD. Endoscopic transsphenoidal surgery. J Neurooncol 2001; 54: 187 – 195
[8] Cappabianca P, Cavallo LM, Colao A, Del Basso De Caro M, Esposito F, Cirillo S, Lombardi G, Divitiis E de. Endoscopic endonasal transsphenoidal approach: outcome analysis of 100 consecutive procedures. Minim Invas Neurosurg 2002; 45: 193 – 200
[9] Cappabianca P, Alfieri A, Colao A, Cavallo LM, Fusco M, Peca C, Lombardi G, Divitiis E de. Endoscopic endonasal transsphenoidal surgery in recurrent and residual pituitary adenomas: technical note. Minim Invas Neurosurg 2000; 43: 38 – 43
[10] Rudnik A, Zawadzki T, Wojtacha M, Bazowski P, Gamrot J, Gałuszka-Ignasiak B, Duda I. Endoscopic transnasal transsphenoidal treatment of pathology of the sellar region. Minim Invas Neurosurg 2005; 48: 101 – 107
[11] Landolt AM. Surgical management of recurrent pituitary tumors. In: Schmidek HH (ed), Schmidek & Sweet Operative Neurosurgical Techniques: Indications, Methods, and Results, 4th edn. Vol. 1. Philadelphia: WM Saunders, 2000: 455 – 466
[12] Griffith HB, Veerapen R. A direct transnasal approach to the sphenoid sinus. Technical note. J Neurosurg 1987; 66: 140 – 142
[13] Cooke RS, Jones RAC. Experience with the direct transnasal transsphenoidal approach to the pituitary fossa. Br J Neurosurg 1994; 8: 193 – 196
[14] Visot A, Gaillard S, Derome PJ. Surgical management of endocrinologically silent pituitary tumors. In: Schmidek HH (ed), Schmidek & Sweet Operative Neurosurgical Techniques: Indications, Methods, and Results, 4th edn. Vol. 1. Philadelphia: WM Saunders, 2000: 424 – 437
[15] Abe T, Ludecke DK. Recent results of secondary transnasal surgery for residual or recurring acromegaly. Neurosurgery 1998; 42: 1013 – 1021
[16] Kurosaki M, Ludecke DK, Abe T. Effectiveness of secondary transnasal surgery in GH-secreting pituitary macroadenomas. Endocr J 2003; 50: 635 – 642
[17] Alfieri A, Jho HD. Endoscopic endonasal approaches to the cavernous sinus: surgical approaches. Neurosurgery 2001; 49: 354 – 360
[18] Jho HD, Ha HG. Endoscopic endonasal skull base surgery: Part 2.The cavernous sinus. Minim Invas Neurosurg 2004; 47: 9 – 15
[19] Koren I, Hadar T, Rappaport ZH, Yaniv E. Endoscopic transnasal transsphenoidal microsurgery versus the sublabial approach for the treatment of pituitary tumors: endonasal complications. Laryngoscope 1999; 109: 1838 – 1840
[20] Cho DY, Liau WR. Comparison of endonasal endoscopic surgery and sublabial microsurgery for prolactinomas. Surg Neurol 2002; 58: 371 – 375

D. Winkler[1]
D. Lindner[1]
G. Strauss[2]
A. Richter[3]
R. Schober[4]
J. Meixensberger[1]

Surgery of Cavernous Malformations with and without Navigational Support – A Comparative Study

Abstract

Background: The aim of this descriptive study was the comparison of the clinical and surgical data of patients who suffered from cavernoma and were treated surgically with and without intraoperative navigation (ultrasound, neuronavigation). **Method:** Between 1995 and 2002, 40 patients were treated for cavernous malformations microsurgically: 24 patients (group I) using a neuronavigation system (STP 4.0, SNN, Germany), 7 patients (group II) using ultrasound (Siemens Omnia with 5.0 MHz Probe) and 9 patients (group III) without any image guidance using anatomic landmarks. **Findings:** With the use of neuronavigation the mean sizes of cavernous malformations, which were resected, were reduced from 25.6 mm (group III) and 24.4 mm (group II) to 16.3 mm (group I) ($p \geq 0.05$). Corresponding to the reduction of the cavernoma size, the mean distances of the vascular lesion to the cortical surface increased from 13.9 mm (group III) and 17.8 mm (group II) to 24.4 mm under neuronavigational support ($p \geq 0.05$). All cavernomas were resected completely in all 40 patients. Postoperative neuroradiological control (MRI) confirmed complete resection in all cases. No significant differences in the clinical outcome could be evaluated in all three groups up to three months postoperatively. **Conclusions:** Use of neuronavigation was associated with a more comfortable and safer surgery of smaller and more deeper-seated cavernomas. In spite of the lack of significance between all groups, the advantages of neuronavigation in planning and realising surgery could be documented, which justify the additional costs and time-consuming acquisition of planning image data and postprocessing as well as intraoperative navigation.

Key words

Cavernoma surgery · neuronavigation · ultrasound

Introduction

Cavernous malformations have received a great deal of attention in recent years due to the improvement of its diagnosis by neuroimaging with magnetic resonance (MR) and because of the different options for surgical therapy using ultrasound and neuronavigation as well as conservative treatment using stereotactic radiation.

Intracerebral cavernous malformations are conglomerates of sinusoid-like enlarged capillaries containing slow-flowing blood or stagnated blood in varying degrees of thrombosis and degradation with thin collagenous walls, often surrounded by varying degrees of gliosis and hematomas of various age [1 – 5]. As dark red to purple, multilobulated masses ("mulberry-like"), they offer a characteristic appearance on MR (T_1-, T_2-weighted images) as the diagnostic method of choice [1, 3 – 7] and an ideal base for image-guided surgery. Patients suffering from cavernous malformations present in the majority signs of headache, vertigo, tinni-

Affiliation
[1] Department of Neurosurgery, University of Leipzig, Leipzig, Germany
[2] ENT Department, University of Leipzig, Leipzig, Germany
[3] Department of Diagnostic Radiology, University of Leipzig, Leipzig, Germany
[4] Department of Neuropathology, University of Leipzig, Leipzig, Germany

Correspondence
Dirk Winkler, M. D. · Klinik für Neurochirurgie · Universität Leipzig · Liebigstr. 20 · 04103 Leipzig · Germany · Tel.: +49/341/971-7509 · Fax: +49/341/971-7500 · E-mail: wind@medizin.uni-leipzig.de

Bibliography
Minim Invas Neurosurg 2006; 49: 15–19 © Georg Thieme Verlag KG Stuttgart · New York
DOI 10.1055/s-2005-919163
ISSN 0946-7211

tus, seizures and haemorrhage-related neurological deficits [1,5–7]. The treatment of newly discovered intracranial lesions generates debates about the appropriate therapy. Microsurgical resection should be the standard treatment in order to eliminate the risk of haemorrhage and to improve the control of seizures. Surgical resection offers a permanent cure for a cavernous malformation [3,6,8]. Stereotactic radiosurgery as an alternative therapeutic option, especially in high risk patients, is presently under discussion regarding long-term effects, efficacy and side effects [6,7].

Besides "conventional" surgery with the consideration of anatomic landmarks, ultrasound as a new surgical tool was introduced and offers a new dimension of surgery. It allows a high level of intraoperative accuracy, real-time imaging and high comfort for the surgeon. Doubtless the use of ultrasound, compared to the later introduced principle of neuronavigation, seems to be by far the cheapest method, both efficient and sufficient for the localisation of the cavernoma in the brain and for resection control during surgery. Furthermore, it allows a haemodynamic detection of associated deep venous anomalies, which cannot be realised by other methods [9–11].

With the use of neuronavigation and the possibility of postprocessing of preoperatively acquired image data, computer-assisted surgery was created [2,6,11–17]. The aim of this technical development and its use are to decrease the surgery-associated tissue traumatisation as well as to minimise or to prevent additional neurological deficits. Basic ideas behind computer-assisted surgery were the integration of presurgically acquired image data, the planning of the surgical intervention corresponding to anatomic and functional specialties and the realisation of the surgical manoeuvre in a safe and comfortable way. The crucial advantages of secondary image processing of preoperatively acquired image data are the possibility of exact detailed reproduction of structures of interest that need to be safeguarded and the option of virtual definition of entry and target coordinates. The planning procedure is user-friendly, safe and comfortable and allows the surgeon to define the best surgical approach based upon both patient's and the tool's coordinate systems controlled via display [16].

Methods and Materials

We described and analysed the neuroradiological, clinical and surgical data as well as the pre- and postoperative neurological status of patients who were operated on for cavernous malformations between 1995 and 2002 with image guidance, that means with the use of neuronavigation (24 patients, group I), ultrasound (7 patients, group II), and without any navigational support (9 patients, group III), respectively. Data were documented prospectively for group I and retrospectively for groups II and III.

Preoperative diagnosis was based on MRI and was confirmed by histopathological examination in all cases. Angiography (7 cases) was performed only in those cases in which the haemorrhage or suspect area was so close to the subarachnoid space in the vicinity of the basal cisterns that an aneurysm had to be ruled out. All cavernomas were resected microsurgically and completely in all 40 patients. Postoperative neuroradiological control (MRI) confirmed complete resection.

In group I tumour resection was performed with neuronavigation using the STP 4.0 system (Carl Zeiss Corp., Germany) and the vectorvision system (Brainlab, Germany). MRI data sets (Magnetom "Vision", Siemens, Germany, 1.5 Tesla) were acquired preoperatively for detection and localisation of the intracranial lesion as well as planning of the neuronavigational procedure [18–24]. With one millimetre slice thickness and no interval between a high level of accuracy could be achieved. A total of 250 T_1-w 3D-images per patient was used (FOV: 25 cm, matrix: 200 × 256, repetition time: 11.4 msec) for data processing. Image data were transferred via network connection or magnetic optical disc (MOD). Contouring of interesting regions (cavernoma) and structures of risk (vessels, ventricles) as well as the image fusion of anatomic and functional image data (fMRI - motor and speech cortex) were realised manually and automatically using a special postprocessing software program. Surgical planning and definition of approach in group I were facilitated by neuronavigation.

In group II identification and visualisation of the cavernoma lesion as well as surgical exposure and tumour resection were done with navigational support using intraoperative ultrasound (Siemens Omnia with 5.0 MHz ultrasound probe) [25]. Intraoperative tumour localisation was based on the visualisation of typical ultrasound signals, which could be acquired intraoperatively in all directions, corresponding to the planned surgical approach and which reflected the lesion localisation and extension in an excellent manner. At the end of surgery tumour resection was controlled in the same way.

In group III tumour localisation was based on diagnostic image data and the experiences of the neurosurgeon to transfer the visualised tumour lesion into the intracranial situs virtually using anatomic landmarks.

The widely accepted removal of cavernomas was performed microsurgically. Final diagnosis was confirmed by histopathological examination. Neurological examination of all patients was performed preoperatively and up to three months postoperatively, a neuroradiological control six months after surgery was done by MRI.

Results

A total of 40 patients with a cavernous malformation was treated microsurgically with and without navigation: 24 patients (group I), 7 patients (group II) and 9 patients (group III). No patient was operated twice and all cavernomas were resected completely. Patients who refused surgery and preferred to wait were excluded. In all cases of our study cavernous malformations were confirmed neuropathologically.

Clinical and surgical data of the navigational group (group I, II) and the conventional group (group III) were analysed: sex and age distribution of all groups as well as surgical data are shown

Table **1** Patient, anaesthesiological and surgical data. The mean size of operated cavernomas differed between navigationally (groups I and II) and conventionally operated groups (group III), meaning that very small cavernomas could resected microsurgically using neuronavigation and that deeply situated cavernomas were operated under neuronavigational support. Other data were comparable in both groups

Patient data	*Neuronavigation Group I*	*Ultrasound Group II*	*Conventional Group III*
mean age (min – max) [years]	35.2 (12 – 60)	38.5 (28 – 63)	37.9 (16 – 61)
male/female	13/11	4/3	3/6
mean time of surgery (min – max) [min]	202.5 (95 – 300)	191.3 (70 – 270)	215.2 (40 – 245)
mean time of anaesthesia (min – max) [min]	300.8 (178 – 436)	230.6 (120 – 310)	240.3 (95 – 380)
mean size of cavernoma (min – max) [mm]	16.3	24.4	25.6
mean distance of cavernoma to cortex [mm]	24.4	17.8	13.9
mean hospital stay [days]	8.6	9.6	11.9

Table **2** Localisation of cavernous malformations in navigation (groups I and II) and conventional groups (group III)

Localisation	*Neuronavigation Group I*	*Ultrasound Group II*	*Conventional Group III*
frontal	4	0	5
temporal	10	3	3
parietal	2	1	0
occipital	6	0	0
basal ganglia	1	0	0
ventricle	1	0	1
cerebellum	0	3	0
total	24	7	9

Table **3** Neurological outcome based on neurological status up to three month after surgery

Clinical outcome	*Neuronavigation Group I*	*Ultrasound Group II*	*Conventional Group III*
unchanged	23	6	5
improved	1	1	2
deteriorated	0	0	2
total	24	7	9

in Tables **1** and **2**. The clinical outcome, the cavernoma size and distance to the cortical surface were the crucial criterions and the base for the discussion and comparison of all groups: in the neuronavigation group the mean cavernoma size was with 16.3 mm the smallest, the mean distance to the cortical surface with 24.4 mm the biggest (Table **1**, Figs. **1** and **2**). The anaesthetic time in the neuronavigation group was with a mean time of

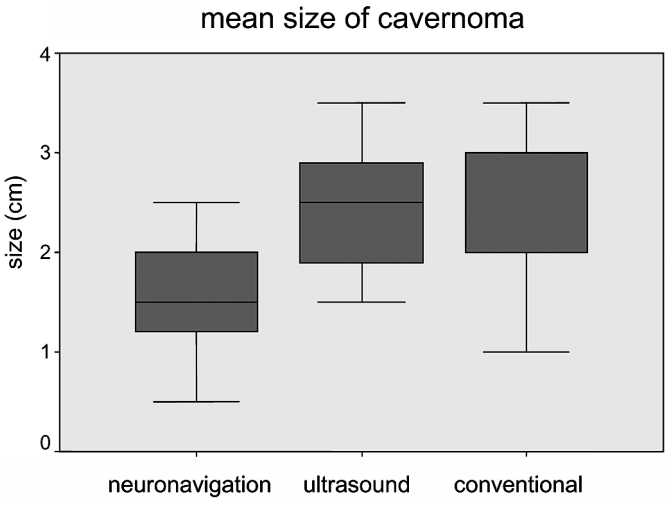

Fig. **1** Comparison of cavernoma size and neurosurgical intervention showing a decrease of cavernoma size with the use of neuronavigation.

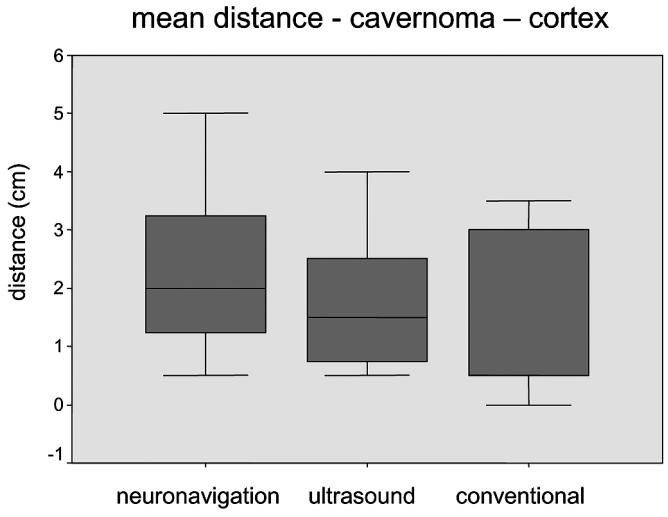

Fig. **2** Using navigational support allows an neurosurgical intervention of deeper-seated cavernomas as an advantage of image-guided surgery.

301 min not significant longer than that in group II (231 min) and group III (240 min, $p \geq 0.05$). The same ratio was found in the operation time: the time interval was in the neuronavigation group 202.5 min compared to 191.3 min in group II and 215.2 min in group III ($p \geq 0.05$). The mean hospital stay of all patients in the navigational groups was 8.6 days (group I), 9.6 days (group II), respectively, but in the conventional group III with 11.9 days it was clearly longer (Table **1**). The outcome categories (i. e., "improved", "unchanged" or "deteriorated") determined for up to three months after surgery reflect the surgery-associated morbidity as well as the result of bleeding episodes, which were one of the clinical findings (Table **3**).

Surgery-associated persisting worsening of the clinical symptoms was observed in two patients in the conventional group (group III): a 54-year-old female patient with a bleeding cavernoma in the precentral region and preoperative contralateral motor deficit of the hand. After surgery the paresis was stronger than before and persisted postoperatively. In another case a 49-

year-old male patient with a superficial temporal cavernoma and a focal epilepsy developed a postoperative bleeding in the resection hole without any space-occupying effect and an circumscriptive oedema. No second surgery was performed. In the consequence this patient suffered a prolonged hospitalisation and dysphasia. In the neuronavigation group only one patient with a temporary latent monoparesis of the arm could be registered. The patient recovered completely after antioedematous therapy four days later.

Discussion

The complex anatomy of the brain and the requirement of exact planning of surgery as well as intraoperative precise orientation were the reasons to integrate the additional technical possibilities of navigational support – ultrasound and neuronavigation. Vascular malformations are relatively common and usually resectable. Advantages of navigation-supported surgery are the precise localisation of intracranial lesions, options of more accurate and minimally invasive openings and consequently the prevention of unnecessary brain manipulation. An increase in the confidence for the neurosurgeon is the consequence.

With the help of ultrasound, cavernoma lesions can be detected in real time in an excellent way as the major advantage of intraoperative image acquisition. Surgery-associated brain shift artefacts can be compensated and do not disturb or influence the identification of the tumour lesion during surgery. Beside the possibility of resection control it allows the visualisation of the intraoperative situation as well as the haemodynamic detection of associated deep venous anomalies, which cannot be realised by other methods [26–28].

The major advantage of neuronavigation-assisted microsurgical removal of cavernomas is the possibility of postprocessing features of neuronavigation, including special visualisation of the tumour in relation to other regions of the brain, 3D reconstruction, section modes, and zoom functions. Three planar views of the surgical route allow one to illustrate the optimal surgical approach in relation to anatomic, pathological and functional areas preoperatively and to define the optimal site and extension of the craniotomy. At the end of the planning procedure, an exact simulation of the planned surgical approach can be done. As a result the extension of the craniotomy as well as brain traumatisation can be limited as much as possible.

In our study, patient's age, sex and symptoms were comparable with the results of other studies [1,4,5,9,11,19,29–31]. In group I the craniotomy was planned preoperatively using the navigational postprocessing features. In the same way the optimal planning access with minimal brain damage could be achieved in most cases by a minimal and safe cortical incision. During surgery navigational devices provided a rapid display of the point of interest in acquired images corresponding to any chosen point in the patient and vice versa. If necessary, modification of the computer-planned trajectory could be made intraoperatively by adjusting the target point to avoid eloquent areas or structures of risk. In groups II and III the craniotomy was realised corresponding to the expected localisation of the vascular lesion. The cortical incision was performed as minimally as possible via a sulcus and without touching any eloquent regions, identified by fMRT preoperatively. Steps of orientation and subsequent identification of the vascular tumour were supported in group II by ultrasound, and in group III by anatomic landmarks. Time intervals of anaesthesia and surgery were the longest in the neuronavigation group, but did not differ essentially in all three groups. Especially in group I these intervals reflect the intraoperative use of navigational devices, including registration of patient and adaptation as well as control of the intraoperative situation. In this study we documented a surgery-associated deterioration of neurological symptoms in two cases in the conventional group and a temporary deterioration in only one case in the neuronavigation group. These incidences do not reflect differences in the specific methods, but are possible complications of surgical intervention and the result of the individual experiences of neurosurgeon, which is confirmed by other authors [9,10,28,32–36]. The size and localisation of the operated cavernomas were not comparable in all groups. Especially in the conventional group in most cases the cavernomas were situated superficially and were visible on microscopic inspection of the cortical surface.

In the recent literature it has been widely reported that navigational-supported surgery of intracranial lesions can improve surgical planning and intraoperative orientation in the operating field [26,27]. Especially in patients with cavernomas invisible by microscopy and in patients with deeper seated cavernomas (corpus callosum, ventricles) the ultrasound and navigation devices were used to increase the surgeon's safety and to decrease the patient's risk as well as to prevent additional surgery-associated traumatisation. With the routine use of navigational devices, the majority of deeper situated and/or small cavernomas below the cortical surface were resected under neuronavigational support in an excellent way. At the end of the introduction of navigational devices the size of cavernomas could be reduced from 25.6 mm (group III) and 24.4 mm (group II) to 16.3 mm (group I) ($p \geq 0.05$) and the distance between vascular lesion and cortical surface could be increased from 13.9 mm (group III) and 17.8 mm (group II) to 24.4 mm by neuronavigational support. The question of whether navigationally supported surgery led to clinical benefits for patients in terms of improved postoperative outcome, reduced postoperative neurological complications, increased safety and lowered costs is difficult to answer. No study evaluating the real benefit to patients has been performed in the past and it is indeed difficult to objectively evaluate navigational methods in cavernoma surgery. Because of the considerable differences in the number of patients in each group, statistical analysis did not lead to valid conclusions. However, the trend of our results shows that the use of neuronavigation forms a good base for resection of small and deep-seated cavernomas. The requirement of statistically valid groups, which are large enough for statistical analysis and which offer the possibility for matching of different features (neurological status, lesion size and site, clinical, surgical, anaesthesiological data) should be the base for further analysis and discussions.

Image-guided navigation is a helpful instrument for neurosurgery of cavernomas. Preoperative (neuronavigation) and intraoperative (ultrasound) acquisition of three planar image data are time-consuming, but allow valid intraoperative orientation

and resection control. Although objective benefits for neurological outcome are not yet validated, the limited cost and time investment allows a microsurgical removal of cavernomas with a high grade of safety, accuracy and reliability. Compared to conventional surgery the establishment of navigation-supported surgery can be recommended unreservedly for the resection of cavernomas of small extension and difficult localisation.

References

[1] Braun V, Antoniadis G, Rath S, Richter H-P. Kavernome. Nervenarzt 1996; 67: 301 – 305
[2] Moriarity JL, Clatterbuck RE, Rigamonti D. The natural history of cavernous malformations. Neurosurg Clinics North America 1999; 10: 411 – 417
[3] Vishteh AG, Nadkarni T, Spetzler RF. Cavernous malformation of the pineal region: short report and review of the literature. Br J Neurosurg 2000; 14: 147 – 151
[4] Zabramski JM, Henn JS, Coons S. Pathology of cerebral vascular malformations. Neurosurg Clinics North America 1999; 10: 395 – 410
[5] Zabramski JM, Wascher TM, Spetzler RF, Johnson B, Golfinos J, Drayer BP, Brown B, Rigamonti D, Brown G. The natural history of familial cavernous malformations: results of an ongoing study. J Neurosurg 1994; 80: 422 – 432
[6] Maesawa S, Kondziolka D, Lunsford D. Stereotactic radiosurgery for management of deep brain cavernous malformations. Neurosurg Clinics North America 1999; 10: 503 – 511
[7] Meixensberger J, Hofmann E, Roosen K. Zerebrale Kavernome – Klinik und Therapie. WMW 1997; 7/8: 194 – 198
[8] McCormick WF, Hardmann JM, Roulter TR. Vascular malformations ("angiomas") of the brain, with special reference to those occurring in the posterior fossa. J Neurosurg 1968; 28: 241 – 251
[9] Awad IA, Robinson J. Cavernous malformation and epilepsy. In: Awad IA, Barrow DL (eds), Cavernous Malformations. Park Ridge, AANS, 1993: 49 – 63
[10] Barrow D, Awad IA. Conceptual overview and management strategies. In: Awad IA, Barrow DL (eds), Cavernous Malformations. Park Ridge, AANS, 1993: 205 – 213
[11] Weil SM, Tew JM. Surgical management of brain stem vascular malformations. Acta Neurochirurgica 1990; 105: 14 – 23
[12] Cohen DS, Lustgarten JH, Miller E, Khandji AG, Goodman RR. Effects of coregistration of MR to CT images on MR stereotactic accuracy. J Neurosurg 1995; 82: 772 – 779
[13] Dorward NL. Neuronavigation – the surgeon's sextant. Br J Neurosurg 1997; 11: 101 – 103
[14] Kelly PJ. Volumetric stereotactic surgical resection of intra-axial brain mass lesion. Mayo Clin Proc 1988; 63: 1186 – 1198
[15] Ryan MJ, Erickson RK, Levin DN, Pelizzari CA, MacDonald RL, Dohrmann GJ. Frameless stereotaxy with real-time tracking of patient head movement and retrospective patient-image registration. J Neurosurg 1996; 85: 287 – 292
[16] Schulder M, Fontana P, Lavenhar MA, Carmel PW. The relationship of imaging techniques to the accuracy of frameless stereotoaxy. Stereotact Funct Neurosurg 1999; 72: 136 – 141
[17] Wirtz CR, Tronnier VM, Bonsantomm MM, Haßfeld S, Knauth M, Kunze S. Neuronavigation – Methoden und Ausblick. Nervenarzt 1998; 69: 1029 – 1036
[18] Alp MS, Dujovny M, Misra M, Charbel FT, Ausman JI. Head registration techniques for image-guided surgery. Neurolog Res 1988; 20: 1 – 37
[19] Brommeland T, Hennig R. A new procedure for frameless computer navigated stereotaxy. Acta Neurochir 2000; 142: 443 – 448
[20] Buchholz RD, Ho HW, Rubin JP. Variables affecting the accuracy of stereotactic localization using computerized tomography. J Neurosurg 1993; 79: 667 – 673
[21] Gumprecht HK, Widenka DC, Lumenta CB. Brainlab vectorvision neuronavigation system: technology and clinical experiences in 131 cases. Neurosurgery 1999; 44: 97 – 105
[22] Kondziolka D, Dempsey PK, Lunsford LD, Kestle JRW, Dolan EJ, Kanal E, Tasker RR. A comparison between magnetic resonance imaging and computed tomography for stereotactic coordinate determination. Neurosurgery 1992; 30: 402 – 407
[23] McInerney J, Roberts DW. Frameless stereotaxy of the brain. Mount Sinai J Med 2000; 67: 300 – 310
[24] Ostertag CB, Warnke PC. Neuronavigation – computerassistierte Neurochirurgie. Nervenarzt 1999; 70: 517 – 521
[25] Tomancok B, Holl K, Wurm G, Pogady P, Fischer J. Stereotaxiegeführtes versus ultraschallgeführtes Operieren – Ein vergleichender Erfahrungsbericht. Zentralbl Neurochir 1996; 57: 123 – 128
[26] Ungersböck K, Aichholzer M, Günthner M, Rössler K, Görzer H, Koos WT. Cavernous malformations. From frame-based to frameless stereotactic localization. Minim Invas Neurosurg 1997; 40: 134 – 138
[27] Matz P, McDermott M, Gutin P, Dillon W, Wilson C. Cavernous malformation. Results of image-guided resection. J Image Guid Surg 1995; 1: 273 – 279
[28] Weber M, Vespignani H, Bracard S, Roland J, Picard L, Barroche G, Auque J, Lepoir J. Intracerebral cavernous angioma. Rev Neurol (Paris) MDN 1989; 145: 429 – 436
[29] Amin-Hanjani S, Ogilvy CS, Ojemann RG, Crowell RM. Risks of surgical management for cavernous malformations of the nervous system. Neurosurgery 1998; 42: 1220 – 1228
[30] Bertalanffy H, Kühn G, Scheremet R, Seeger W. Indications for surgery and prognosis in patients with cerebral cavernous angiomas. Neurol Med Chir 1992; 32: 659 – 666
[31] Woydt M, Krone A, Soerensen N, Roosen K. Ultrasound-guided neuronavigation of deep-seated cavernous haemangiomas: clinical results and navigation techniques. Br J Neurosurg 2001; 15: 485 – 495
[32] Fahlbusch R, Strauss C, Huk W. Pontine-mesencephalic cavernomas: Indications for surgery and operative results. Acta Neurochir Suppl (Wien) 1991; 53: 37 – 41
[33] Huhn S, Rigamonti D, Hsu F. Indications for surgical intervention. In: Awad IA, Barrow DL (eds), Cavernous Malformations. Park Ridge, AANS, 1993: 87 – 99
[34] Ojemann RG, Crowell RM, Ogilvy CS. Management of cranial and spinal cavernous angiomas. Clin Neurosurg 1993; 40: 98 – 123
[35] Robinson JR, Awad IA, Little JR. Natural history of the cavernous angioma. J Neurosurg 1991; 75: 709 – 714
[36] Sakai N, Yamada H, Tanigawara T, Asano Y, Andoh T, Tanabe Y, Takada M. Surgical treatment of cavernous angioma involving the brainstem and review of the literature. Acta Neurochir (Wien) 1991; 113: 138 – 143

A Minimally Invasive Endoscopic Transsphenoidal Approach with an Endonasal Septal Pushover Technique by Using a Modified Nasal Speculum

N. Nakao
K. Nakai
T. Itakura

Abstract

Whereas the endoscopic endonasal transsphenoidal approach has been applied in patients with pituitary lesions as a potentially efficacious and less invasive surgical technique, the sinonasal step of a series of the surgical procedures is generally not well known to neurosurgeons. This is one of the reasons why the endoscopic technique has not been fully been adopted as a routine surgical procedure approaching towards the sella. The present paper describes the technical details of a purely endoscopic approach using an endonasal septal pushover technique. We also present a newly designed nasal speculum specialized for this endoscopic endonasal technique. As compared to the endoscopic endonasal approach previously reported, the surgical procedure required for sphenoidotomy with the aid of the modified speculum was simplified and thereby less time-consuming. This technique has been performed in 40 patients with several types of pituitary lesions. All patients recovered rapidly without significant rhinological complications. Despite a limited number of cases, our experience suggests that this simplified endoscopic technique could encourage a more routine use of endoscopes in the endonasal approach for pituitary lesions.

Key words

Pituitary adenoma · cavernous sinus · endoscopic surgery

Introduction

The endoscopic endonasal transsphenoidal approach has been used as a potentially efficient and less invasive surgical procedure for pituitary lesions [1–5]. One striking advantage of the endoscopic technique is its peculiar ability of visualization. An endoscope provides a panoramic view of the sphenoid sinus. This makes it possible for the surgeon to recognize the bony bulge covering vital structures around the sella, such as the carotid artery and optic nerves. With angled views afforded by an endoscope, moreover, blind manipulation can be avoided in the resection of lateral and suprasellar lesions. There are also some drawbacks and limitations which may be responsible for the fact that the endoscopic endonasal technique has been slow to be adopted as a routine surgical procedure approaching towards the sella. The endoscopic transsphenoidal approach requires different surgical skills from those needed for microsurgery. Surgeons have to handle surgical instruments in a relatively narrow working space with a two-dimensional view. An unfamiliarity of neurosurgeons with sinonasal surgery is also an obstacle to widespread use of the endoscopic transsphenoidal approach for pituitary lesions. With the endoscopic endonasal surgical technique most commonly reported [1–5], sphenoidotomy is performed without the use of a nasal retractor or speculum. Therefore, this requires a series of surgical procedures which are basically derived from endoscopic sinonasal surgery routinely made by endoscopic rhinologists.

We have applied an endoscopic technique to sphenoidotomy with an endonasal sepal pushover technique originally reported by Griffith and Veerapen [6]. Since this approach consists of rela-

Affiliation
Department of Neurological Surgery, Wakayama Medical University, Wakayama, Japan

Correspondence
Naoyuki Nakao, M. D. · Department of Neurological Surgery · Wakayama Medical University · 811–1 Kimiidera · Wakayama 641–0012 · Japan · Tel.: +81/734/41-0609 · Fax: +81/734/47-1771 · E-mail: nnakao@wakayama-med.ac.jp

Bibliography
Minim Invas Neurosurg 2006; 49: 20–24 © Georg Thieme Verlag KG Stuttgart · New York
DOI 10.1055/s-2005-919148
ISSN 0946-7211

tively simple surgical procedures, sphenoidotomy is rapidly and safely completed with minimum disruption of normal tissue in the nasal cavity. We converted this microsurgical technique into purely endoscopic surgery by using a rigid endoscope and a nasal speculum specially designed for the endoscopic endonasal approach. In this report, we describe this technique and our experience with 40 patients.

Patients and Methods

Equipment

We used 4-mm rigid endoscopes with 0- and 30-degree angled lenses (Olympus). In all cases, the endoscope is mounted on an endoscope holder (Olympus) during the entire procedure of the endoscopic surgery. The navigation system used for image-guided surgery was the StealthStation frameless stereotactic system (Medtronic Sofamor Danek) consisting of a 3D digitizer based on optical tracking system interfaced with a computer workstation. Preoperative CT and MR imaging data were obtained by using a CT unit (HiSpeed Advantage, GE Medical System, Milwaukee, WI) and a 1.5-T MR imaging unit (Magnetom Vision, Siemens Corp., Erlangen, Germany), respectively [7]. We used a nasal speculum (Fujita Medical Instruments, Tokyo) which was modified specially for endonasal endoscopic surgery. As compared to a conventional nasal speculum (Fujita Medical Instruments, Tokyo) commonly used in the microsurgical endonasal transsphenoidal approach, the blade of the newly designed speculum is thinner and more slender (Fig. **1**). Furthermore, the blade tip of the speculum is designed to fan out with a limited extent of the opening of the blade base which is supposed to contact with the nostril. This mechanism is achieved by means of the fact that the angle between the hinge portion and the shaft of the speculum is reduced as compared to that of a conventional speculum. When the blade is fully opened, the outer and inner widths of the blade base are 13 mm and 10 mm, respectively. With this modification we are able to attenuate stretch-derived injury to the nostrils, and a relaxing alar incision is not needed even in patients with extremely small nostrils as frequently seen in the Japanese woman.

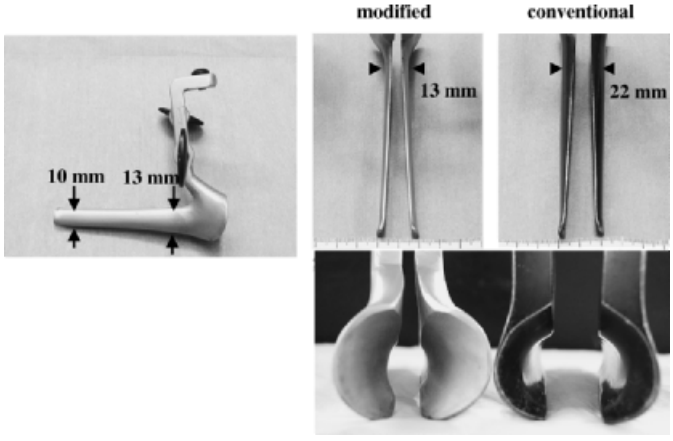

Fig. **1** A nasal speculum modified specially for the endoscopic endonasal transsphenoidal approach. As compared to the conventional nasal speculum used for the microscopic endonasal approach, the blade of the modified nasal speculum is thinner and more slender, and is designed to fan out with a more limited extent of the opening of the blade base which is supposed to contact with the nostril.

Surgical procedures

CT and/or MR images with a 1 – 2 mm slice thickness are preoperatively performed with six to eight fiducial markers being stuck to the patient's forehead and face. The data are then transferred to the workstation of the StealthStation via a magnetooptical disc. After general anesthesia with orotracheal intubation, the patient is placed supine with the trunk slightly elevated. The head is fixed in a Mayfield headrest to which the navigation reference arc is attached. The patient's registration based on the preoperative image data is repeated until the error is within 2 mm as previously described [7]. The oropharyngeal cavity is packed with a roll of gauze. Cottonoids soaked with diluted adrenaline (1 : 100,000 w/v) are placed in the nasal cavity while the endoscope equipment is set up. The 4-mm rigid endoscope with 0-degree angled lens is mounted on an endoscope holder, and introduced through either the right or left nostril, depending on which provides the larger space between the nasal septum and the middle turbinate. Approach toward the sphenoid rostrum is made through the space between the nasal septum and the middle turbinate (Fig. **2A**). At this step of the procedure, the middle turbinate is gently displaced laterally, and is not needed to be outfractured. The neuronavigation is employed as necessary to determine the direction of the approach. Once the nasal septum close to its base is brought into view through the space medial to the middle turbinate, an approximately 1-cm linear mucosal incision is made in a vertical direction at the junction of the anterior wall of the sphenoid sinus and the posterior bony septum (Fig. **2B**). After the mucosa is dissected from the base of the septal bone to gain the space into which the nasal speculum is put, the blade tip of the nasal speculum is inserted into the submucosal space under the endoscopic view (Fig. **2C**). The septal bone is then fractured at its junction to the anterior wall of the sphenoid sinus, and is dislocated towards the contralateral side (Fig. **2C**). At this point of the procedure, much attention was paid to confirm that the tip of the speculum is entirely placed in the submucosal space to avoid mucosal laceration. Whereas this is usually achieved by turning the tip of the speculum to the contralateral side, care must be taken not to forcibly turn the blade of the speculum. From that surgical phase onward, the endoscope is placed inside the speculum. While the blade of the speculum is gradually opened and the nasal septum is pushed away from the sphenoid rostrum, submucosal dissection is made bilaterally to fully expose the anterior wall of the sphenoid sinus (Fig. **2D**). The edge of the incised mucosa should be bloodless and fully retracted laterally by the tip of the speculum blade. This procedure is important to avoid a blood-derived blur of the lens of the endoscope at the following surgical steps. The posterior aspect of the vomer (i. e., the keel bone) remaining in the anterior wall of the sphenoid sinus is noted, and served as a guide to the midline (Fig. **2D**). With a small bone chisel and alligator forceps, the anterior wall of the sphenoid sinus is widely removed particularly toward the inferior direction. A microdrill is occasionally required to extend the inferior portion of the opening of the sphenoid rostrum, depending on the extent of the pneumatization of the sphenoid sinus. The sphenoid septa are removed by using alligator forceps so that a panoramic view from the planum sphenoidale superiorly to the clival indentation inferiorly (Fig. **2E**) is

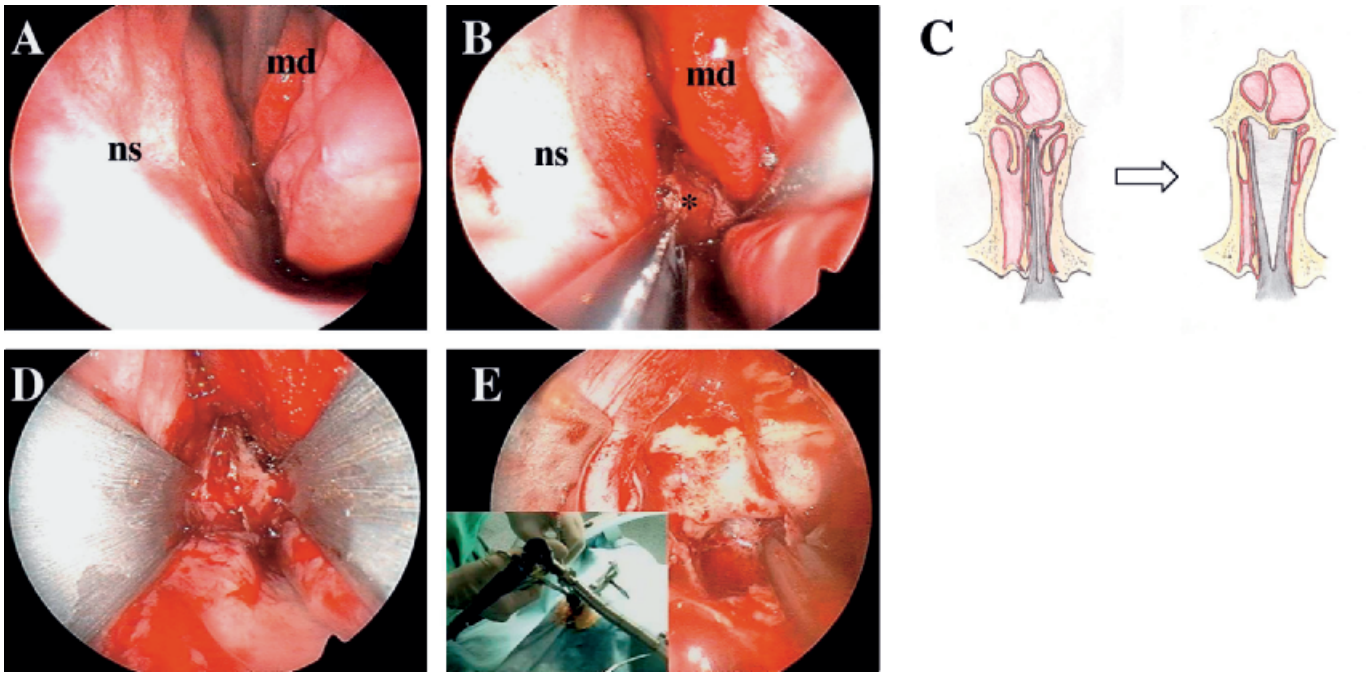

Fig. **2** Endoscopic views and schematic illustrations showing a series of procedures for endoscopic endonasal sphenoidotomy using a septal pushover technique. **A** Endoscopic approach towards the sphenoid rostrum is made through the space between the nasal septum and the middle turbinate. At this step of the procedure, the middle turbinate is gently displaced laterally, and need not be outfractured. md = middle turbinate; ns = nasal septum. **B** After an approximately 1-cm linear mucosal incision is made in a vertical direction at the junction of the anterior wall of the sphenoid sinus and the posterior bony septum, the mucosa is dissected from the base of the septal bone (*) to obtain the space into which the nasal speculum is inserted. **C** The blade tip of the nasal speculum is put into the submucosal space under the endoscopic view. The posterior part of the septal bone is then fractured and dislocated toward the contralateral side by turning the tip of the speculum to the contralateral side. While the speculum blade is gradually opened, submucosal dissection is made bilaterally to expose the anterior wall of the sphenoid sinus. **D** The keel bone remaining in the anterior wall of the sphenoid sinus serves as a guide to the midline. **E** The anterior wall of the sphenoid sinus is widely removed particularly towards the inferior direction. The sphenoid septa are removed by using an alligator forceps so that a panoramic view from the planum sphenoidale superiorly to the clival indentation inferiorly is obtained. The inset shows an intraoperative photograph. While a rigid endoscope is mounted to an endoscope holder, a surgeon handles two surgical instruments put into the sphenoid sinus through a surgical corridor secured with the aid of a modified nasal speculum.

gained. Pieces of the resected bone are saved for reconstruction of the sellar floor. The following surgical procedures including those for the opening of the sella, the removal of the lesions and the sellar reconstruction are performed in a manner similar to that previously reported [2–4,8,9]. Whereas a 0-degree angled lens is used in most of the procedures above, lesions present in the suprasellar region as well as those extending into the cavernous sinus are extirpated under direct visualization with a 30-degree angled endoscope. In three patients where a CSF leakage was recognized during the operation, abdominal free fat grafts were placed to repair the CSF fistula. The speculum is removed gradually at the end of the procedure. After the nasal septum is placed at the midline, the structures of both nasal cavities are restored. Since the extent of submucosal septal dissection is limited to its basal part, nasal packing is not used.

Results

We performed a total of 41 procedures using this endoscopic approach in 40 patients with sellar and parasellar lesions. In one patient with a Rathke's cleft cyst, a purely endoscopic repair of a CSF fistula was performed two weeks after an endoscopic drainage of the cyst. They were 26 women and 14 men among, and the mean age was 52 years (range: 23–80 years). Among those included 21 patients with non-functioning adenomas, 3 with acromegaly, 5 with prolactinomas, 9 with Rathke's cleft cysts, one with a meningioma and one with a mucocele in the sphenoid sinus. Among the 21 patients with non-secreting adenomas, total resection was made in 14 patients and subtotal resection in 4 patients. In the remaining three patients, tumor removal was partial. Among the three patients, one patient with recurrent adenoma underwent partial removal leaving residual tumor in the bilateral cavernous sinuses. In the other two patients undergoing partial removal, the adenoma was extremely hard, exhibiting an extensive suprasellar growth. In all of the 3 patients with acromegaly, the results of endocrinological evaluations met the cure criteria of the Cortina consensus [8] with clinical improvements. In one patient with acromegaly, a less enhanced mass lesion was present exclusively in the right cavernous sinus. Under direct visualization by use of a 30-degree angled endoscope, the inferomedial portion of the dura of the cavernous sinus was opened, and the tumor was totally extirpated with great care not to injure the internal carotid. Among the 5 patients with prolactinomas, prolactin levels were normalized with associated clinical improvements in 3 patients without adjunctive medical treatment and in 2 patients with administration of cabergoline. In the 9 patients with Rathke's cleft cysts, decompression of the cyst and biopsy of the cyst wall were performed. Whereas none of those patients underwent radical resection of the cyst, no recurrence

of the cyst occurred during a follow-up period of 3 – 36 months. In one patient with sellar meningioma exhibiting suprasellar and cavernous sinus extensions, tumor removal was limited to the extent from the intrasellar to the suprasellar part. One patient with a huge mucocele in the sphenoid sinus presented with a unilateral abducens palsy, and underwent drainage of the cyst content and removal of the sinus mucosa with a consequent complete recovery of the nerve palsy.

None of the patients complained of nasal pain or discomfort after surgery. Among the present series of the patients undergoing endoscopic surgery, there were three patients with recurrent adenomas. Those three patients had previously undergone sublabial surgery and reported that postoperative recovery from the endoscopic endonasal procedure was much easier and less painful than that from the sublabial procedure. There was no sinonasal complications such as postoperative nasal bleeding, perforation of the nasal septum, nasal mucosal synechia and rhinosinusitis. A postoperative CSF leak developed in two patients: one patient with acromegaly and one with Rathke's cleft cyst. The patient with acromegaly underwent spinal drainage with a consequent cessation of CSF leakage. In another patient with Rathke's cleft cyst, as described above, a CSF fistula was successfully repaired endoscopically using an abdominal free fat graft. There were no patients who postoperatively suffered from an insufficiency of the anterior pituitary function. One patient with a recurrent adenoma developed permanent diabetes insipidus after surgery, and required desmopressin therapy. No other complications were encountered.

Discussion

Our experience with 40 patients indicates that this endoscopic technique allows for a fast and accurate approach to the sella. In all cases except for one where the base of the septal bone was thick, the sellar floor was reached within an average of 10 minutes of starting the procedure. This method is also less complicated, and possibly less invasive to the normal structures in the nasal cavity than the previously published technique of endoscopic endonasal surgery [1 – 5]. In the endoscopic endonasal surgical technique commonly reported [1 – 5], sphenoidotomy is achieved without the use of a nasal speculum. Therefore, this technique requires several surgical procedures to gain an adequate space that serves for a surgical corridor. Thus, the middle turbinate is outfractured to obtain a working space in the sphenoethmoid recess with subsequent identification of the sphenoid sinus ostium. The nasal septum is then detached from the sphenoid rostrum by using a microdrill or simply by being fractured. The removal of the sphenoid rostrum was made by enlarging the sphenoid sinus ostia using rongeurs or a microdrill. Among the procedures above, the approach toward the sphenoid ostium is a crucial step of the procedure to which neurosurgeons are generally unaccustomed. By contrast, such sinonasal surgical procedures are not needed in our technique. A surgeon brings the posterior part of the nasal septum into view, followed by an insertion of a modified nasal speculum into the submucosal space of the base of the nasal septum. After the septum is dislocated towards the contralateral side by using the modified speculum, a sufficient working space is gained to facilitate the subsequent surgical procedures. Furthermore, as in the case with the endoscopic surgery without using the nasal speculum, postoperative nasal packing is not needed since the extent of submucosal septal dissection is limited to its basal part. One can argue that the insertion of a nasal speculum in the nasal cavity makes the handling of surgical instruments restricted in the endoscopic surgery. Based on the experience with an use of our modified nasal speculum, however, this instrument with a minimum stretch force on the nostril fully retracts mucosal edges that can be an obstacle to both the insertion and handling of surgical instruments. Thus, the speculum provides an appropriate surgical corridor through which surgical instruments can be taken in and out without hindrance. In addition, whereas the entrance of the modified speculum is small, the blade tip fans out just anterior of the opening of the sphenoid rostrum so that the sphenoid sinus can fully be used as a broad working space.

A potential advantage of the present purely endoscopic approach over the microscopic direct endonasal approach remains to be discussed since these two techniques adopt the same surgical route to the sella. It is accepted that the microscopic direct endonasal approach has the advantage of a simpler and less time-consuming sphenoidotomy with fewer postoperative rhinological complications [6,9,10]. Nonetheless, this approach also has some drawbacks in that it provides a more restricted exposure and a surgical trajectory which is slightly off midline [6,9,10]. Surgical microscopes need the retraction of superficial structures (i.e., the nostrils), which otherwise hinder the entry of the light beam. In the microscopic endonasal approach with the conventional nasal speculum, a wider opening of its blade can entail an excessive stretch force on the nostril, and therefore a relaxing alar incision is needed in patients with extremely small nostrils as seen frequently in the Japanese women. Zada et al. [10] indeed reported in a series of 100 patients undergoing the microscopic endonasal approach that 20% of the patients required a relaxing alar incision for speculum placement. In contrast, endoscopes can visualize a deep-seated object even with a small entry of the approach. Our technique fully utilizes this advantage of endoscopes. Thus, even in patients with very small nostrils, our endoscopic approach by using the modified speculum can afford both an excellent operative view and a sufficient surgical corridor with a minimal invasiveness to the nostrils. Of the current series of 40 patients, there were five women with extremely small nostrils. Despite the very small nostrils, a wide opening of the blade tip of the speculum was feasible without making a relaxing alar incision. Furthermore, a panoramic view of the sphenoid sinus provided by endoscopes makes it possible for the surgeon to recognize the bony bulge covering vital structures around the sella, such as the carotid artery and optic nerves. Surgeons can make the opening in the sellar floor as large as possible while viewing the surrounding vital structures. In addition, the panoramic visualization can alleviate the problem of a slightly off midline surgical trajectory. Angled views afforded by an endoscope help to avoid blind manipulation in dealing with lateral and suprasellar lesions. As in our cases, lesion sites which are not normally visualized with a surgical microscope can directly be brought into view. These peculiar visualizing abilities possibly contribute to a decreased incidence of complications as reported elsewhere [1,4].

In endoscopic surgery, surgical instruments have to be handled in a relatively narrow working space with a two-dimensional view, and therefore the endoscopic transsphenoidal approach requires different surgical skills from those needed for microsurgery. Although surgical instruments modified for use in endoscopic techniques as well as a stereoscopic endoscope have been developed [4,11], the preciseness of endoscope-controlled manipulations of surgical instruments cannot yet reach the level of that achieved with microsurgery. Considering the current state of the endoscopic technique, the surgical approach itself employed in the endoscopic surgery should be simplified in order to attenuate the incidence and severity of the procedure-related complications. In this context, our technique that affords a more simplistic and minimally invasive approach than other endoscopic techniques [1 – 5] in terms of a series of techniques required for sphenoidotomy could help to make the endoscopic endonasal approach for pituitary lesions more effective and safe. Despite a limited number of cases, the present study also suggests that this simplified endoscopic technique can encourage a routine use of endoscopes in the endonasal approach for pituitary lesions.

References

[1] Cappabianca P, Cavallo LM, Colao AM, de Divitiis E. Surgical complications associated with the endoscopic endonasal transsphenoidal approach for pituitary adenomas. J Neurosurg 2002; 97: 293 – 298

[2] Cappabianca P, Cavallo LM, Colao AM, Del Basso De Caro M, Esposito F, Cirillo S, Lombardi G, de Divitiis E. Endoscopic endonasal transsphenoidal approach: Outcome analysis of 100 consecutive procedures. Minim Invas Neurosurg 2002; 45: 1 – 8

[3] Cappabianca P, Cavallo LM, de Divitiis E. Endoscopic endonasal transsphenoidal surgery. Neurosurgery 2004; 55: 933 – 941

[4] Jho H-D, Carrau RL. Endoscopic endonasal transsphenoidal surgery: experience with 50 patients. J Neurosurg 1997; 87: 44 – 51

[5] Jho H-D, Carrau RL. Endoscopic transsphenoidal surgery. In: Schmidek HH (eds). Schmidek & Sweet Operative Neurosurgical Techniques: Indications, Methods, and Results, 4th edn. Philadelphia: WB Saunder, Vol 1, 2000: 385 – 397

[6] Griffith HB, Veerapen R. A direct transnasal approach to the sphenoid sinus. Technical note. J Neurosurg 1987; 66: 140 – 142

[7] Nakao N, Nakai K, Itakura T. Updating of neuronavigation based on images intraoperatively acquired with a mobile computerized tomographic scanner: Technical note. Minim Invas Neurosurg 2003; 46: 117 – 120

[8] Giustina A, Barkan A, Casanueva FF, Cavagnini F, Frohman L, Ho K, Veldhuis J, Wass J, Werder K von, Melmed S. Criteria for cure of acromegaly: A consensus statement. J Clin Endocrinol Metab 2000; 85: 526 – 529

[9] Cooke RS, Jones RAC. Experience with the direct transnasal transsphenoidal approach to the pituitary fossa. Br J Neurosurg 1994; 8: 193 – 196

[10] Zada G, Kelly DF, Cohan P, Wang C, Swerdloff R. Endonasal transsphenoidal approach for pituitary adenomas and sellar lesions: assessment of efficacy, safety, and patient impressions. J Neurosurg 2003; 98: 350 – 358

[11] Cappabianca P, Alfieri A, Thermes S, Buonamassa S, de Divitiis E. Instruments for endoscopic endonasal transsphenoidal surgery. Neurosurgery 1999; 45: 392 – 396

T. Hori
Y. Okada
T. Maruyama
M. Chernov
W. Attia

Endoscope-Controlled Removal of Intrameatal Vestibular Schwannomas

Abstract

The use of endoscopes for surgery of the cerebellopontine angle tumors is steadily obtaining widespread acceptance. The objective of the present study was a laboratory and clinical evaluation of the safety of the endoscope-controlled microneurosurgical removal of the intrameatal vestibular schwannomas through a retrosigmoid approach. The anatomical investigation was done on formalin-fixed cadaver heads and dry temporal bones. Clinical series included 33 consecutive patients (23 women and 10 men; mean age 50 ± 15 years). A bayonet-style rigid endoscope with 70 angle of view and 4 mm outer diameter was found to be optimal for observation of the internal auditory canal. Its insertion in the cerebellopontine cistern should be preferably done under control through an operating microscope. Endoscope-controlled manipulations necessitate the use of a special holder system, which provides a stable position of the device and allows bimanual manipulations by the surgeon. A thermographic evaluation did not reveal a significant increase of the local temperature due to use of the endoscope. Use of the endoscope permitted removal of the neoplasm from the most lateral part of the internal auditory canal and identification of the nerve of tumor origin. In total, 28 tumors underwent total removal, and anatomical preservation of the facial nerve was attained in 31 cases. Damage of the facial nerve by the endoscope was met once. In 8 out of 16 patients, who showed serviceable hearing before surgery, this was preserved after tumor removal. In conclusion, endoscope-controlled removal of the intrameatal vestibular schwannomas seems to be a technically feasible, effective and safe procedure. Nevertheless, good equipment and special training are absolutely necessary for attainment of optimal results.

Key words

Vestibular schwannoma · endoscope-controlled removal · neuroendoscopy · internal acoustic meatus

Introduction

Complete microneurosurgical excision represents the ideal treatment option for symptomatic patients with vestibular schwannomas [1]. On average 96 % of the tumors can be removed totally, which provides the best possible long-term local control [2]. However, the treatment is accompanied by the well-known risk of postoperative complications, such as hearing loss, facial nerve palsy, and cerebrospinal fluid (CSF) leak. Many technical adjuncts were proposed for their prevention. Recently, there has been growing interest in the use of neuroendoscopes during surgery for cerebellopontine angle (CPA) tumors [3 – 15], because the possibility “to look around the corner” is very attractive for early identification of the cranial nerves and inspection of the internal auditory canal (IAC). However, the efficacy of the technique is not yet completely known. Moreover, there is some concern about possible endoscope-related complications due to poor overview of the operative field, the limited two-dimension-

Affiliation
Department of Neurosurgery, Neurological Institute, Tokyo Women’s Medical University, Tokyo, Japan

Correspondence
Prof. Tomokatsu Hori, M. D. · Department of Neurosurgery · Neurological Institute · Tokyo Women’s Medical University · 8–1 Kawada-cho · Shinjuku-ku · Tokyo 162–8666 · Japan · Tel.: +81/3/3353-8111 (ext. 26216) · Fax: +81/3/5269-7438 · E-mail: thori@nij.twmu.ac.jp

Bibliography
Minim Invas Neurosurg 2006; 49: 25–29 © Georg Thieme Verlag KG Stuttgart · New York
DOI 10.1055/s-2006-932125
ISSN 0946-7211

al image, and possible local increase of temperature in the vicinity to the tip of the device [10,11,13]. Therefore, we conducted both a laboratory and a clinical study on the safety of the endoscope-controlled removal of the intrameatal vestibular schwannomas.

Materials and Methods

Laboratory investigation

Endoscope-controlled microneurosurgical removal of an intrameatal vestibular schwannoma through a retrosigmoid approach was simulated on 2 formalin-fixed cadaver heads and 2 dry temporal bones. After craniotomy, which was done by a high-speed drill, the rigid bayonet-style endoscope was inserted into the CPA. Commercially available 19-cm and 23-cm long devices with 0 , 30 , and 70 angles of view, and outer diameters of 2.7 and 4 mm were tested consequently. Two sets of observations were done: initially the endoscope connected with videocamera and cold light source was manipulated freehand; thereafter all manipulations were repeated while the device was fixed in the "EndoArm", a specially designed endoscope holder integrated with a video system (Olympus Co., Tokyo, Japan) [16].

After observation of the CPA, the endoscope was removed and drilling of the posterior wall of the IAC was done with its further inspection by various types of endoscopes, which were manipulated either freehand or were fixed in the "EndoArm" (Fig. **1**). During observation of the CPA, opening of the IAC by a high-speed drill, and its endoscopic inspection the thermographic study were performed using a portable infrared camera TVS 100 ME (Nippon Avionics Inc., Tokyo, Japan).

Clinical study

During 2004 and 2005, 33 consecutive patients underwent endoscope-controlled microneurosugical removal of intrameatal vestibular schwannomas at the Department of Neurosurgery of the Tokyo Women's Medical University. There were 23 women and 10 men; mean age constituted 50 ± 15 years. The tumor was located on the left side in 16 cases, and on the right side in 17. There were 31 initially diagnosed and 2 recurrent neoplasms. Three schwannomas were purely intrameatal, 8 had limited extension into the CPA, 7 filled the CPA completely, but did not show compression of the brain stem, and 15 caused more or less prominent brain stem compression. Before surgery 31 patients had either normal, or nearly normal facial nerve function (House-Brackmann grade 1 – 2 [17]), and 16 patients had functionally preserved hearing (Gardner-Robertson class I-II [18]).

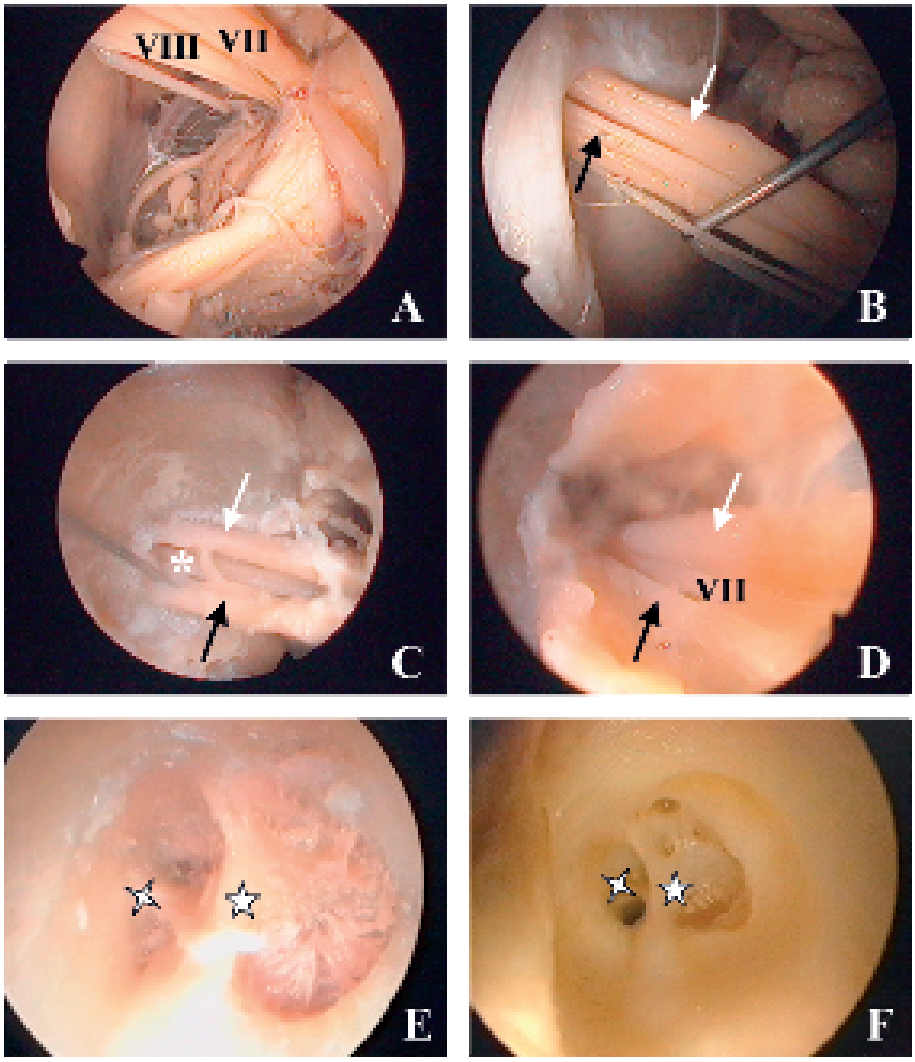

Fig. **1** Neuroendoscopic view of the right CPA during anatomic dissection: identification of origin of the VII and VIII cranial nerves from the brain stem (**A**), observation of the cisternal portion of the nerves (**B**), observation of the nerves after removal of the posterior wall of the IAC (**C**), observation of the most lateral part of the IAC (**D**), identification of the Bill's bar and transverse crest after removal of the nerves (**E**) and complete removal of the soft tissues (**F**). Marked: facial nerve (VII), vestibulocochlear nerve (VIII), superior vestibular nerve (black arrow), inferior vestibular nerve (white arrow), cochlear nerve (asterisk), Bill's bar (crest), and transverse crest (star).

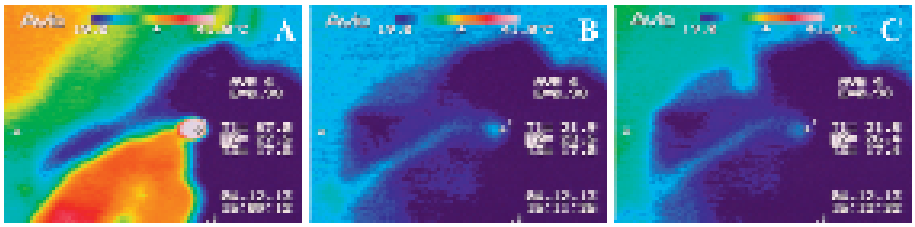

Fig. **2** Thermographic study during simulated endoscope-controlled procedure for intrameatal tumor: the local temperature dramatically increased during drilling of the posterior wall of the IAC (**A**), but normalized thereafter (**B**), and did not changed significantly during the use of endoscope (**C**).

All procedures were planned as routine microneurosurgical operations, so if necessary these could be completed without the use of endoscope. General anesthesia, lateral oblique position of the patient, standard retrosigmoid approach, motor and somatosensory evoked potentials, auditory brain response, facial nerve monitoring, and cochlear nerve action potentials were used routinely, in the same way as described elsewhere [13,14,19,20]. After microsurgical intracapsular debulking of the tumor in the CPA, the posterior wall of the IAC was removed by a high-speed drill. A rigid endoscope fixed in the "EndoArm" was inserted into the CPA under control through an operating microscope. Subsequent removal of the residual tumor from the CPA and IAC was attained utilizing concurrently both microscope- and endoscope-controlled techniques with the use of routine microneurosurgical instruments. Regular irrigation of the wound by Ringer's lactate solution was done during use of the endoscope.

Results

Laboratory investigation

The endoscopes with 0 , 30 , and 70 angles of view were found to be equally useful for observation of the CPA through the retrosigmoid approach. Inspection of the IAC seemed to be optimal using the endoscope with a 70 angle of view and outer diameter 4 mm. The insertion of this device into the CPA and its positioning for visualization of the IAC were found to be difficult without microscopic control. Both freehand fixation of the endoscope and use of the "EndoArm" seemed to be equally suitable for inspection of the CPA and IAC. However, endoscope-controlled microsurgical manipulations could not be effectively done without use of the endoscope-holder system, which provided a stable position of the device and allowed bimanual manipulations by the surgeon. During drilling of the posterior wall of the IAC a thermographic study revealed a prominent increase of the local temperature. Alternatively, the presence of an endoscope connected with a working cold light source in the CPA did not lead to significant changes of the local temperature (Fig. **2**).

Clinical study

Use of the endoscope permitted removal of residual tumor from the most lateral part of the IAC (Fig. **3**). In all, total tumor removal was done in 28 cases, subtotal removal in 3, and partial removal in 2 cases. Anatomic preservation of the facial nerve was attained in 31 cases. In one case the facial nerve was mechanically damaged by the endoscope itself, which necessitated its direct suturing in the CPA. In 8 out of 16 patients, who showed serviceable hearing preoperatively, this was preserved after tumor removal. No one case of thermal injury to the cranial nerves, postoperative CSF leak, or infection was observed. Histological examination revealed typical schwannomas in all cases; mean MIB-1 index constituted 2.3 ± 1.9 %.

Final endoscopic inspection at the end of the procedure gives us an opportunity to define the nerve of tumor origin, either definitely (in 18 cases), or most probably (in 14 cases). Schwannomas arising from the superior vestibular and inferior vestibular nerves were represented in 16 cases each (Figs. **4** and **5**). In one case with partial tumor removal the nerve of tumor origin was not defined. Its identification was found to be easier if dilatation of the fundus of the IAC due to tumor growth was present. Meanwhile, no associations were found between the nerve of tumor origin and age and gender of the patient, side and MIB-1 index of the neoplasm, and the presence of useful hearing before surgery.

Discussion

Modern neuroendoscopic devices, both rigid and flexible, provide a wide angle of view, superb illumination with a cold light, and perfect depth of focus in combination with high magnification. Their use during microsurgical procedures allows to reduce the size of the craniotomy, to improve visualization in the operative field, and to look around important anatomic structures, thus eliminating the need for extensive retraction [4,6,11–13,21–23]. Furthermore, the development of "virtual endoscopy" [24,25], which permits to simulate the surgical procedures preoperatively, based on the data of neuroimaging, can significantly increase the clinical efficacy of the technique in the future.

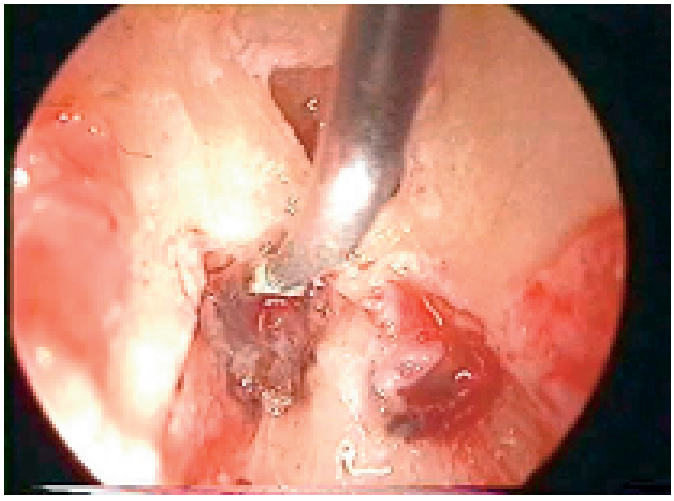

Fig. **3** Endoscope-controlled removal of the intrameatal vestibular schwannoma from the lateral part of the IAC.

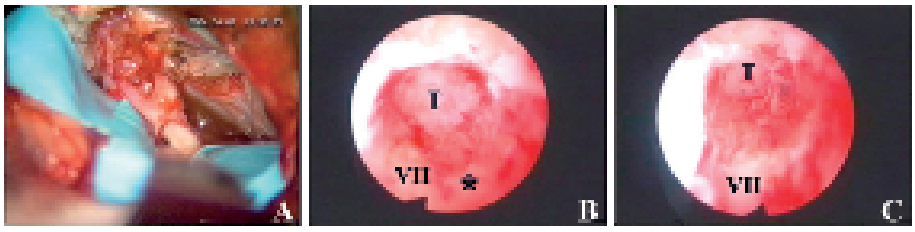

Fig. **4** Endoscope-controlled microneurosurgical removal of the right-sided vestibular schwannoma: view of the tumor in the IAC after removal of its posterior wall (**A**) and observation of the neoplasm originated from the superior vestibular nerve in the most lateral part of IAC (**B** and **C**). Marked: facial nerve (VII), cochlear nerve (asterisk), and tumor (T).

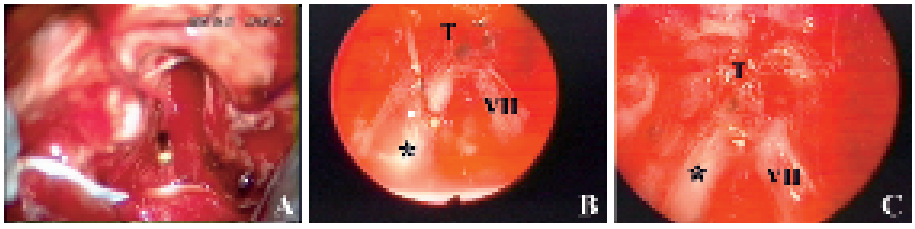

Fig. **5** Endoscope-controlled microneurosurgical removal of the left-sided vestibular schwannoma: view of the tumor after removal of the posterior wall of the IAC (**A**) and endoscopic observation of the neoplasm originated from the inferior vestibular nerve in the most lateral part of the IAC (**B** and **C**). Marked: facial nerve (VII), cochlear nerve (asterisk), tumor (*T*), and electrode for cochlear nerve action potentials (white arrow).

The advantages of the endoscopic inspection during microsurgical removal of vestibular schwannomas had been highlighted in several previous reports [3–15]. These mainly include early identification of the cranial nerves in the CPA, possibility of revision of the most lateral part of the IAC for the presence of the residual neoplasm, and visualization of the non-sealed petrous bone air cells for prevention of postoperative CSF leak. With the adjunct of endoscopy, tumors can be removed more completely, with less morbidity, and the degree of their resection can be assessed more precisely [3,7,10,13,23]. The length of drilling of the posterior wall of the IAC can be reduced, and inadvertent opening of the intraosseous endolymphatic sac and posterior semicircular canal, which has a crucial importance in hearing-preservation vestibular schwannoma surgery, can be avoided [9–12]. The technique may be useful for identification of the source of problematic bleeding during removal of the neoplasm [15]. Finally, as was shown in the present series, use of the endoscope permits an exact delineation of the nerve of tumor origin.

While endoscopic inspection during surgery for vestibular schwannomas has obtained widespread acceptance, the advantages of endoscope-controlled removal of these tumors are less clear. Wackym et al. [13] and Magnan et al. [14] advocated use of this technique for the dissection of the residual neoplasm from the most lateral part of the IAC. Goksu et al. [10] reported the results of such procedures in 8 patients with serviceable hearing and small intrameatal vestibular schwannomas: total removal, functional preservation of the facial nerve, and anatomic preservation of the cochlear nerve was attained in all cases, whereas useful hearing was preserved in four cases. In the present series, which included a significant proportion of large tumors, total removal of the neoplasm was attained in 85% of the cases, anatomic preservation of the facial nerve in 94% of cases, and preservation of the serviceable hearing in 50% of those, who showed its presence before surgery.

Our clinical results confirm that integration of endoscope-controlled removal of the intrameatal part of the tumor into microneurosurgical excision of vestibular schwannomas is technically feasible, effective, and safe. Nevertheless, several lessons have been learnt. First, use of rigid endoscopes, which are usually recommended for endoscope-assisted skull base surgery [6,21,23], may be complicated during endoscope-controlled procedures due to nearly coaxial positions of the endoscopic device and microinstruments. This disadvantage can be overcome if bayonet-style endoscopes and microinstruments are used. Second, several endoscopes should be available during surgery and used according to the particular goals. While 0 , 30 , and 70 angles of view endoscopes were found to be useful for manipulations in the CPA, only the latter device was suitable for observation of the IAC. Third, angled rigid endoscopes may be difficult to pass in the operative wound without risk of inadvertent damage to the neurovascular structures [5,6,23]. Mechanical injury of the facial nerve by the endoscope was met once in the present series. Therefore, we strongly recommend microscopic guidance during insertion of the 70 angle of view device into the CPA.

There is known concern that prolonged use of endoscope can be accompanied by an increase of the local temperature in the vicinity to its tip followed by thermal injury to critical neurovascular structures [11,13]. This was not, however, confirmed by the conducted laboratory thermographic study. In fact, it was found that local temperature in the CPA during the use of an endoscope connected with a working light source, is much lower, compared with those during removal of the posterior wall of the IAC by a high-speed drill. Moreover, in no one case of our clinical series the thermal injury to the cranial nerves was marked. Definitely, the possibility of this complication may depend on the model of the device, duration of its use, type of light source, and individual sensitivity of the cranial nerves. However, in general, the risk of thermal injury during use of the endoscope should not be considered too high, and regular irrigation of the wound by Ringer's lactate solution seems to serve as a sufficient preventive measure.

Intracranial neuroendoscopic procedures are usually performed through a narrow corridor in the vicinity to important neurovascular structures. While endoscopic inspection can be done by

freehand fixation of the device, endoscope-controlled microneurosurgical manipulations require its precise position, because monomanual surgical manipulations may be not only non-effective, but even dangerous if an occasional shift of the endoscope occurs in the surgical wound [5,9–11,13,21–23]. This necessitates the use of special holder, which can provide a stable position of the device in the surgical wound and permits bimanual manipulations by the surgeon and assistant. Several such systems are currently available. One of these is the "EndoArm", which was used in the present study, and can be suitable for endoscopic inspection, endoscope-assisted, and endoscope-controlled microneurosurgery. It provides excellent maneuverability within 6 degrees of freedom, smooth manipulations with avoidance of strenuous maneuvers of the surgeon, accurate fixation in any direction, and safe release, which result in a high level of clinical safety of the device [16].

Conclusion

Endoscopic inspection during surgery for vestibular schwannomas allows early identification of the cranial nerves, revision of the most lateral part of the IAC for presence of the residual neoplasm, delineation of the nerve of its origin, and visualization of the non-sealed petrous bone air cells for prevention of postoperative CSF leak. Endoscope-controlled microneurosurgical removal of the intrameatal tumors is technically feasible, effective, and safe, and permits to attain dissection of the neoplasm from the most lateral part of the IAC. The risk of thermal injury to the cranial nerves due to use of endoscopes seems to be low. Nevertheless, special training is absolutely necessary, because endoscopic procedures are accompanied by definite learning curve. Availability of good equipment, including an endoscope-holder system, is also very important for attainment of optimal surgical results.

References

[1] Chernov M, DeMonte F. Skull base tumors. In: Levin VA (ed). Cancer in the nervous system, 2nd edn. Oxford: Oxford University Press, 2002: 300–319

[2] Yamakami I, Uchino Y, Kobayashi E, Yamaura A. Conservative management, gamma-knife radiosurgery, and microsurgery for acoustic neurinomas: a systematic review of outcome and risk of three therapeutic options. Neurol Res 2003; 25: 682–690

[3] McKennan KX. Endoscopy of the internal auditory canal during hearing conservation acoustic tumor surgery. Am J Otol 1993; 14: 259–262

[4] Magnan J, Chays A, Lepetre C, Pencroffi E, Locatelli P. Surgical perspectives of endoscopy of the cerebellopontine angle. Am J Otol 1994; 15: 366–370

[5] Rosenberg SI, Silverstein H, Willcox TO, Gordon MA. Endoscopy in otology and neurootology. Am J Otol 1994; 15: 168–172

[6] Matula C, Tschabitscher M, Diaz Day J, Reinprecht A, Koos WT. Endoscopically assisted microneurosurgery. Acta Neurochir (Wien) 1995; 134: 190–195

[7] Tatagiba M, Matthies C, Samii M. Microendoscopy of the internal auditory canal in vestibular schwannoma surgery: technique application. Neurosurgery 1996; 38: 737–740

[8] Valtonen HJ, Poe DS, Heilman CB, Tarlov EC. Endoscopically assisted prevention of cerebrospinal fluid leak in suboccipital acoustic neuroma surgery. Am J Otol 1997; 18: 381–385

[9] Jennings CR, O'Donoghue GM. Posterior fossa endoscopy. J Laryngol Otol 1998; 112: 227–229

[10] Goksu N, Bayazit Y, Kemaloglu Y. Endoscopy of the posterior fossa and dissection of acoustic neuroma. J Neurosurg 1999; 91: 776–780

[11] King WA, Wackym PA. Endoscope-assisted surgery for acoustic neuromas (vestibular schwannomas): early experience using the rigid Hopkins telescope. Neurosurgery 1999; 44: 1095–1102

[12] Low WK. Enhancing hearing preservation in endoscopic-assisted excision of acoustic neuroma via the retrosigmoid approach. J Laryngol Otol 1999; 113: 973–977

[13] Wackym PA, King WA, Poe DS, Meyer GA, Ojemann RG, Barker FG, Walsh PR, Staecker H. Adjunctive use of endoscopy during acoustic neuroma surgery. Laryngoscope 1999; 109: 1193–1201

[14] Magnan J, Barbieri M, Mora R, Murphy S, Meller R, Bruzzo M, Chays A. Retrosigmoid approach for small and medium-sized acoustic neuromas. Otol Neurotol 2002; 23: 141–145

[15] Gerganov VM, Romansky KV, Bussarsky VA, Noutchev LT, Iliev IN. Endoscope-assisted microsurgery of large vestibular schwannomas. Minim Invas Neurosurg 2005; 48: 39–43

[16] Morita A, Okada Y, Kitano M, Hori T, Taneda M, Kirino T. Development of hybrid integrated endoscope-holder system for endoscopic microneurosurgery. Neurosurgery 2004; 55: 926–932

[17] House WF, Brackmann DE. Facial nerve grading system. Otolaryngol Head Neck Surg 1985; 93: 184–193

[18] Gardner G, Robertson JH. Hearing preservation in unilateral acoustic neuroma surgery. Ann Otol Rhinol Laryngol 1988; 97: 55–66

[19] Ojemann RG. Retrosigmoid approach to acoustic neuroma (vestibular schwannoma). Neurosurgery 2001; 48: 553–558

[20] Ciric I, Zhao J-C, Rosenblatt S, Wiet R, O'Shaughnessy B. Suboccipital retrosigmoid approach for removal of vestibular schwannomas: facial nerve function and hearing preservation. Neurosurgery 2005; 56: 560–570

[21] Perneczky A, Fries G. Endoscope-assisted brain surgery: Part 1 – evolution, basic concept, and current technique. Neurosurgery 1998; 42: 219–225

[22] Fries G, Perneczky A. Endoscope-assisted brain surgery: Part 2 – analysis of 380 procedures. Neurosurgery 1998; 42: 226–232

[23] Teo C. Endoscopic-assisted tumor and neurovascular procedures. Clin Neurosurg 2000; 46: 515–525

[24] Boor S, Maurer J, Mann W, Stoeter P. Virtual endoscopy of the inner ear and the auditory canal. Neuroradiology 2000; 42: 543–547

[25] Vrabec JT, Briggs RD, Rodriguez SC, Johnson Jr RF. Evaluation of the internal auditory canal with virtual endoscopy. Otolaryngol Head Neck Surg 2002; 127: 145–152

Thecaloscopy through Sacral Bone Approaches, Cadaver Study: Further Anatomic Landmarks

S. Mourgela[1]
S. Anagnostopoulou[2]
J. P. Warnke[3]
A. Spanos[1]

Abstract

Endoscopy of the spinal canal, for interventional studies, diagnosis and therapy, is a scientific topic that has attracted the interest of neurosurgeons, anesthesiologists and orthopedic surgeons for the past twenty years. Endoscopy of the thecal sac was assumed to be less important than endoscopy of the ventricular system by neurosurgeons. Nevertheless, during the last years it has attained increasing scientific interest, firstly because of the introduction of small diameter flexible endoscopes and secondly due to the growing interest for minimal invasive diagnostic and therapeutic procedures in modern neurosurgery. Until now thecaloscopy was performed by the ISGT (International Study Group for Thecaloscopy) using co-axial downward orientated approaches. We have examined transsacral approaches to facilitate the navigation of flexible scopes in the lumbosacral subarachnoid space, and thus we now introduce further recognizable endoscopic anatomic landmarks.

Key words

Thecaloscopy · filum terminale · sacral spinal rootlets · coccygeal spinal rootlets

Introduction

The author is a member of the International Study Group for Thecaloscopy (ISGT), a study group of neurosurgeons, united under a common interest for exploration of the lumbar subarachnoid space using flexible endoscopes and under a growing interest in the anatomy of the thecal sac, the pathological entities originating from this anatomical area and the probable therapeutic possibilities and interventions [1]. The cadaver studies on fresh post-mortem cadavers were performed in the Anatomy Institute of Vienna University, using coaxial, downward-orientated approaches under the supervision of Prof. M. Tschabitscher [1–3]. A further study on cadavers, using transsacral approaches, featuring upward-directed endoscopy, was performed in the Department for Anatomy, Medical School of the University of Athens, on phenol-formalin embalmed cadavers, under the supervision of Prof. S. Anagnostopoulou.

It is nowadays common knowledge that certain pathological entities originating from morphological structures of the thecal sac are suitable for an endoscopic approach. Pathomorphology of the leptomeningeal layers around nerve rootlets and filum terminale is widely regarded to be the cause of certain clinical conditions, such as low back pain and other pain syndromes.

To perform transsacral thecaloscopy, a neurosurgeon needs certain anatomic landmarks, some of which have already been mentioned in previous reports on thecaloscopy [2]. In this article we describe some further anatomic landmarks for transsacral thecaloscopy, such as the last part of filum terminale internum, as well as the sacral and coccygeal nerve rootlets.

Filum terminale

The filum terminale is the anatomic continuation of the spinal pia mater, about 20 cm in length, prolonged downward from the

Affiliation
[1] Neurosurgical Department, "Agios Savas" Anticancer Institute, Athens, Greece
[2] Department of Anatomy, Medical School, University of Athens, Athens, Greece
[3] Neurosurgical Department, Paracelsus Klinik, Zwickau, Germany

Correspondence
S. Mourgela, M. D. · Neurosurgical Department · "Agios Savas" Anticancer Institute · Leoforos Alexandras 171 · 115 22 Athens · Greece · Tel.: +30/210/692-5520 · Fax: +30/210/692-5520 · E-mail: sofiamou@otenet.gr

Bibliography
Minim Invas Neurosurg 2006; 49: 30–33 © Georg Thieme Verlag KG Stuttgart · New York
DOI 10.1055/s-2006-932147
ISSN 0946-7211

apex of the conus medullaris. It consists of two parts, an upper and a lower section. The upper part, or filum terminale internum, measures about 15 cm in length, is enclosed within the thecal sac, is surrounded by the nerve rootlets forming the cauda equina and reaches as far as the lower border of the second sacral vertebra. The lower part or filum terminale externum or coccygeal ligament, measures about 5 cm in length, is enclosed in a sheath of dura mater (filum durae matrix spinalis), extending downwards from the apex of thecal sac and is attached to the back of the first segment of the coccyx.

Dorsal and ventral sacral and coccygeal nerve rootlets

There are five pairs of sacral and one pair of coccygeal spinal nerves. In general, each spinal nerve is attached to the medulla spinalis by two roots, an anterior or ventral and a posterior or dorsal, the latter being characterized by the presence of the spinal ganglion. Dorsal and ventral nerve roots differ not only functionally but also morphologically, by their size. They emerge from the posterior and the anterior surfaces of the medulla spinalis, correspondingly, as a number of rootlets or filaments (filia radicularia). These filaments coalesce to form nerve roots in the intervertebral foramen. In the thecal sac only filaments or rootlets exist. Dorsal nerve roots, in general, are thicker than ventral nerve roots by a ratio of 3.2 : 1, owning to the greater size and number of rootlets because of the fact that the dorsal nerve roots contain sensory fibers for more than one dermatome, whilst the ventral nerve roots contain fibers for only one myotome.

The roots of the lower lumbar and upper sacral nerves are the largest, and their individual filaments the most numerous of all the spinal nerves, while the rootlets of the coccygeal nerve are the smallest. The first and second sacral nerves are the largest, whilst the third, fourth and fifth diminish progressively in size from the upper level downwards. The first coccygeal nerve is even smaller than these nerves. The second and third coccygeal nerves represent a few strands of nerve fibers which adhere to the outer surface of filum terminale externum [4].

Materials and Methods

The aim of our study on cadavers was to describe a new co-axial, upward-directed approach for thecaloscopy. A study using four phenol-formalin embalmed adult human cadavers was performed.

All cadavers were placed in prone position and the lumbar spine was elevated, in the knee-elbow position. Three methods were used to fill the subarachnoid space with saline:

- a translaminar method – with ectomies of the laminae and insertion of an instillation catheter in the thecal sac,
- by performing lumbar puncture, and
- through the endoscope, with irrigation of the subarachnoid space with saline through the working channel.

Two surgical approaches were used to reach the sacral dura mater. First, a midline skin incision was performed over the anatomic area of the sacral hiatus. The sacral hiatus was found and the endoscope was inserted through it to reach the apex of the thecal sac (see Fig. **2**). Then the dura was penetrated and the endoscope was inserted for further navigation in the subarachnoid space. In cases of a higher position of the thecal sac and a narrow sacral canal, a laminectomy of S1 and S2 was performed. A detachment of the paravertebral muscles in the upper sacral area was performed, followed by laminectomy of S1 and S2 laminae and dura exposure (Fig. **1**). A flexible, steerable endoscope (Zeppelin, diameter 2.8 mm, 37 cm long, one working channel of 1-mm in diameter and one irrigation channel less than 1-mm), was then inserted.

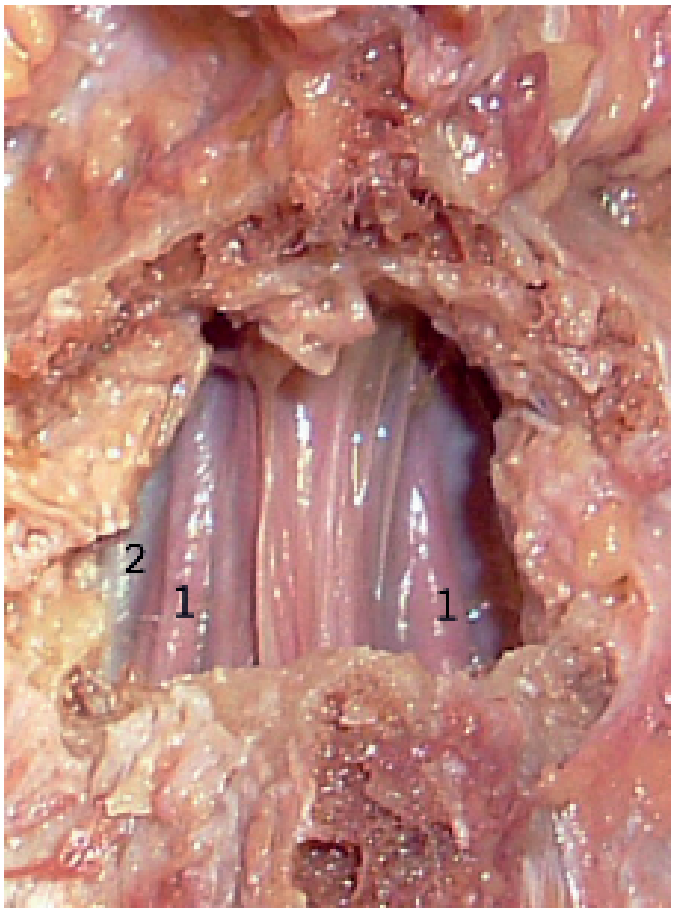

Fig. **1** Transacral approach – laminectomy at S1 and S2 level; 1 = nerve rootlet, 2 = dura mater.

All structures were identified and named (Fig. **3**). There was a slight difficulty to guide the endoscope at the level of the sacrovertebral angle. At this point the endoscope tip was manipulated upwards and brought to face the posterior surface of the dura. Another helpful manipulation to pass the sacrovertebral angle was irrigation with saline through the working channel of the endoscope. The endoscopic procedure was recorded on S-VHS video tape (Fuji). After removal of the endoscope the dura was opened and the structures were observed microsurgically (Fig. **4**). The ventral and dorsal, sacral and coccygeal roots were separated. After that the free part of the neural filum terminale was easily identified because all the nerve rootlets in that anatomic position have left the thecal sac and entered the nerve pockets at the foraminal levels. At this stage micro- and macrophotographs were taken (Fuji Digital Camera A205s).

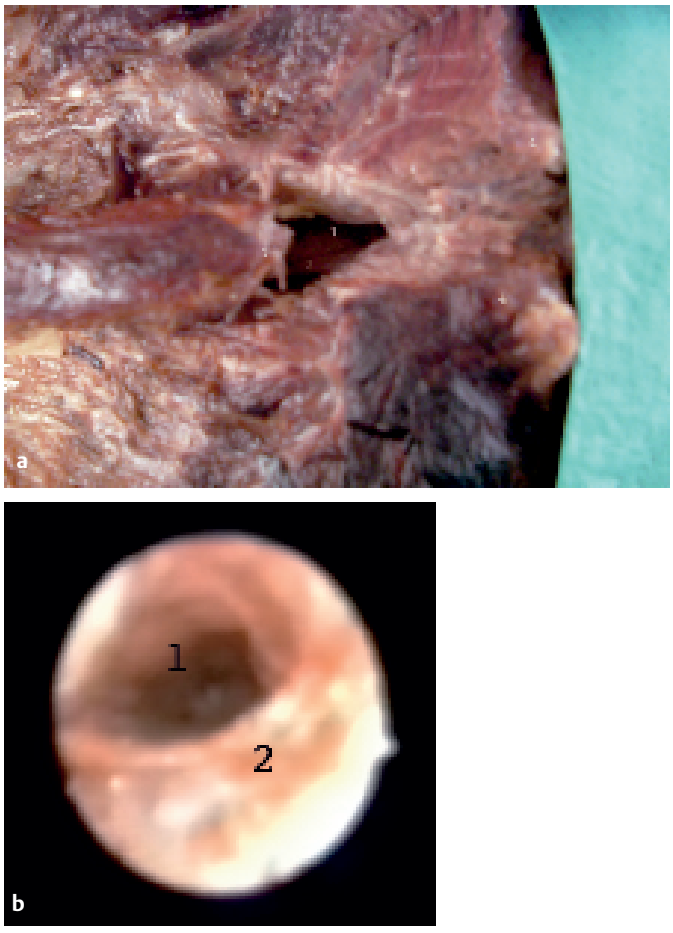

Fig. **2** **a** Transhiatal approach, macroscopic view; 1 = bed of sacral hiatus, 2 = filum terminale, 3 = ridge of sacral hiatus, 4 = coccygeal protuberantia. **b** Transhiatal approach, endoscopic view; 1 = extradural sacral canal, 2 = epithelium covering the sacral canal.

Results

The ISGT has already proved that endoscopic inspection of the thecal sac is an easy, safe and reliable method. The medical endoscopic equipment fulfils the specific criteria of this anatomic region for inspection. Anatomic structures suitable for using as landmarks in this particular region are listed below.

Filum terminale

This anatomic structure consists of two parts, the filum terminale internum and the filum terminale externum. What is of great interest for thecaloscopy is the filum terminale internum which reaches as far as the second sacral vertebra and its last 2 cm that can be reached during the endoscopic transsacral procedure. It is enclosed within the thecal sac, and is surrounded by the nerve rootlets, from which it can be recognized by its bluish-white colour and lack of outer blood vessels. The filum terminale consists mainly of fibrous connective tissue and glial cells and is continuous with pia mater [2].

Sacral and coccygeal nerve rootlets

The first and second sacral nerve rootlets are large, white in colour covered by vessels, whilst the third, fourth and fifth sacral nerve rootlets are diminishing in size from the upper level downwards. The first coccygeal nerve rootlets are very thin, whilst the second and third coccygeal nerve rootlets are nerve strands covering the filum terminale externum.

Discussion

It is already known from prior studies that endoscopy of the thecal sac can be performed by using reliable anatomic structures. Orientation using the transsacral approach described above has the advantage to visualize directly the filum terminale without interference of nerve rootlets.

At this level, the filum terminale as well as the dorsal and ventral coccygeal and sacral nerve rootlets differ even more in size and can be identified endoscopically. The constancy of the position of all these structures allows them to be used for orientation and navigation within the sacral subarachnoid space. The filum is covered by an envelope of transverse crossing fibers of connective tissue and pia mater, whilst nerve rootlets are covered by pia mater containing feeding vessels.

It is sometimes difficult to penetrate the dura mater because of its elasticity. At the penetration site the endoscope is inserted and its tip is advanced to face the anterior wall of the dura. At the level of the sacrovertebral angle the endoscope tip is ad-

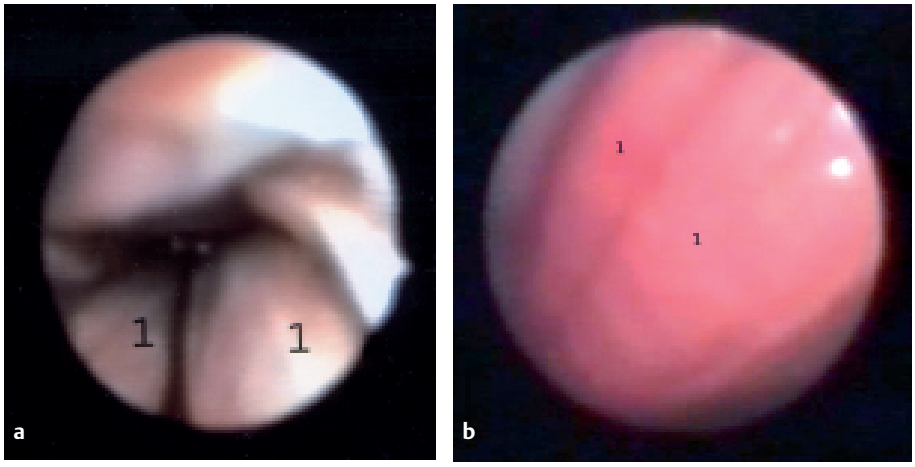

Fig. **3** Endoscopic view of the subarachnoid space; 1 = nerve rootlet.

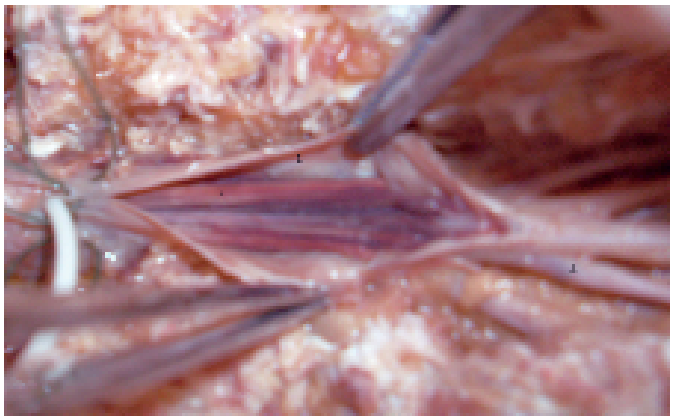

Fig. **4** Macroscopic view of the nerve rootlets; 1 = dura mater, 2 = nerve rootlet, 3 = nerve root.

vanced to the posterior wall of the dura. The endoscope should be inserted only 2 cm into the subarachnoid space. This may decrease the risk of the malpositioning.

Endoscopy through the sacral hiatus offers the neurosurgeon the possibility to perform epiduroscopy before thecaloscopy [5, 7 – 10]. In cases of high positioning of thecal sac apex, a laminectomy of the hypoplastic, according to the size of the lumbar vertebrae, first sacral laminae facilitates thecaloscopy. In cases of a narrow sacral extradural canal a possibility is the insertion of an endoscope of an even smaller diameter, only for inspection, diagnosis and probably prognosis of spinal diseases.

We have found transsacral intradural subarachnoid endoscopy to be an effective method for inspection of the lumbar subarachnoid space and a possible method for treating tethered cord syndrome in some instances, if the individual anatomy allows it. This success of thecaloscopy when coupled with a low morbidity rate adds a new technique to the armamentarium of the spine surgeon. As the learning curve for the procedure is difficult, we do recommend cadaver and other hands-on experience with thecaloscopic techniques before using it clinically.

The intraoperative use of fluoroscopy is necessary for the neurosurgeon to know exactly the height he is working on. Finally, the method requires attention and a very good knowledge of neuroanatomy.

Acknowledgements

We would like to express our gratitude to Univ.-Prof. M. Tschabitscher for the inspiration and his scientific support, and to G. Kazdaglis, M. D., for his laboratory assistance.

References

[1] Warnke JP, Tschabitscher M, Nobles A. Thecaloscopy: the endoscopy of the lumbar subarachnoid space, Part I: Historical review and own cadaver studies. Minim Invas Neurosurg 2001; 42: 61 – 64
[2] Warnke JP, Mourgela S, Tschabitscher M, Dzelzitis J. Thecaloscopy, Part II: Anatomical landmarks. Minim Invas Neurosurg 2001; 44: 181 – 185
[3] Warnke JP, Köppert H, Bensch-Schreiter B, Dzelzitis J, Tschabitscher M. Thecaloscopy, Part III: First clinical application. Minim Invas Neurosurg 2003; 46: 94 – 99
[4] Sacral and coccygeal nerves. In: Gray's Anatomy of the Human Body. Philadelphia: Lea & Febiger 1918
[5] Karakhan VB, Filimov BA, Grigoryan YA, Mitropolsky VB. Operative spinal endoscopy: stereotopography and surgical possibilities. Acta Neurochi Suppl (Wien) 1994; 61: 108 – 114
[6] Schütze G, Kurtze H. Percutaneous investigation of the epidural space using a flexible endoscope. A contribution to epiduroscopy. Reg Anesth 1993; 8 (1S): 24
[7] Jerosch J, Grönemeyer D, Gevargez A, Filler TJ, Peuker ET. Möglichkeiten der Spinaloskopie im Rahmen der minimal invasiven Intervention – eine experimentelle Untersuchung. Biomedizinische Technik 1999; 44: 243 – 246
[8] Ooi Y, Satoh Y, Sugawara S, Mikanagi K, Morisaki N. Myeloscopy. International Orthopaedics (SICOT) 1997; 21: 107 – 111
[9] Schütze G, Kurtze H. Direct observation of the epidural space with a flexible catheter-secured epiduroscopic unit. Regional Anesthesia 1994; 19: 85 – 89
[10] De Antoni DJ, Claro ML, Poehling GG, Hughes SS. Translaminar lumbar epidural endoscopy: Technique and clinical results. J Southern Orthop Assoc 1998; 7: 6 – 12

Selective Use of the Paraophthalmic Balloon Test Occlusion (BTO) to Identify a False-Negative Subset of the Cervical Carotid BTO

W. S. Lesley
B. K. Bieneman
H. J. Dalsania

Abstract

Background: The extracranial, internal carotid artery balloon test occlusion is helpful in predicting ischemic stroke resulting from operative occlusion of the internal carotid artery. However, balloon test occlusion is falsely negative in up to 20% of patients. With selected use of the paraophthalmic internal carotid artery balloon test occlusion, our group has identified a patient subset that developed ischemia resulting from supraclinoid internal carotid artery occlusion, in spite of passing the standard balloon test occlusion. **Methods:** Patient charts were reviewed for all balloon test occlusion referrals over a two-year period. Diagnostic angiography and standard cervical internal carotid artery balloon test occlusion were performed. The presence of retrograde ophthalmic blood flow was determined by angiography during cervical balloon test occlusion. Balloon test occlusion was then performed in those patients who both demonstrated retrograde ophthalmic blood flow during the cervical balloon test occlusion and those who were considered candidates for planned supraclinoid internal carotid artery sacrifice during skull base surgery. **Results:** Ten patients were referred for carotid balloon test occlusion. One patient who refused balloon test occlusion was excluded. Two patients (2/9 or 22%) failed the initial balloon test occlusion. Two of the seven remaining patients (and one who failed balloon test occlusion) demonstrated retrograde ophthalmic arterial flow during cervical balloon test occlusion. Of the patients who passed the initial balloon test occlusion, one failed paraophthalmic carotid artery balloon test occlusion. Surgical planning in one patient (1/7 or 14%) was significantly modified because of the results of the paraophthalmic carotid artery balloon test occlusion. **Conclusion:** Paraophthalmic internal carotid artery balloon test occlusion is indicated when planning supraclinoid internal carotid artery sacrifice in patients who demonstrate retrograde ophthalmic arterial flow during uneventful cervical carotid balloon test occlusion.

Key words

Balloon test occlusion · carotid · paraophthalmic

Abbreviations

BTO:	balloon test occlusion
CCA:	common carotid artery
ECA:	external carotid artery
ICA:	internal carotid artery
pBTO:	paraophthalmic internal carotid artery balloon test occlusion

Introduction

Endovascular cervical carotid artery balloon test occlusion (BTO) has been performed since 1964 when Serbinenko carried out the first procedure [1,2]. In recent years, BTO has become standard practice for the evaluation of collateral cerebral blood flow prior

Affiliation
Saint Louis University Health Sciences Center, Departments of Radiology and Surgery
Sections of Surgical Neuroradiology and Cerebrovascular Neurosurgery, St. Louis, MO, USA

Correspondence
Walter S. Lesley, M. D. · Scott & White Clinic · Scott, Sherwood and Brindley Foundation · The Texas A&M University System Health Science Center · Department of Radiology · Section of Surgical Neuroradiology · 2401 South 31st Street · Temple, Texas 76508 · USA · Tel.: +1/254/724-2412 · Fax: +1/254/724-0502 · E-mail: wlesley@swmail.sw.org

Bibliography
Minim Invas Neurosurg 2006; 49: 34–36 © Georg Thieme Verlag KG Stuttgart · New York
DOI 10.1055/s-2005-919149
ISSN 0946-7211

to planned carotid sacrifice during skull-base surgery. In effect, BTO attempts to predict the patient's ability to clinically tolerate the permanent loss of an internal carotid artery (ICA) [3,4]. Unfortunately, 12 – 20% of patients who pass the BTO will nevertheless incur delayed or immediate neurological deficits following ICA sacrifice [5,6]. By modifying the BTO so that the ophthalmic segment of the internal carotid artery (ICA) is temporarily occluded, elimination of the collateral ophthalmic arterial supply may unmask an unsuspected high-risk candidate for supraclinoid ICA ligation. Since, to the best of our knowledge, such a technique has not been specifically addressed in the peer-reviewed literature, we explored the utility, safety and technical aspects of performing paraophthalmic internal carotid artery balloon test (pBTO) in these patients.

Patients and Methods

This retrospective study was approved by the Saint Louis University Investigational Review Board. Patients referred for BTO were identified from the procedural database of the Surgical Neuroradiology Division at Saint Louis University. A detailed medical chart review was then obtained in those patients for whom supraclinoid ICA sacrifice was concurrently planned for either complex skull-base neoplasm resection or aneurysmal trapping.

Each patient was brought to the angiography suite after obtaining written, informed consent. Blood pressure, electrocardiogram, arterial oxygen saturation and respiratory rate were continuously monitored. Intravenous conscious sedation was not given so as to fully evaluate the patient's neurological status during BTO. Intravenous fentanyl citrate was administered as needed for analgesia. If not previously obtained, a transfemoral cerebral and cervical, digital subtraction angiogram was performed to evaluate the bilateral common, internal and external carotid vasculature.

A 6-French guiding catheter, which was continuously maintained to heparinized saline flush, was positioned within the mid-cervical common carotid artery. In addition to the standard 3000 units of intravenous heparin that were given at the start of the diagnostic angiogram, additional heparin aliquots (500 – 3000 units) were injected periodically throughout the BTO procedure in order to maintain an activating clotting time of 200 – 300 seconds. A 4.1- or 5-mm diameter, Endeavor balloon (Target Therapeutics, Fremont, CA) was advanced through the guiding catheter and into the mid-cervical ICA. Under fluoroscopy, the balloon was slowly inflated over 5 – 10 seconds with Isovue 300 contrast (Bracco Diagnostics, Inc., Princeton, NJ). With the balloon inflated, ICA occlusion was documented by control common carotid artery (CCA) angiography at 0, 10 and 20 minutes. The presence of retrograde filling of the ophthalmic artery with corresponding flow into the ophthalmic segment of the ICA was specifically sought during BTO. Neurological evaluation was completed by the Surgical Neuroradiology Service. The balloon was deflated after 20 minutes of BTO, or immediately before this time if clinical evidence of cerebral ischemia developed.

pBTO was performed if the patient exhibited clinical tolerance to the initial BTO, and if retrograde ophthalmic artery opacification was seen during BTO. In patients subjected to pBTO, the balloon was positioned within the ophthalmic segment of the ICA. This maneuver was facilitated by slightly inflating the balloon, which promotes flow-directed propagation during balloon positioning under fluoroscopy. With the ophthalmic artery origin covered by the balloon, the balloon was further inflated. Roadmap guidance ensured that inadvertent balloon over-inflation did not occur. Control CCA angiography and neurological testing were again performed for a maximum of 20 minutes as described with the initial BTO. A final control angiogram was obtained to exclude the presence of any balloon-related cervical or intracranial ICA trauma, or distal thromboembolism.

Results

A total of ten patients was referred for BTO. One patient refused BTO. Of the nine patients subjected to BTO, two (2/9 or 22%) clinically failed cervical BTO. Retrograde ophthalmic arterial flow was noted in one of these two patients, and in two of the remaining seven patients who passed BTO. Of the patients who passed cervical BTO, one (1/7 or 14%) failed pBTO at 6 minutes. Because of the demonstrated clinical intolerance to pBTO, this patient's surgical plan was changed to incorporate extracranial-to-intracranial arterial bypass with radial artery graft harvest in conjunction with skull base craniotomy (Fig. **1**). Overall, no bal-

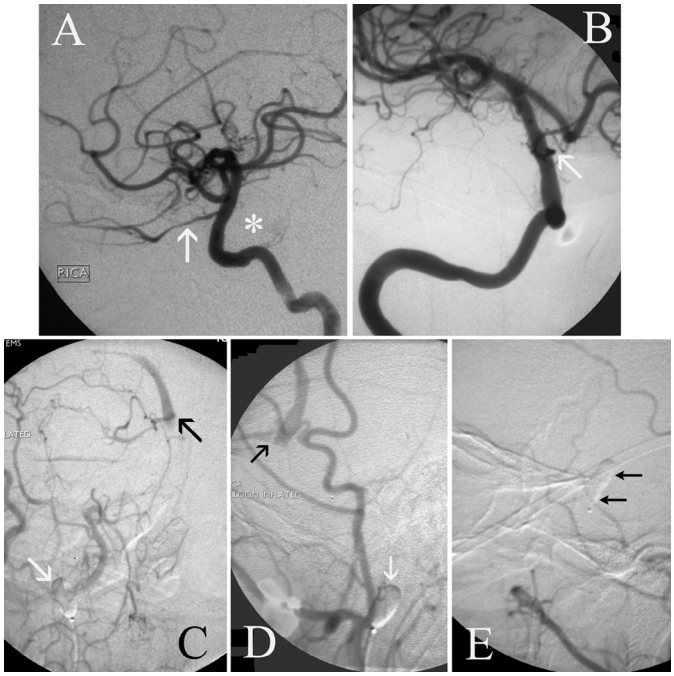

Fig. **1** Cervical and paraophthalmic ICA balloon test occlusion (BTO). Baseline lateral (**A**) and anterior oblique (**B**) right ICA angiogram demonstrates antegrade filling of the ophthalmic artery (arrow). Note the splaying of the ICA (asterisk) due to a cavernous sinus neoplasm. Anterior oblique (**C**) and lateral (**D**) right CCA angiogram during cervical ICA BTO confirms occlusion of the proximal ICA by the balloon (white arrow). The external carotid artery (ECA) branches are seen filling the ophthalmic artery which, in turn, supplies retrograde flow to the supraclinoid ICA (black arrow). Lateral view (**E**), right CCA angiogram demonstrates that with the balloon (arrows) positioned at the paraophthalmic segment of the ICA, the ECA collateral blood supply is eliminated.

loon occlusion-related death or permanent neurological deficit occurred in this series.

Discussion

Beginning in 1914, when Matas [7] preoperatively assessed patients for tolerance to carotid artery ligation through the simple means of manually compressing the cervical carotid artery, further refinements have ultimately led to the provocative BTO. Although both simple and sound in concept, the BTO nevertheless fails to predict stroke in as many as 1 in 5 patients subjected to ICA sacrifice. This unacceptably high, false-negative result has prompted numerous investigators to modify the BTO, either by challenging the patient's cerebrovascular reserve by pharmacologically-induced hypotension, or by seeking quantifiable predictors of carotid ligation outcome, including the measurement of cerebral perfusion with magnetic resonance imaging, xenon-computed tomography or single-photon emission computed tomography during BTO. These modifications will likely reduce, but not entirely eliminate, this adverse subset since following permanent ICA occlusion, thrombus can develop at the ICA stump with a resulting embolic shower downstream to a cerebral hemisphere already compromised by diminished blood flow [5].

To the unwary, the results of ICA BTO might not appear to be dependent upon a proximal or distal balloon placement as the ICA may mistakenly be thought of as a closed, isolated system. But because of several anastomotic connections between the external carotid artery and the vertebrobasilar system – especially the ophthalmic and posterior communicating arteries, intolerance to supraclinoid ICA sacrifice may not be recognized if these collaterals are not appropriately restricted during the BTO. In the sole cohort patient who passed the standard BTO while demonstrating retrograde ophthalmic blood flow, the additional challenge with pBTO clearly identified a critical collateral cerebral vascular supply. As a consequence, radial artery graft by-pass surgery was planned in conjunction with craniotomy and supraclinoid ICA ligation.

As observed from the outcomes of this series, three general rules emerge for carotid balloon test occlusion:

- the presence or absence of retrograde ophthalmic arterial flow during cervical BTO does not predict patient tolerance of cervical BTO;
- the presence of retrograde ophthalmic arterial flow during cervical BTO will not predict patient tolerance of pBTO;
- BTO should be performed at the exact site of the planned permanent vessel occlusion.

However, it should be emphasized that the theoretical risk of serious procedure-related complication is higher for pBTO because placement and inflation of a balloon within the intradural ICA subjects the patient to potential vessel rupture with subsequent morbidity or death. We therefore recommend that for patients with planned supraclinoid ICA occlusion, the cervical BTO be performed first, followed by pBTO if clinical tolerance and retrograde ophthalmic flow are observed during the initial BTO. Careful consideration should be given in determining the patient's ability to remain cooperative and motionless during pBTO.

Standard cervical BTO is not without risk. Mathis et al. [8] reported a 0.4% incidence of BTO-related permanent stroke and a 1.2% occurrence of carotid dissection. Although no complications were observed in our series, the continuous technological advancements in catheters, balloons and guidewires that have occurred since the previous reports are possibly the greatest factor for this improvement.

Conclusion

Paraophthalmic BTO is indicated to predict clinical tolerance to supraclinoid carotid sacrifice in all patients who pass cervical ICA BTO and in whom retrograde ophthalmic arterial flow is demonstrated during cervical ICA BTO.

History

Presented at the 6th Annual Joint Meeting, AANS/CNS/ASITN, Phoenix, AZ, 2003, USA.

References

[1] Serbinenko FA. Occlusion of the cavernous portion of the carotid artery with a balloon as a method of treating carotid-cavernous anastomosis. Vopr Neirokhir 1971; 35: 3 – 9
[2] Teitelbaum GP, Larsen DW, Zelman V et al. A tribute to Dr. Fedor A. Serbinenko, founder of endovascular neurosurgery. Neurosurgery 2000; 46: 462 – 469
[3] Ezura M, Takahashi A, Yoshimoto T. Combined intravascular parent artery and ophthalmic artery occlusion for giant aneurysms of the supraclinoid internal carotid artery. Surg Neurol 1997; 47: 360 – 363
[4] Russell E, Goldberg K, Oskin J et al. Ocular ischemic syndrome during carotid balloon occlusion testing. AJNR 1994; 15: 258 – 262
[5] Dare AO, Chaloupka JC, Putman CM et al. Failure of the hypotensive provocative test during temporary balloon test occlusion of the internal carotid artery to predict delayed hemodynamic ischemia after therapeutic carotid occlusion. Surg Neurol 1998; 50: 147 – 155
[6] McIvor NP, Willinsky RA, TerBrugge KG et al. Validity of test occlusion studies prior to internal carotid artery sacrifice. Head Neck 1994; 16: 11 – 16
[7] Matas R. Testing the efficiency of the collateral circulation as a preliminary to the occlusion of the great surgical arteries. JAMA 1914; 63: 1441 – 1447
[8] Mathis JM, Barr JD, Jungreis CA et al. Temporary balloon test occlusion of the internal carotid artery: experience in 500 cases. AJNR 1995; 16: 749 – 754

E. Gadelha Figueiredo
M. Castillo De La Cruz
N. Theodore
P. Deshmukh
M. C. Preul

Modified Cervical Laminoforaminotomy Based on Anatomic Landmarks Reduces Need for Bony Removal

Abstract

We describe a modified keyhole laminoforaminotomy (LF) using anatomic landmarks on the posterior aspect of the cervical vertebral body to decompress the intervertebral foramen with minimal bone removal. Twenty-four procedures were performed at C3 – 4, C4 – 5, and C5 – 6; 12 at C6 – 7; and 3 at C7 – TI. Facets and laminae structures were identified based on relative surgical perspectives. Bony resection was limited as follows: 1) inferior limit; inferior border of the superior facet; 2) superior limit, superior border of the superior facet; 3) lateral limit, a vertical line linking the junction of the lamina-facet to the lateral end of the superior limit; and 4) lateral aspect of the dural sac. Fluoroscopy was used to confirm that the intervertebral space was reached. The amount of bony removal was quantified for the superior and inferior laminae and facets. The length of the exposed nerve root was measured. The intervertebral foramen was exposed and the intervertebral disc reached in all specimens. Fluoroscopy showed that the center of the exposure remained at the same height with the intervertebral space. The mean length of the nerve root was 4.6 mm; the mean percentage of bony resection was 21.8 %, 7.5 %, 11.3 %, and 11.5 % for the superior and inferior laminae and facets, respectively. Opening the intervertebral foramen posteriorly consistently exposed sufficient nerve root length and allowed access to the intervertebral disc. The technique offers the most direct and safest method of decompressing the intervertebral foramen while minimizing bony resection. This simple surgical procedure may help reduce postoperative morbidity.

Key words

Cervical laminoforaminotomy · cervical pedicle · facet joint · surgical technique

A cervical laminoforaminotomy (LF) is indicated for radiculopathy related to osteoarthritic foraminal stenosis or a lateral soft disc herniation. The levels most frequently affected are C5 – 6, C6 – 7, C4 – 5 and C7 – TI [1]. Compared to anterior approaches, the LF has several advantages. No fusion is involved, and no morbidity is associated with retraction and dissection of the neurovisceral structures in the neck (e. g., tracheal edema, esophageal dysfunction, neurovascular complications). However, excessive bony removal of the facet joint and laminae can decrease segmental stability and increase scar formation [2, 3] and must be avoided.

Few anatomic studies have addressed the amount of bone removed in a posterior LF [2, 4]. Several authors have described their technique and offered technical points to perform a cervical LF [1, 5 – 15]. However, no anatomical landmarks have been described for a keyhole LF that can be used to provide the most direct and consistent route to the neural foramen and the disc while minimizing bony resection and preserving optimal function.

Affiliation
Division of Neurological Surgery, Barrow Neurological Institute, St. Joseph's Hospital and Medical Center, Phoenix, AZ, USA

Correspondence
Mark C. Preul, M. D. · Newsome Chairman of Neurosurgery Research · Barrow Neurological Institute · Division of Neurosurgery · St. Joseph's Hospital and Medical Center · 350 West Thomas Road · Phoenix, AZ 85013 · USA · Fax: +1/602/406-4153 · E-mail: mpreul@cox.net and mark.preul@chw.edu

Bibliography
Minim Invas Neurosurg 2006; 49: 37–42 © Georg Thieme Verlag KG Stuttgart · New York
DOI 10.1055/s-2006-932146
ISSN 0946-7211

We describe a technical modification of the keyhole LF based on anatomic landmarks in the posterior aspect of the cervical laminae. These landmarks can be used to limit bony resection as much as necessary without affecting the surgical exposure. The exposure of the nerve root and the amount of bone resected were quantified.

Materials and Methods

Twelve injected cadaver heads with necks were used to perform a modified keyhole LF on both sides of the cervical spine at C3 – 4, C4 – 5, C5 – 6, C6 – 7 and C7 – T1. The mean age of the specimens was 64.4 years (range: 54 to 68 years). The posterior aspects of the cervical spines were exposed completely, and the laminae and facet joints from C3 to the most distal level were dissected. The complete cervical spine was not available in every specimen; therefore, 24 procedures were performed at C3 – 4, C4 – 5, C5 – 6; 12 at C6 – 7; and 3 at C7 – T1. To avoid confusion, we considered all superior and inferior anatomic structures of a superior vertebra as superior and all superior and inferior structures of an inferior vertebra as inferior. Hence, instead of using anatomic nomenclature, we identified the facets and laminae based on their relative surgical perspectives.

The established anatomic limits of the modified LF were as follows: 1) inferior limit, inferior border of the superior facet; 2) superior limit, superior border of the superior facet; 3) lateral limit, a vertical line linking the junction of the lamina-facet to the lateral end of the superior limit; and 4) lateral aspect of the dural sac (Fig. **1**).

Using a standard surgical microscope, the junction between the lamina and the inferior border of the superior facet was drilled using a 3-mm diamond drill (Fig. **2a**). The drilling progressed superiorly to the superior border of the superior facet. This first stage of bony resection corresponded to the lateral limit of the LF (Fig. **2b**). At this point, part of the joint surface of the inferior facet was exposed.

The drilling progressed medially from the inferior border of the superior facet. As the bone was removed, the ligamentum flavum and the vertebral venous plexus became visible (Fig. **2c**). Removing portions of the ligamentum flavum exposed the dural sac. At this point the inferior and medial limits of the LF were delineated. The resection of the lamina progressed to the superior edge of the lateral limit. A straight line linking these points constitutes the superior limit of the bony resection. The joint surface of the superior facet included within these boundaries was also removed (Fig. **2d**).

This approach exposed the lateral aspect of the dural sac, a third to a half of the proximal intervertebral neural foramen, and a considerable portion of the nerve root. This exposure is sufficient to decompress the intervertebral foramen and to remove herniated soft disc. To remove a large or calcified disk herniation, it also may be necessary to remove a small portion of the laminae (Fig. **2e** and Fig. **2f**). Bony resection was limited to the lateral aspect of the superior border of the inferior lamina situated above the level of the inferior border of the superior facet, part of the lateral aspect of the superior lamina, a minimal amount of the superior facet, and the minimal portion of the inferior facet included within the boundaries of the exposure (Fig. **1**, Fig. **2d** and Fig. **3**).

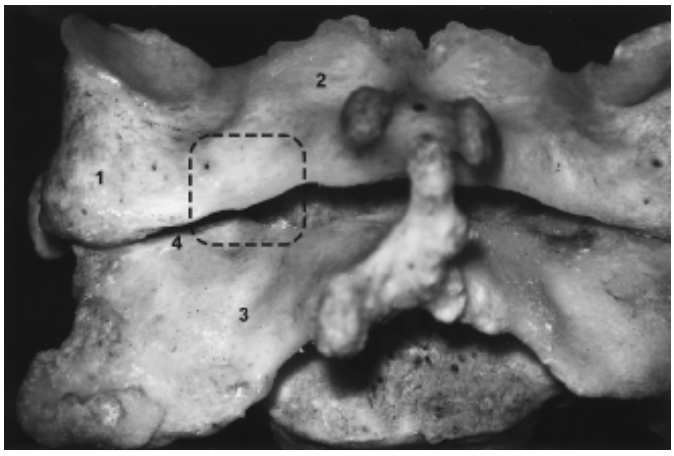

Fig. **1** Posterior aspect of the cervical vertebrae (C5 – 6). The delineated area represents the area of bony removal. The superior line is at the level of the superior border of the facet of the superior vertebra (superior facet); the inferior line is at the level of the inferior border of the superior facet; the lateral limit is a line passing the junction between the lamina and facet linking the superior and inferior limits. The medial limit is defined as when the lateral border of the dural sac is visualized; (1) superior facet, (2) superior lamina, (3) inferior lamina, and (4) inferior facet.

After the dissection was completed using the above landmarks, the disc space was localized under the surgical microscope. A 3.0-cm needle was introduced at every level studied. Lateral and posteroanterior fluoroscopy was used to confirm that the needles were in the disc and that the intervertebral space could be approached (Fig. **4a** and Fig. **4b**).

Quantification of bone removal

In six specimens, the area in the posterior aspect of the hemilaminae and facets in each level was measured with an electronic digital caliper (General Tools, New York, NY) to quantify the amount of bony resection. The areas of the superior and inferior hemilaminae and the areas of the inferior and superior facets were measured. Two points (superior and inferior) were selected at the medial edge of the laminae, one at the inferior junction of the lamina and facet and the other at the most lateral aspect of the lamina. These two points defined the medial boundary for calculating the area of the facets. Laterally, the rostral and caudal points constituted the lateral boundary. After resection, the amount of the bone removed from the posterior aspect of the hemilaminae and the facet joint was measured and calculated as a percentage of the total area. The middle point of the nerve root at its exit and at its distal exposure were considered to determine the length of nerve root that could be exposed.

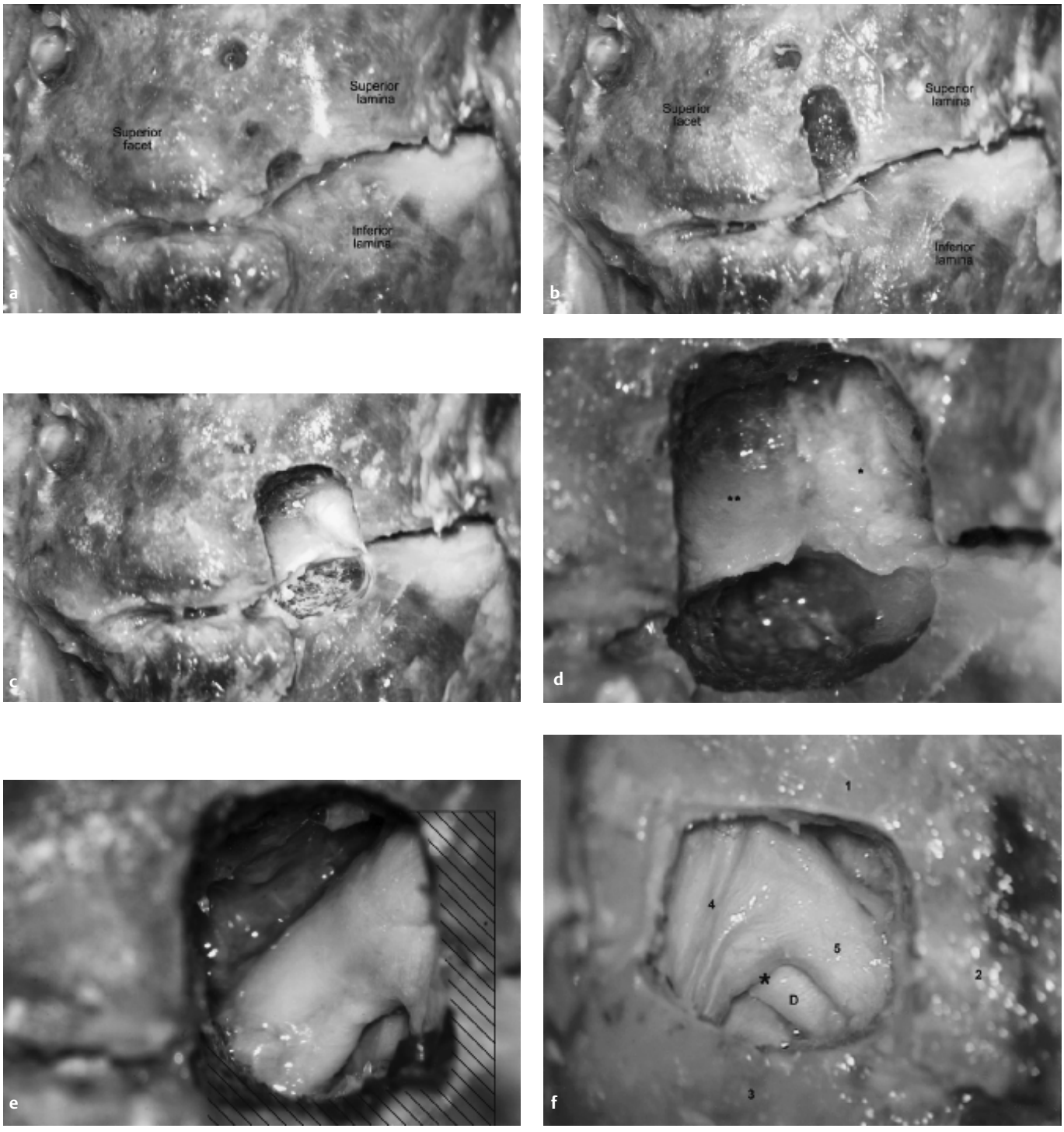

Fig. **2** Stepwise dissection of the cervical spine. **a** Drilling starts at the junction of the facet and lamina. **b** Bony removal progresses rostrally and ends at the level of the superior border of the facet. **c** The inferior limit corresponds to a horizontal line at the level of the inferior border of the superior facet. **d** In this magnified view, the ligamentum flavum is visible medially (*). The portion of the inferior facet that must be removed is included within the limits (**). **e** This exposure ensures decompression of the intervertebral foramen and is sufficient to remove a soft disc herniation. Additional bone may need to be removed from the inferior vertebra to dissect a calcified or large disc herniation (shaded area). **f** Final aspect of the modified laminoforaminotomy with additional bone removed from the laminae. The intervertebral foramen is opened, and the floor, roof, and nerve root are exposed; (1) superior lamina, (2) superior facet, (3) inferior lamina, (4) dural sac, (5) nerve root, (*) nerve root axilla, and (D) intervertebral disc.

Results

Using the modified LF with bony removal limited by the defined landmarks, we were able to expose the nerve root and to reach the posterolateral portion of the cervical disc in all specimens (Fig. **2e**, Fig. **2f**, Fig. **3a**, Fig. **3b**). Fluoroscopic control showed that the keyhole remained at the same height as the intervertebral space (Fig. **4a** and Fig. **4b**).

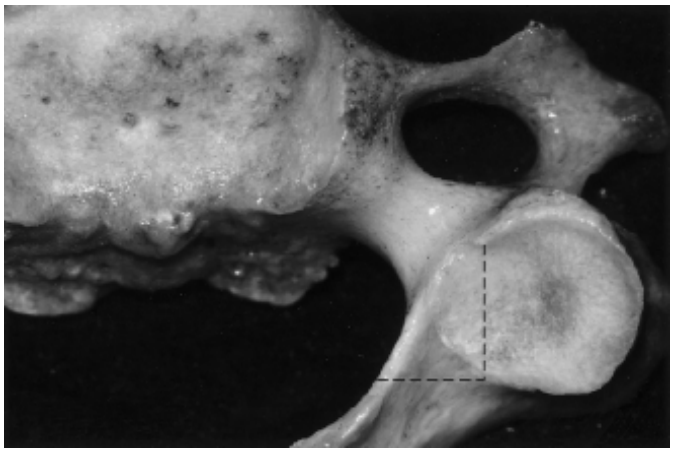

Fig. **3** Superior view of the cervical vertebra. The dotted line represents the bone removed from the inferior facet and lamina. One-half to two-thirds of the intervertebral foramen may be approached by using these landmarks.

Table **1** Length of nerve root exposed after a modified laminoforaminotomy

Cervical level	*Length of exposed nerve root [mm]*
C3 – C4	3.9 ± 0.5
C4 – C5	4.6 ± 0.4
C5 – C6	4.4 ± 0.3
C6 – C7	5.1 ± 0.5
C7 – T1	5.3 ± 0.7

The mean length of nerve root that could be exposed depended on the level (Table **1**), but averaged 4.6 mm. The roof, floor, and anterior wall of the intervertebral space could be exposed in all specimens, even with minimal bony resection.

Bony resection was limited to 21.8 % of the superior hemilamina, 7.5 % of the inferior hemilamina, and 11.3 % and 11.5 % of the superior and inferior facets, respectively (Table **2**).

Discussion

Lesions causing cervical radiculopathy have been approached through anterior and posterior approaches. During an anterior approach, dissection of visceral structures in the neck can cause surgical morbidity, such as lesions of the esophagus, trachea, carotid artery, and neurological deficits. When fusion is involved, problems with grafting and loss of motion of the fused segments can occur. For selected patients, a posterior approach offers a more benign course than an anterior discectomy with fusion. Shorter hospital stays, less operative time, lower costs, prevention of fusion, and preservation of functional mobility are noticeable advantages of the posterior route. Furthermore, the recent trend toward minimally invasive techniques and keyhole operations favors the LF [12]. However, excessive bony resection can reduce segmental stability and increase scar formation [2, 3].

The surgical technique used in earlier studies described exposure of the nerve root as the final objective. In this approach, which was popularized by Scoville et al. [10], a keyhole was placed to remove the medial portion of the facet and parts of the lamina above and below the nerve root. Bone was excised as needed to expose the foramen. However, no anatomic landmarks were included. Several authors have described their technical nuances,

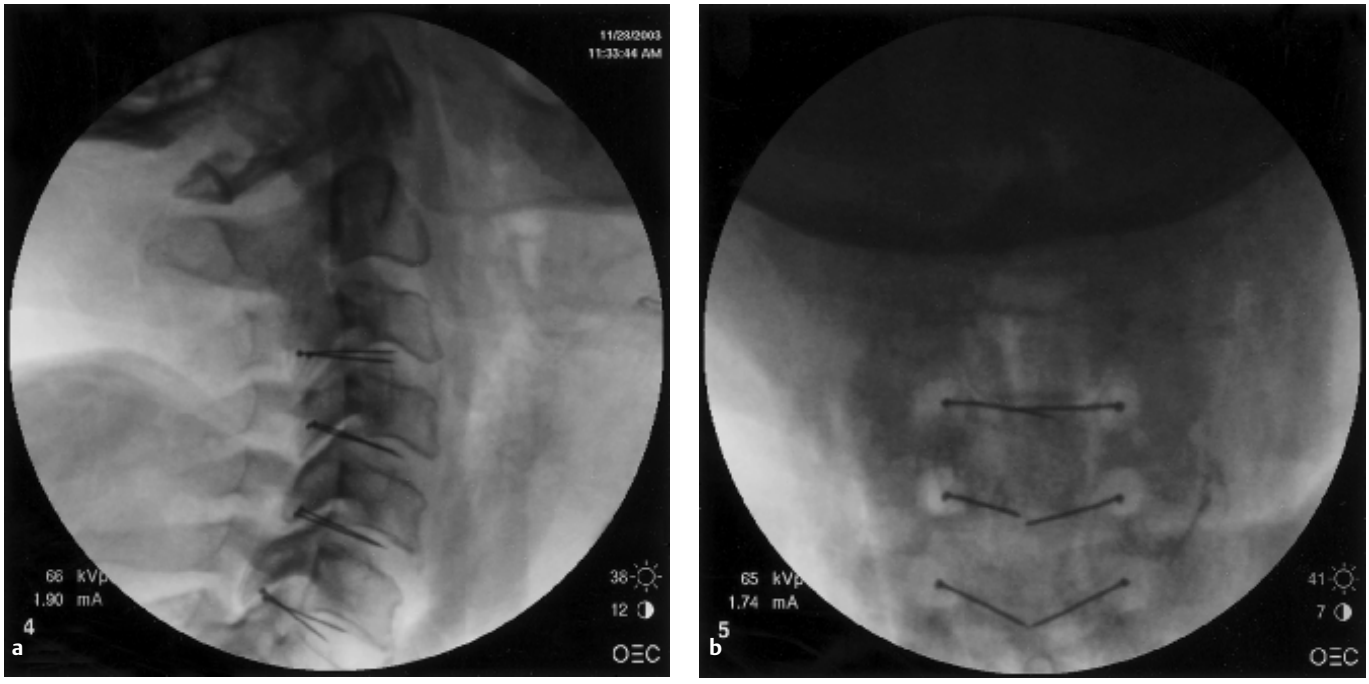

Fig. **4** **a** Lateral fluoroscopic view after a laminoforaminotomy (LF) of C3 – 4, C4 – 5, C5 – 6, and C6 – 7 has been performed on both sides. All pins are in the disc. **b** Posteroanterior fluoroscopic view of the cervical spine shows the keyhole LF on both sides and its relation to the intervertebral space. Each pin is in the disc.

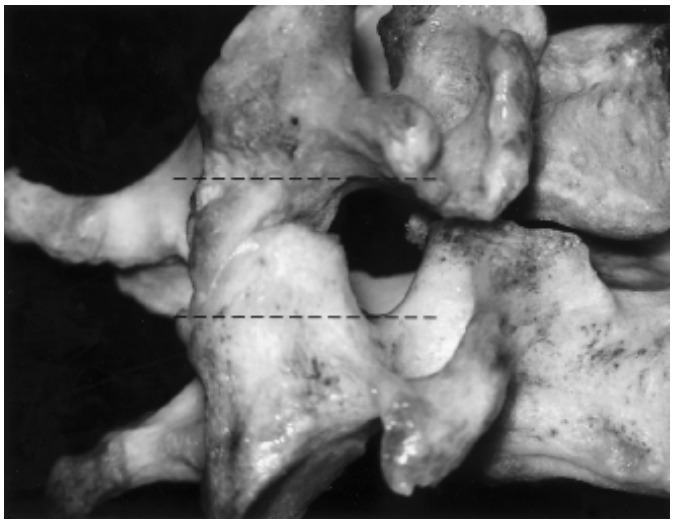

Fig. **5** Anterolateral view of the intervertebral foramen. The superior border of the pedicles projects toward the posterior surface of the vertebra at the level of the inferior border of the superior facet (upper line A). The inferior border of the pedicles projects posteriorly at the level of the superior border of the superior facet (lower line B). Bony resection beyond these limits does not improve the working space in the intervertebral foramen.

however no anatomic landmarks have been provided to limit the bony resection [1,2,5,6,8,9,11–15].

Although the amount of bony resection depends on the patient's anatomy and surgeon's experience, excessive bony resection of the facet joint must be avoided. Removal of more than 50% of the facet joint creates segmental hypermobility and instability [3,16].

Advanced technologies have changed the practice of neurosurgery. Contemporary microscopes, endoscopes, and newly designed surgical instruments make it possible to use small incisions with minimal retraction and tissue removal. In many clinical situations, minimally invasive surgical procedures have gained popularity compared to traditional procedures. However, to be minimally invasive while maintaining maximal effectiveness, these procedures should be based on consistent anatomic information. LF must guarantee minimal bony removal and concomitantly ensure consistent exposure of the neural foramen, disc space, and nerve root. Using the anatomic landmarks described here, we could reliably expose the related anatomy while limiting resection of bone. This technical modification may help surgeons to optimize the effectiveness of the keyhole LF and to reduce related surgical morbidity.

Anatomically, the intervertebral foramen is limited ventrally by the posterolateral aspect of the uncovertebral junction, intervertebral disc, and inferior portion of the supra-adjacent vertebra; inferior and superiorly by the respective pedicles; and posteriorly by the medial and anterior aspects of facet joints and by the adjacent part of the articular column [17,18].

In our study the inferior border of the superior facet was the inferior limit of the LF. The cervical pedicles project from the vertebral body anteromedially to posterolaterally and give rise to the superior and inferior articular processes. The superior border of the pedicles projects into the posterior aspect of the vertebra almost at the level of the inferior margin of the inferior facet (Fig. **5**). The inferior margin of the inferior facet is obscured by the inferior border of the superior facet. The inferior border of the pedicle also projects at the level of the superior border of the superior facet. By using these posterior points as landmarks to define the superior and inferior limits of bony resection, we could reach the floor and roof of the foramen and limit bony resection to what was strictly necessary.

The intervertebral foramen has a main medial-to-lateral axis that can be exposed laterally by removing a minimal portion of the medial aspect of the superior facet at the level of the junction facet and lamina. Resection of the inferior facet is limited only to the portion included in the limits of the exposure (Fig. **2d**). This procedure ensures adequate decompression of the intervertebral foramen and offers adequate access to remove a soft disc herniation. A large or calcified disc herniation may require further resection of the lamina. However, no additional bone has to be removed from the facets (Fig. **2e** and Fig. **2f**).

The tip of the uncinate process is higher than the superior border of the lamina, but it is lower than the superior border of the superior facet [4]. The superior border of the vertebral body remains at the midpoint between the superior and inferior borders of the superior facet (Fig. **4a** and Fig. **4b**). This anatomic relationship appears to hold constant even in patients with degenerative pathology including bony spurs, facet hypertrophy, and disc herniation, which some of our specimens displayed. Thus, besides providing surgical access to the floor, roof, and anterior wall of the intervertebral foramen, the center of this exposure is at the same level of the intervertebral space. Fluoroscopy confirmed the reliability of these landmarks for opening the foramen to obtain complete exposure of the nerve root and to reach the disc (Fig. **4a** and Fig. **4b**).

These landmarks could be used consistently to expose an adequate length of the nerve root to open the intervertebral foramen

Table **2** Area of bone removed after a modified laminoforaminotomy

Location	*Total area [mm2]*	*Area of modified laminoforaminotomy [mm2]*	*Bony removal [%]*
Superior hemivertebra	328.0 ± 35.7	71.78 ± 11.1	21.8
Inferior hemivertebra	346.2 ± 29.6	26.0 ± 3.2	7.5
Superior facet	103.8 ± 9.9	11.7 ± 1.5	11.3
Inferior facet	107.9 ± 9.1	12.4 ± 1.4	11.5

posteriorly and to reach the intervertebral disc. Concomitantly, the extent of the bony removal was limited to 21.8 % of the superior hemilamina, to 7.5 % of the inferior hemilamina, and to 11 % of the facets. This approach may be tailored on an individual basis. It offers the safest and most direct way to decompress the intervertebral foramen while minimizing bony resection. We believe this anatomic description contributes to an understanding of this procedure and may reduce the morbidity associated with cervical spine surgery.

References

[1] Henderson CM, Hennessy RG, Shuey Jr HM, Shackelford EG. Posterior-lateral foraminotomy as an exclusive operative technique for cervical radiculopathy: a review of 846 consecutively operated cases. Neurosurgery 1983; 13: 504 – 512

[2] Ebraheim NA, Xu R, Bhatti RA, Yeasting RA. The projection of the cervical disc and uncinate process on the posterior aspect of the cervical spine. Surg Neurol 1999; 51: 363 – 367

[3] Raynor RB, Pugh J, Shapiro I. Cervical facetectomy and its effect on spine strength. J Neurosurg 1985; 63: 278 – 282

[4] Raynor RB. Anterior or posterior approach to the cervical spine: an anatomical and radiographic evaluation and comparison. Neurosurgery 1983; 12: 7 – 13

[5] Aldrich F. Posterolateral microdiscectomy for cervical monoradiculopathy caused by posterolateral soft cervical disc sequestration. J Neurosurg 1990; 72: 370 – 377

[6] Ducker TB, Zeidman SM. The posterior operative approach for cervical radiculopathy. Neurosurg Clin N Am 1993; 4: 61 – 74

[7] Epstein NE. A review of laminoforaminotomy for the management of lateral and foraminal cervical disc herniations or spurs. Surg Neurol 2002; 57: 226 – 233

[8] Rock JP, Ausman JI. The use of the operating microscope for cervical foraminotomy. Spine 1991; 16: 1381 – 1383

[9] Rodrigues MA, Hanel RA, Prevedello DM, Antoniuk A, Araujo JC. Posterior approach for soft cervical disc herniation: a neglected technique? Surg Neurol 2001; 55: 17 – 22

[10] Scoville WB, Dohrmann GJ, Corkill G. Late results of cervical disc surgery. J Neurosurg 1976; 45: 203 – 210

[11] Tomaras CR, Blacklock JB, Parker WD, Harper RL. Outpatient surgical treatment of cervical radiculopathy. J Neurosurg 1997; 87: 41 – 43

[12] Witzmann A, Hejazi N, Krasznai L. Posterior cervical foraminotomy. A follow-up study of 67 surgically treated patients with compressive radiculopathy. Neurosurg Rev 2000; 23: 213 – 217

[13] Woertgen C, Holzschuh M, Rothoerl RD, Haeusler E, Brawanski A. Prognostic factors of posterior cervical disc surgery: a prospective, consecutive study of 54 patients. Neurosurgery 1997; 40: 724 – 728

[14] Fager CA. Management of cervical disc lesions and spondylosis by posterior approaches. Clin Neurosurg 1977; 24: 488 – 507

[15] Harrop JS, Silva MT, Sharan AD, Dante SJ, Simeone FA. Cervicothoracic radiculopathy treated using posterior cervical foraminotomy/discectomy. J Neurosurg Spine 2003; 98: 131 – 136

[16] Cusick JF, Yoganandan N, Pintar F, Myklebust J, Hussain H. Biomechanics of cervical spine facetectomy and fixation techniques. Spine 1988; 13: 808 – 812

[17] Tanaka N, Fujimoto Y, An HS, Ikuta Y, Yasuda M. The anatomic relation among the nerve roots, intervertebral foramina, and intervertebral discs of the cervical spine. Spine 2000; 25: 286 – 291

[18] Xu R, Kang A, Ebraheim NA, Yeasting RA. Anatomic relation between the cervical pedicle and the adjacent neural structures. Spine 1999; 24: 451 – 454

Y.-G. Jiang
J. Xiang
F. Wen
L.-Y. Zhang

Microsurgical Excision of the Large or Giant Cerebellopontine Angle Meningioma

Abstract

Objective: The object of this study was to analysis the therapeutic effects of microsurgical excision in cases with the large or giant cerebellopontine angle meningioma. **Methods:** We retrospectively analyzed the 56 patients who suffered from the large or giant cerebellopontine angle meningioma and underwent the microsurgical therapy, for which the suboccipital-retrosigmoidal approach was adopted in 38 cases, the temporal-occipital craniotomy, presigmoidal approach in 6 cases, the temporal-occipital craniotomy, inferotemporal tentorium cerebelli approach in 8 cases, and the temporal-occipital craniotomy, supratentorial or infratentorial allied approach in 4 cases. **Results:** The tumors of 44 cases were all resected (Simpson I, II), with a total resection rate of 78.6%, and there was no operative mortality. After surgery, symptoms improved in 40 cases and remained unchanged in 10 cases. Among 54 cases, recrudescence was seen in 2 cases (3.7%) and being able to take care of themselves in 50 cases (92.6%) at 6 months through 6 years follow-up after surgery. **Conclusion:** A rationally selected surgical approach, a microscopic technology applied in the operation to appropriately treat and protect vein, nerve and brain stem, which can ideally excise the tumors, together can increase the survival ability of patients.

Key words

Cerebellopontine angle (CPA) · meningioma · microsurgery · effect

CPA meningioma accounts nearly for 6–8% [1] of the whole encephalic meningiomas, and for 40–50% [2] of meningiomas of the posterior cranial fossa. Most of the tumor fundus is attached on the endocranium of the inferior-petrosal-sinuous and sigmoid sinus, adjacent to the jugular foramen, always being hemispheric, tuberculous or lobulated shaped, sometimes taking on a compressed shape. Because of its deep location, the narrow visual field of operation and the proximity of post-cranial nerves, brain stem and important blood vessels, the operation for this pathology has a high lethal and crippled rate [1–6]. The tumor grows slowly, has a chronic disease history and its inchoate symptom is not clear. When an obvious symptom occurs, the tumor has usually formed a large or giant CPA meningioma. It adheres closely to its surrounding tissues, so it is still a difficulty of neurosurgery to remove the tumor while preserving its surrounding nerves and important blood vessels as much as possible [1,4–7]. We have succeeded in removing large or giant CPA meningiomas in 56 cases from January 1998 to December 2004, without any operative mortality. Now we have analyzed our results as described in the following.

Patients and Methods

General information

Written, informed content was obtained from each patient in the group. We included 56 patients suffering from CPA large or giant meningiomas in this group, accounting for 10.8% (56/520) of encephalic meningiomas in the corresponding period, for 35.0% (56/160) of meningiomas of the posterior cranial fossa, and for

Affiliation
Department of Neurosurgery, The Second Xiangya Hospital of Central South University, Changsha, Hunan Province, P.R. China

Correspondence
Yu-Gang Jiang, M. D. · Department of Neurosurgery · The Second Xiangya Hospital of Central South University · 86# Renming Road · Changsha · Hunan Province 410011 · People's Republic of China · Tel.: +86/731/552-4222 ext 2238 · E-mail: 13707315567@hnmcc.com

Bibliography
Minim Invas Neurosurg 2006; 49: 43–48 © Georg Thieme Verlag KG Stuttgart · New York
DOI 10.1055/s-2005-919151
ISSN 0946-7211

56.0% (56/100) of CPA meningiomas; there were 18 male patients and 38 female patients. Their ages ranged from 14 to 62 years, with an average age of 41.5 years. The course of disease was from 3 months to 8 years, with an average of 2.2 years. Types of tumors [3]: giant type in 24 cases (diameter ≥ cm), large type in 32 cases (diameter < 7 cm, > 4.5 cm).

Clinical presentation: There are different degrees of intracranial hypertension, following with symptoms such as post-cranial nerve injury, compressed brain stem and cerebella physical signs. Among them, intracranical symptoms such as headache, vomiting, and papilledema were seen in 56 cases, trigeminal neuralgia in 6 cases, facial numbness in 24 cases, facial paralysis in 12 cases, abducent nerve paralysis in 4 cases, tinnitus and hypoacusis in 30 cases, drinking choke and anarthria in 12 cases, vertigo in 18 cases, unsteady walk and ataxia in 24 cases, unilateral limb weak in 12 cases, hemidisturbance of sensation in 8 cases.

Iconography examination: Cerebral CT and MRI have been carried out on 56 patients. CT scanning result showed a nodal or foliaceous equidensity or slightly high-density block image with calcification for CPA meningioma in 14 cases and arachnoid cyst besides meningioma in 8 cases. The bony "window" position showed petrous bone damage and hyperosteogeny in 14 cases. Only one case was found with internal auditory artery enlarging. After contrast agent injection, the focus was reinforced evenly and its boundary was clear. MRI scanning showed that the tumor is characterized by iso-T_1 or longer T_1, and iso-T_2 or longer T_2. After intensifying, most are evenly reinforced, and the tumor extensively adheres to the putamen of the retro-petrous pyramid surface. Visible flowing-void images were shown in 50 cases, dural tail sign in 26 cases and low-signal ring edema belt around the tumor in 30 cases. CT and MRI showed that there were different degrees of hydrocephalus and compressed brain stem and cerebella in 56 cases, four ventricles were pressed to narrow and deformed to displaced in 40 cases, tumor was found in the CPA in 20 cases, in the CPA-slope in 26 cases, in the CPA-slope-opposite CPA in 6 cases, and CPA and slope up to the sella turcica and parasella in 4 cases. There were 8 cases for total cerebral angiography, showing that the tumor was supplied by the internal carotid artery and vertebral basilar artery and different blood vessel replacements such as the arteria cerebelli inferior anterior, the posterior inferior cerebellar artery, the superior artery of the cerebellum and the labyrinthine artery.

Operative methods

For this group of cases we always adopted microsurgery to remove the tumor, with the suboccipital-retrosigmoidal approach in 38 cases, of which the tumor was only in the CPA in 20 cases, mainly in the CPA but involving the clivus ossis sphenoidalis in 12 cases, and with the tumor in CPA involving the clivus ossis sphenoidalis to the opposite CPA in 6 cases. The subtemporal-presigmoidal approach was adopted in 6 cases, in which the tumor lies in the CPA, mainly involving in middle-bottom clivus ossis sphenoidalis. There were 8 cases for the temporal-occipital craniotomy, presigmoidal approach, in which the tumor was in the CPA mainly involving the clivus ossis sphenoidalis in 6 cases. In 2 cases, the tumor is in the saddle area of the clivus ossis sphenoidalis of the CPA. In addition, there are four patients whose tumors were quite huge, spanning the supratentorial region and connecting with the saddle area and the metasellar of the clivus ossis sphenoidalis of the CPA, so that a temporal-occipital craniotomy with supratentorial or infratentorial allied approach was adopted. According to MRI results prior to surgery (Fig. **1**), we made suitable bony "windows" and performed the ventricle puncture to release the cerebrospinal fluid. If necessary, with rapidly intravenous injection of 20% mannitol (250 mL), and to excise the dura mater after the intracranial pressure was reduced. We opened the cisterna cerebellomedullaris and cerebellopontine pool to further reduce the intracranial pressure. When cutting the tentorium of the cerebellum, we protected the IV and VI cranial nerves from damage. It was quite difficult to expose the tumor pedicel because the tumor is large; therefore we first cut the large interior-tumor block. After the tumor has been diminished, the tumor wall caves in and the blood vessel of tumor pedicel is exposed, we then stopped the blood supply to the tumor. In principle, we first stop the arterial blood supply to the tumor and then deal with the drainage vein and any blood supply artery around the tumor should be preserved as much as possible, and do our best to reduce or protect the VII-XII cerebral nerves from damage. The tumor nidus penetrating into Meckel's bursa and petrosal sinus or side sinus should be cut in order to reduce the recrudescence. After removal of the tumor, it is necessary to cut the affected endocranium and to get rid of the affected bone so as to guarantee a Simpson I and II resection standard (Figs. **2** and **3**).

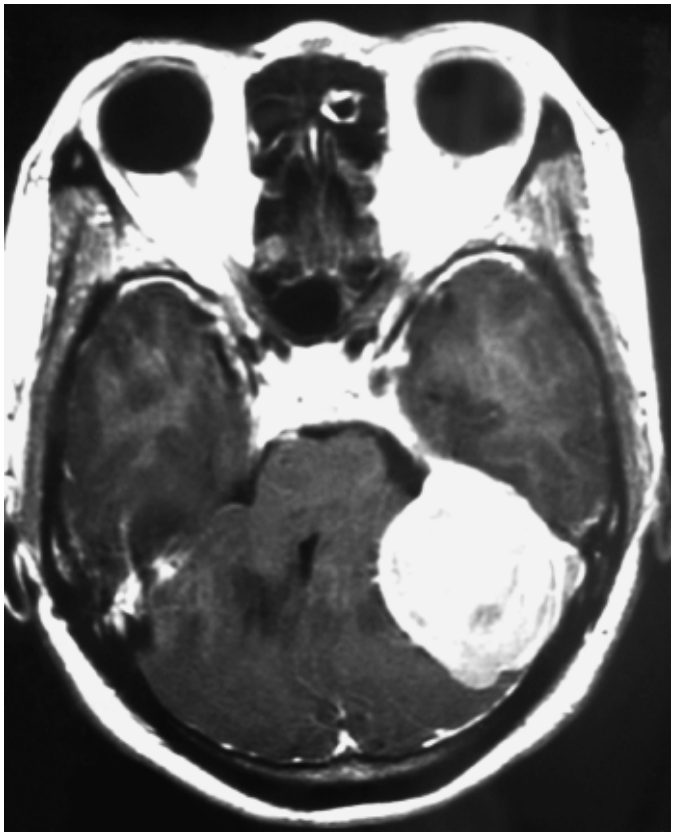

Fig. **1** Before surgery for CPA meningioma. MRI scan of CPA meningioma: the tumor is characterized by iso-T_1 or longer T_1, and iso-T_2 or longer T_2. After intensifying, most are evenly reinforced, and the tumor extensively adheres to the putamen of the retro-petrous pyramid surface. There are different degrees of compressed brain stem and cerebella, the ventricles are pressed to narrow and deformed due to displacement.

Fig. **2** One week after surgery for CPA meningioma. MRI scan displayed that the tumor was excised completely after surgery.

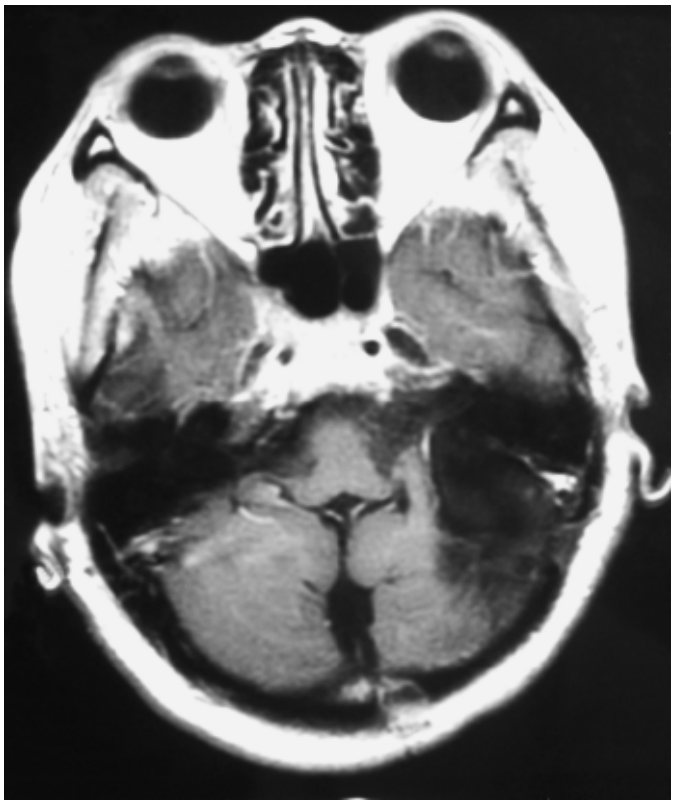

Fig. **3** One year after surgery for CPA meningioma. MRI re-examination displayed no recrudescence.

Results

The type of tumor pathology (Fig. **4**) was fibroblastic in 26 cases (46.5%), syncytial in 16 cases (29.3%), psammomatous in 10 cases (17.9%), angioblastoma in 2 cases (3.6%) and compound type in 2 cases (3.6%). Complete excision of the tumor (Simpson I and II) in was achieved in 44 cases (78.6%) (Figs. **1 – 3**) and partial excision in 12 cases (21.4%), without any operative mortality. Facial nerve function was preserved in 38 cases (67.9%) (House-Brackmann I and II) and hearing was preserved in 36 cases (64.3%).

After surgery, the symptoms improved in 40 cases (71.4%), remained unchanged in 10 cases (17.9%), and were aggravated in 6 cases (10.7%). After operation, lung infections arose in 6 cases, which have been cured through tracheotomy, anti-infection therapy, improving discharge of phlegm, and so on. Bleeding in the upper digestive tract occurred in 4 cases, which have been cured through hemostasia, inhibition of gastric acid and protecting the stomach, leakage of cerebrospinal fluid was seen in 2 cases, which have been cured through lumbar puncture and catheter placement, local puncture, pressure dressing and anti-infection therapy. Bilateral transverse sinus thrombosis was observed in 1 case, which was cured after one week through anticoagulation and dilating the blood vessels. Swallowing difficulty and hoarseness and other symptoms of post-cranial injuries were noted in 4 cases after surgery, in 2 cases the above symptoms disappeared in half a month post-surgery and in the other 2 cases in 3 months. Coma and hemiplegia developed in 1 patient, in whom consciousness was recovered 15 days later and hemiplegia also recovered half a year later. The duration of the follow-up survey for 56 patients is from 6 months to 6 years, with an average follow-up period of 3.5 years. 2 patients died in the meantime due to other diseases. Among the 54 cases, 26 patients (48.2%) basically recovered and are engaged in work (including light jobs), 24 patients (44.4%) are basically able to con-

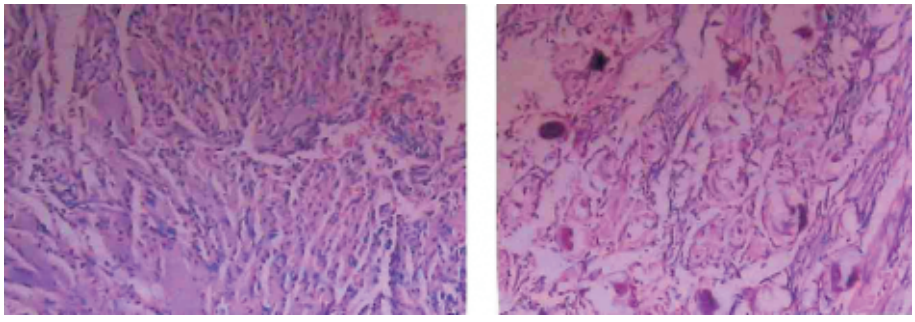

Fig. **4** Pathological diagnosis of the tumor. Pathologic examination of the tumor identified it as a psammomatous meningioma.

tinue their own living and 4 patients (7.4%) still cannot handle their own living. There are two recrudescent cases (3.7%), who are the patients with partial tumor removal and their recrudescent times are 1.5 and 2.6 years, respectively. But there appears to be no recrudescent phenomenon after repeated operative therapy. The symptom comparison of 54 patients before surgery and after surgery is shown in Table **1**.

Discussion

CPA meningioma has a rich blood supply and a bigger volume and is connected closely to the brain stem, cranial nerves and important blood vessels; as a result, it is quite difficult to remove it and the removal rate is about 48.3 – 82% [4,5]. The main reasons for a poor treatment result are the unsuitable selection of the approaches, poor exposure and injury to important blood vessels, nerves and brain stem. The removal rate for large and giant CPA meningiomas is even lower. The application of microsurgical technology in our hospital has dramatically improved the curative effect for diseases of this kind.

Operative approach

Before operation, the iconography examination is of a crucial significance to select the operative approach. According to the tumor's location and growing orientation, blood supply and its size, we can fully expose the tumor, while avoiding damaging the brain stem, cranial nerves and sinus venosus, which is the basic principle to select the operative approach [8]. Our group mainly adopts the following four operative approaches.

1) Suboccipital-retrosigmoidal approach: The advantage is that it is closely adjacent to the CPA area, with full exposure and small trauma. For those who have suffered from tumor just in the CPA or mainly in the CPA but involving in the clivus ossis sphenoidalis, this approach can achieve the objective to wholly remove the tumor. There are reports [6] that, by adopting the suboccipital-retrosigmoidal approach, the cutting path to remove the tumor is shorter and the exposure performance is quite good, so we can orthoptically preserve the important nerves and blood vessels around the tumor. It should be applied first of all. The majority of our patient group (67.9%) was treated with this approach, which has achieved a good effect, that is, the vast majority of tumors has been wholly excised or sub-excised. With dissociating interior or inferior tumors, the facial and auditory nerves, post-cranial nerves and posterior inferior cerebella artery should be protected from injury. Also, with dissociating upper tumors, the trigeminal nerve, anterior inferior cerebella artery and superior artery of cerebellum should be protected from injury. Due to the huge size of the tumor, the facial nerve is usually pressed and becomes thinner or turns to a white membrane that adheres to the arachnoid and is relatively difficult to identify. So when dissociating the surrounding tissues of the tumor, we use electrical coagulation as little as possible so as to avoid damage to the tissues around the tumor. If possible, neuroelectrical physiology monitoring can be carried out. As for the 6 cases with extension into the opposite side of the CPA, we adopt the endoscope-assisted microneurosurgery technology (EAM), which is relatively efficient to expose and remove the tumor and avoids severe traction of the brain stem. In the case of operating on the tumor adjacent to the side brain stem, we pay attention to the protection of perforators. In addition to blocking the blood-supplying artery to the tumor, other perforators should be protected as much as possible, so as to prevent secondary ischemic damage.

2) Temporal-occipital craniotomy, presigmoidal approach: This is applicable to those patients whose tumor fundus is in the CPA and petrosal peak, growing towards the middle/inferior clivus and middle cranial fossa. According to the operative practice of our group, this approach can effectively expose the base of the middle cranial fossa and middle/inferior clivus, so as to shorten the distance to the clivus. At the moment, we cut off the blood supply to the tumor as early as possible. If the petrosal bone is eroded, we can use a grinding drill to partially grind the petrosal bone. However, this approach has the disadvantage of big trauma. Therefore, we try our best to utilize the cistern to release the cerebrospinal fluid. In the case of lifting slightly the temporal lobe, the height between the temporal lobe and basis cranii shall be no more than 1 – 1.5 cm, so as to minimize the damage to temporal lobe and cerebellum. When uplifting the upper tumor, we guard against vein damage to the superior petrosal sinus and the inferior petrosal sinus. There were 2 cases of massive hemorrhage due to vein rupture during our operation, but it has been stanched with isinglass sponge via electrical coagulation. A leakage of the cerebrospinal fluid occurred in 2 cases that may be related with looseness of the bone wax sealed in the mastoid air cells, which has been cured by lumbar puncture and catheter placement, local puncture, pressure dressing and anti-infection. In addition, the transverse sinus thrombosis shall be considered seriously after surgery. Bilateral transverse sinus thrombosis can lead to intracranial hypertension symptoms. If necessary, a magnetic resonance venography (MRV) examination should be performed for its diagnosis [9]. Bilateral transverse sinus thrombosis has occurred in one case of this group, which has been cured by anti-coagulation and blood vessel dilatation, and so on.

3) Temporal-occipital craniotomy, inferotemporal tentorium cerebelli approach: this approach can fully expose the upper clivus, saddle area and petrosal region and tentorium of cerebellum, we can expand towards the middle slope via grinding the

Table **1** Symptom comparison of 54 patients before and after surgery

	Headache	*Trigminal neuralgia*	*Facial numbness*	*Facial paralysis*	*Tinnitus*	*Hearing loss (unilateral)*	*Drinking choke*	*Unsteady walk*	*Weakness of unilateral limbs*	*Hemi-disturbance of sensation*
before	52	6	24	12	30	30	12	24	12	8
after	20	2	16	18	20	20	4	14	2	2

petrosal bone. By this approach, the tentorium of the cerebellum is excised after releasing the cerebrospinal fluid, so as to directly block the blood supply from meninges and reduce bleeding in the operation. But it is necessary to protect the IV and VI cranial nerves from damage when excising the tentorium of the cerebellum. By cutting the tentorium of the cerebellum along 1 cm behind the superior petrosal sinus paralleling with the superior petrosal sinus until the tentorium edge, we can see the displaced trochlear nerve. During the operation, we can see that the Labbe vein flows into the transverse sinus. When uplifting the temporal lobe, we protect it in order to avoid cerebral edema after operation, especially aphasia due to its left-sided injury. This approach was applied to 8 cases in this group, whose tumors are totally removed, without III, IV and VI cranial nerve damage and Labbe vein injury, and they all recovered well. But its disadvantage is that we cannot reach the inferior clivus.

4) Temporal-occipital craniotomy, supratentorial or infratentorial allied approach: This approach removes $^{2}/_{3}$ of the posterior mastoid, and Trautmann triangle bone of the petrosal fundus, wholly separating the transverse sinus and the sigmoid sinus, cutting off the tentorium of the cerebellum. It integrates the supra- and infratentorium and shortens the operation path. Also, the whole tumor, either its interior and exterior or its top and bottom, and the facial nerve, trigeminal nerve, post-cranial nerves and brain stem can all be seen clearly. Four cases of giant CPA meningiomas spanning the whole cerebral tentorium and widely involving in the saddle area and metasellar of clivus ossis sphenoidalis of the CPA were treated with this approach. The approach shows the tumor even more clearly. The tumors are excised wholly and the procedure is performed to preserve the facial nerve. However, this approach needs a long time to perform the operation, with a great deal of bleeding and it has a relatively large injury. Also, all cranial nerves (III – XII) may be damaged. In our group two cases were operated on by adopting this approach and the posterior cranial nerve was damaged, characterized by difficult swallowing and hoarseness, which basically recovered 3 months later.

Microsurgical skills

1) Treatment of blood vessels: It is reported that bleeding after surgery is the main complication of the CPA meningioma [4], therefore it is very important to appropriately deal with the blood vessels. Our experience is as follows: 1) before operation, we determine in detail, via cerebral angiography or MRA examination, whether important blood vessels such as arteria cerebelli inferior anterior, posterior inferior cerebellar artery, superior artery of cerebellum and labyrinthine artery, basilar artery and its branch are displaced or not and the direction and distance of displacement [10]. 2) We apply microsurgical technology to detach the tumor membrane and arachnoid mater. In two cases, the imaging showed that the tumor embraced the arteria cerebelli inferior anterior and in the other two cases, it embraced the posterior inferior cerebellar artery, however, we could still find the interface between blood vessel and tumor to protect the blood vessel. It is reported in the literature that it is quite hard to find the interface of this kind in compressed meningioma [11], so we should avoid unfavorable trauma to blood vessels when removing the tumor concerned. 3) We should not cut off the blood vessel until guaranteeing that it is the vessel supplying blood to the tumor. As performing the operation, we use an electrical coagulation method to excise the vessel at a position near the tumor, so as to avoid damaging the perforators in the brain stem and cranial nerve. 4) Care should be taken not to cut off the blood vessels with a bigger caliber in order to avoid damaging the anterior inferior cerebella artery, posterior inferior cerebella artery or upper cerebella artery and so on. If these blood vessels are really embraced in the tumor concerned, we shall be patient when detaching them. If it is quite difficult to dissociate them due to a close adhesiveness, we can preserve a lamella tumor that will be cured by radioactive therapy and the like. 5) As for the petrosal vein that is shut out the line of sight and affected by the operation, we apply the electric coagulation method to block the vein so as to avoid bleeding after vein avulsion. There was no ataxia in 15 cases after the petrosal vein had been cut off in the operation.

2) Protection of cranial nerves: The protection of cranial nerves is also an important factor influencing the operative result [12]. The cranial nerves around the tumor usually cannot be recognized by the naked eye due to compression by the tumor, displacement, transmutation and denaturalization. During the operation, the white membrane on the tumor surface is usually the compressed cerebral nerve, so we shall by all means avoid rashly cauterizing or cutting it off; on the contrary, it should be tracked down and identified along its course. After identifying the cranial nerve, we can cut the arachnoid open along its long axes and separate the cranial nerve. And then use a micro-absorber to absorb the fluid with cotton slip and pad the cotton slip between tumor wall and cranial nerve, so as to protect the blood-supplying artery from damage that may cause the ischemic cranial nerve injury. In this group, there were two cases of posterior cranial nerve injury after surgery, which may be related to electrically cauterizing the tumor walls around the cranial nerve and damaging small perforators with nerve. The nerve function gradually recovered half a month later by applying nimodipine to improve the microcirculation. As for the 12 patients who suffered from severe posterior cranial nerve injury before operation, we carry out the plan of "early cut, early pull", that is, we did a tracheotomy and inserted nasal cannula for nasal feeding at the early stage after surgery. After improvement and recovery of the cough reflex, we pull out the trachea cannula. The patient recovers well. The preservation of facial and auditory nerves is an important factor to evaluate the operative effect [13]. We apply the facial or auditory nerve stimulation instrument to supervise the facial and auditory nerves. We gradually converge contralaterally through the interior auditory canal side retrograde or from the brain stem side by conduction, and gradually separate the facial nerves from the auditory nerves during the course of peeling off the tumor concerned. However, to anatomically preserve the facial or auditory nerves does not mean the preservation of their function after surgery. In this group of cases, we always anatomically preserved the facial or auditory nerves, but there were still 32.1 % of patients whose facial nerve function and 35.7 % whose auditory nerve functions have been damaged after surgery. We think it may be related to long-term compression of the huge tumor leading to an insufficiency of the nerve's blood supply, denaturalization and necrosis, as well as to severing of its blood-supplying artery.

3) Protection of the brain stem: A distinct characteristic of large or giant CPA meningioma is that it jostles and adheres to the brain stem [4,14]. There were 38 patients whose brain stems have been deformed distinctly as seen on CT and MRI examinations in this group. With reference to the literature [6,15], we think that we can assess the damage to the brain stem and cranial nerves and the tumor's blood supply via systematic examination of the nerves, neuroiconography and brainstem evoked potentials, which are beneficial to wholly excising the tumor and reducing complications. The side operation on the brain stem must be performed orthoptically with the microscope, to separate the tumor along the arachnoid membrane interval between brain stem and tumor. A tumor extending into the brain stem sometimes may gradually pulsate out by itself when excising the tumor to a certain extent. We can see the brain stem and its surface nerves and blood vessels in the interior of the tumor, the trigeminal nerve at its anterior upper part, the anterior inferior cerebella artery at its inferior part, and the upper cerebellar artery at its posterior upper part, which should all be protected properly. In particular, the tumor wall should be dissociated fully from the arachnoid mater, avoiding undue pulling of blood vessels, so as to prevent secondary blood vessel convulsion. One patient who had been operated on had brain stem damage, and had coma and paralysis after surgery. We think this may have been caused by insufficient dissociation of arachnoid mater and pulling of blood vessels. But he recovered consciousness after 15-day rescue treatment, and his sequela of light paralysis also recovered half a year later. There are usually many arteries at the brain stem side to supply the tumor, which should be cut off one by one by an electric coagulation method. At the same time, we should pay attention to avoiding the heat injury of electric coagulation. If it is quite difficult to remove the tumor due to a close adhesion between tumor and brain stem, we can leave over a gobbet of tumor, because we cannot unilaterally pursue a complete excision.

Conclusion

The good curative effect of this group of cases attributes to the correct operative approach, excellent exposure and application of microneurosurgical technology, which minimizes greatly the damage to important nerves, blood vessels and the brain stem.

References

[1] Sekhar LN, Jannetta PJ. Cerebellopontine angle meningiomas, Microsurgical excision and follow-up results. J Neurosurg 1984; 60: 500–505
[2] Martinez R, Vaquero J, Areitio E, Bravo G. Meningiomas of the posterior fossa. Surg Neurol 1983; 19: 237–243
[3] Chan RC, Thompson GB. Morbidity, mortality, and quality of life following surgery for intracranial meningiomas, a retrospective study in 257 cases. J Neurosurg 1984; 60: 52–60
[4] Voss NF, Vrionis FD, Heilman CB, Robertson JH. Meningiomas of the cerebellopontine angle. Surg Neurol 2000; 53: 439–447
[5] Rhoton Jr AL. Meningiomas of the cerebellopontine angle and foramen magnum. Neurosurg Clin N Am 1994; 5: 349–377
[6] Gerganov V, Bussarsky V, Romansky K, Popov R, Djendov S, Dimitrov I. Cerebellopontine angle meningiomas. Clinical features and surgical treatment. J Neurosurg Sci 2003; 47: 129–135
[7] Roberti F, Sekhar LN, Kalavakonda C, Wright DC. Posterior fossa meningiomas: surgical experience in 161 cases. Surg Neurol 2001; 56: 8–21
[8] Sepehrnia A, Knopp U. The combined subtemporal-suboccipital approach: a modified surgical access to the clivus and petrous apex. Minim Invas Neurosurg 2002; 45: 102–104
[9] Quinones-Hinojosa A, Binder DK, Hemphill 3rd JC, Manley GT. Diagnosis of posttraumatic transverse sinus thrombosis with magnetic resonance imaging/magnetic resonance venography: report of two cases. J Trauma 2004; 56: 201–204
[10] Lange M, Duc LD, Hom P, Fink U, Oeckler R. Cerebellopontine angle meningiomas (cpam) – clinical characteristics and surgical results. Neurol Neurochir Pol 2000; 34: 107–113
[11] Samii M, Ammirari M. Surgery of skull base meningiomas. Berlin: Springer Verlag, 1992: 73–85
[12] Bassiouni H, Hunold A, Asgari S, Stolke D. Meningiomas of the posterior petrous bone: functional outcome after microsurgery. J Neurosurg 2004; 100: 1014–1024
[13] Batra PS, Dutra JC, Wiet RJ. Auditory and facial nerve function following surgery for cerebellopontine angle meningiomas. Arch Otolaryngol Head Neck Surg 2002; 128: 369–374
[14] Iwai Y, Yamanaka K, Yasui T, Komiyama M, Nishikawa M, Nakajima H, Kishi H. Gamma knife surgery for skull base meningiomas. The effectiveness of low-dose treatment. Surg Neurol 1999; 52: 40–45
[15] Marangos N, Maier W, Merz R, Laszig R. Brainstem response in cerebellopontine angle tumors. Otol Neurotol 2001; 22: 95–99

H. Z. Zhang
Q. Lan

Design and Microsurgical Anatomy of the Retrosigmoid-Retrocondylar Keyhole Approach without Occipital Condyle Removal

Abstract

Objective: The goal of this study was to design a new retrosigmoid-retrocondylar keyhole approach based on the minimally invasive keyhole idea and to explore its feasibility and indications, which can be regarded as the base of this keyhole approach in clinical use. **Methods:** 8 adult cadaveric heads fixed in formalin and with intracranial vessels perfused by colored latex were used in this study. To search for the most suitable length and shape of the skin incision, we examined two kinds of incision (a longitudinal "S" shape and a straight one) and two lengths (5 cm and 7 cm, respectively). Due to the complexity and thickness of the suboccipital muscles, two ways of muscle dissection were compared: 1) the muscles were incised perpendicularly in layers; 2) the muscles were detached and reflected in layers. A 3-cm diameter retrosigmoid-retrocondylar bone flap was made with a craniotome. Many anatomic structures could be observed under the microscope when the cerebellar hemisphere was retracted. After comparing and balancing the above steps in all specimens, a feasible, duplicable retrosigmoid-retrocondylar keyhole approach was devised. **Results:** The proper incision of the retrosigmoid-retrocondylar keyhole approach was a longitudinal "S" shaped skin incision about 7 cm in length with its superior border 2 cm behind the middle point of mastoid and inferior margin at the level of C-2. The method of detachment and reflection of occipital muscles was superior to the method of cutting them perpendicularly. By means of adjusting the head position and the angle of microscope, the ipsilateral vertebral artery, posterior inferior cerebellar artery, anterior inferior cerebellar artery, VII, VIII, IX, X, XI, XII cranial nerves and the ventral lateral aspect of medulla oblongata were exposed via this keyhole approach. **Conclusions:** The novel retrosigmoid-retrocondylar keyhole approach has practical value for clinical applications. With the techniques of modern microsurgery, several diseases such as an aneurysm situated at the vertebral artery or the posterior inferior cerebellar artery, a small hypoglossal neurinoma and tumor located at the ventral lateral aspect of the medulla oblongata, may be operated via this retrosigmoid-retrocondylar keyhole approach without drilling the occipital condyle.

Key words

Microsurgical anatomy · occipital condyle · skull base · keyhole · surgical approach

Introduction

Lesions located along the lower clivus and the anterior portion of the foramen magnum have always been a surgical challenge because of the depth of the surgical field, the complexity of nerves and blood vessels, and the difficulty of lesion exposure [1, 2]. The far lateral approach has been thought of as a suitable approach since it can provide access to the upper ventral spinal canal, the anterior portion of the foramen magnum, the lower and middle clivus, and the jugular foramen [3–5]. With the rapid development of minimally invasive microsurgical techniques, however, several disadvantages of the conventional far lateral approach, such as extensive brain exposure, more complications and significant morbidity and mortality, have emerged gradually. In recent years, the advantages of microsurgical operation via a keyhole

Affiliation
Department of Neurosurgery, Second Affiliated Hospital, Soochow University, Suzhou, JiangSu, P.R. China

Correspondence
Qing Lan, M. D., Ph. D. · Department of Neurosurgery · Second Affiliated Hospital · Soochow University · 1055 Sanxiang Road · Suzhou · JiangSu 215004 · People's Republic of China · Tel.: +86/512/6778-3937 · Fax: +86/512/6778-4303 · E-mail: qlanq@netscape.net

Bibliography
Minim Invas Neurosurg 2006; 49: 49–54 © Georg Thieme Verlag KG Stuttgart · New York
DOI 10.1055/s-2005-919152
ISSN 0946-7211

approach have been realized by more and more neurosurgeons. Based on the magnification effect of a certain keyhole, lesions situated at special anatomic positions, especially in the skull base, are more feasible to be exposed and treated via the keyhole approach with exquisite microsurgical techniques [6–8]. Many keyhole approaches like supraorbital keyhole, subtemporal keyhole, retromastoid keyhole and pterional keyhole approach have been proved to be much better and more predominant than traditional ones [9–12]. Enlightened by the keyhole idea and with the aim to decrease the corresponding invasion of the conventional far lateral approach, we tried to melt the keyhole idea into this approach and devise a new keyhole approach. In this article, we report a novel approach design, describe the relevant microsurgical anatomy of the retrosigmoid-retrocondylar keyhole approach and evaluate its feasibility.

Materials and Methods

The studies were performed in 8 cadeveric specimens (bilateral dissection in all heads), which were prepared, and injected with colored latex into the bilateral internal carotid arteries, vertebral arteries and internal carotid veins, respectively. The dissections were made with the aid of a microscope (Leica OHS-1), a high-speed drill (Aesculap GA820), a digital camera (Nikon 4500), and some microsurgical instruments specially designed for keyhole surgery.

The head, fixed rigidly in a special headholder, was placed in the lateral position, which enabled the ear and mastoid to be the highest structures. To probe into the most suitable length and shape of the skin incision, we examined two kinds of incision (a longitudinal "S" shape and straight one) and two lengths (5 cm and 7 cm, respectively). Due to the complexity and thickness of the suboccipital muscles, two ways of muscle dissection were compared: 1) the muscles were incised perpendicularly in layers; 2) the muscles were detached and reflected in layers. A 3-cm diameter retrosigmoid-retrocondylar bone flap was made with a craniotome. When the cerebellar hemisphere was retracted many anatomic structures could be observed under the microscope. After comparing and balancing the above steps in all specimens, a feasible, duplicable retrosigmoid-retrocondylar keyhole approach was devised.

Results

Comparison of different methods related to this approach

Skin incision shape: The longitudinal "S" shaped incision was superior to the straight incision, for instance, less tension of the bilateral skin of the incision and more exposure of the surgical field were provided by the effect of "two small skin flaps" of the "S" shaped incision.

Length of incision: In the 7-cm incision, we could not only detach and reflect the suboccipital muscles of each layer easily, but also gain the exposure of all the important structures of this area, including hemilamina of the arch of the posterior atlas, the vertebral artery and the posterolateral portion of foramen magnum could be exposed satisfactorily. However, a 5-cm incision could not meet the needs of reflecting muscles fully and exposing enough surgical field.

Methods of muscles dissection: When the suboccipital muscles were divided by cutting, it was difficult to distinguish the layers of the muscle and as a result, the vertebral artery is liable to be injured. In contrast, by detaching the muscles from their attachments and reflecting them, the distance between the skin and bone window was shortened; one could obviously discern the layers of the suboccipital muscles, and the vertebral artery could be protected in the early stage of the operation by identifying the suboccipital triangle.

The specific procedures of the retrosigmoid-retrocondylar keyhole approach

Head positioning: The head was placed in a lateral position with the face oriented moderately flexed and the vertex down, keeping the ear and mastoid as the highest structures. The vertex down head position was the key step to provide an improved inferior to superior viewing angle for the surgeon [13].

Skin incision: A 7-cm "S" shaped incision began 2 cm behind, and at the level of the middle of the mastoid. The incision curved gently downward, ending at the level of C2 (Fig. **1**).

Muscular stage: The superficial layer of muscle was composed of the trapezius and sternocleidomastoid muscles. The sternocleidomastoid muscle was cut at the level of the superior margin of the incision and reflected anteriorly, while preserving a cuff of its upper attachment for convenience of future closure (Fig. **2**). The trapezius did not need to be undermined in this keyhole approach. After reflecting the sternocleidomastoid muscle, the middle layer of muscle, which includes the splenius capitis, longissmus capitis, semispinalis capitis, and longus cervicis muscles, could be identified. Dissecting the splenius capitis muscle, and reflecting it medially exposed the longissimus capitis muscle, the deep lamina of the deep cervical fascia, and the occipital artery and vein (Fig. **3**). In this keyhole approach, the occipital artery could be exposed from the segment of the occipital groove. After piercing between the superior oblique and the posterior belly of the digastric muscles, the occipital artery coursed medially under the longissimus capitis and crossed the semispinalis capitis muscle (Figs. **4** and

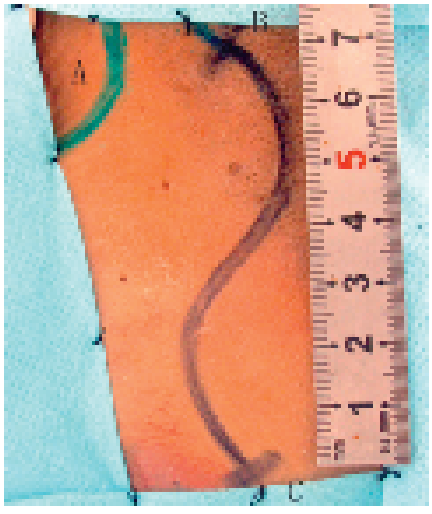

Fig. **1** A left longitudinal "S" shaped skin incision behind the mastoid: A = left mastoid, B = vertex side, C = neck side.

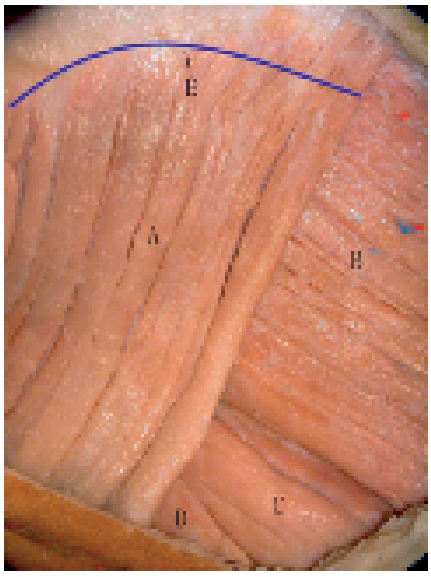

Fig. **2** Exposure of 1 to 2 layers of muscle after skin incision: A = sternocleidomastoid muscle, B = splenius capitis muscle, C = levator scapular muscle, D = splenius cervicis muscle, E = incision line illustrated preserving a cuff of the upper attachment of the splenius capitis muscle for convenience in the future closure.

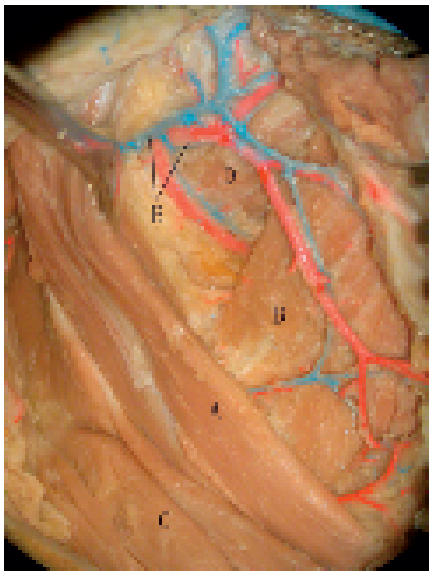

Fig. **3** After reflecting the splenius capitis muscle the 2 to 3 layers of muscle could be observed clearly: A = longissimus capitis muscle, B = semispinalis capitis muscle, C = levator scapular muscle, D = superior oblique muscle, E = occipital artery and vein.

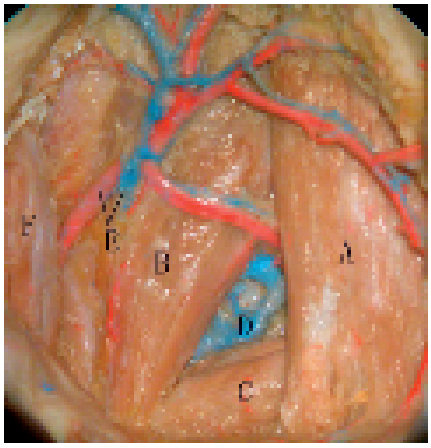

Fig. **4** The course of the occipital artery and vein and the 3 layers of muscle could be exposed after reflecting the longissimus capitis and levator scapular muscles: A = semispinalis capitis muscle, B = superior oblique muscle, C = inferior oblique muscle, D = venous plexus surrounding vertebral artery, E = occipital artery and vein, F = posterior belly of the digastric muscles.

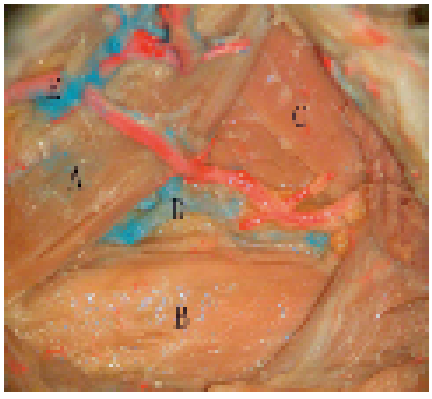

Fig. **5** The suboccipital triangle could be exposed after dissecting the semispinalis capitis muscle: A = superior oblique muscle, B = inferior oblique muscle, C = major rectus capitis muscle, D = venous plexus surrounding vertebral artery, E = occipital artery and vein.

5). Generally, the occipital artery and vein have two or three branches, respectively, in this area; for convenience of further deep exposure, the medial ones should be cut, while the lateral one could be preserved by loosening it from surrounding tissues. Reflecting the longissimus capitis and semispinalis capitis muscles downward exposed the inner layer of muscle, including the superior and inferior obliques, and the rectus capitis major and minor muscles [1,2]. It was critical in this layer to identify the suboccipital triangle (Fig. **5**), which was formed by the superior and inferior obliques, and the major rectus capitis muscle. The structures in the triangle included the vertebral artery and the C1 nerve, both of which lie in a groove on the upper surface of the lateral portion of the posterior arch of the atlas. The superior oblique muscle was detached at its insertion on the transverse process of the atlas and reflected upwardly and medially. The major rectus capitis was cut at its upper margin and reflected inferiorly and medially. The inferior oblique muscle did not need to be dissected.

Manipulation of vascular structures: The portion of the vertebral artery in the suboccipital triangle was surrounded by a rich venous plexus [14] (Fig. **6**), which flowed into two systems: one drained by the internal jugular vein and another draining into the vertebral venous plexus. The posterior condylar emissary vein, which passed through the posterior condylar canal, formed a communication between the vertebral venous plexus and the sigmoid sinus [15] (Fig. **6**). Since bleeding from these venous plexus is often fierce and difficult to control, care should be taken to avoid injuring them. In this approach, the posterior condylar emissary vein should be cut close to occipital bone, and posterior condylar canal could be packed with bone wax. In addition, the bony membrane of the condylar fossa was dissected and reflected inferiorly to protect the vertebral artery and surrounding venous plexus. If these veins were ruptured at surgery, they could be controlled by bipolar coagulation and packed with surgicel [16,17].

Bony drilling and dura opening: After exposing the retrocondylar occipital bone (Fig. **7**), a small suboccipital craniotomy about 3 cm in diameter was performed, with its lateral border to the sigmoid sinus, opening the lateral rim of the foramen magnum (Figs. **8** and **9**). The inferior border of the bone window was just at the posterior margin of the occipital condyle and posterior

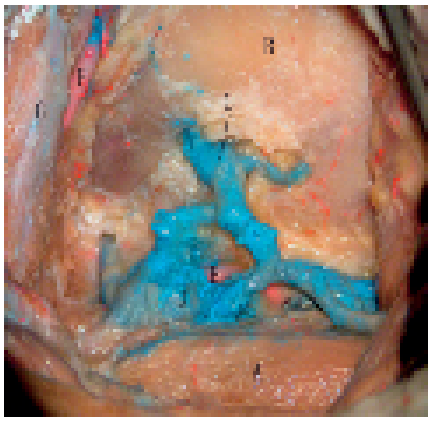

Fig. **6** After reflecting the superior oblique and major rectus capitis muscles, the posterior condylar emissary vein could be seen having communication with the vertebral venous plexus: A = inferior oblique muscle, B = occipital bone, C = posterior condylar emissary vein, D = venous plexus surrounding vertebral artery, E = vertebral artery, F = occipital artery, G = posterior belly of the digastric muscles.

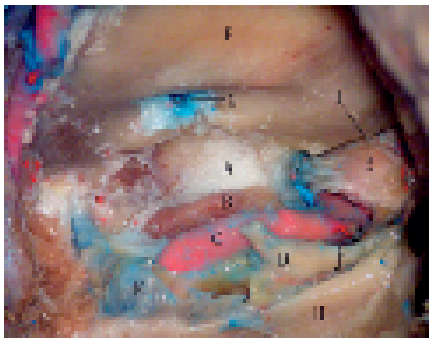

Fig. **7** The posterior condylar emissary vein should be cut close to the occipital bone (in this photo we removed the posterior condylar emissary vein and most of the venous plexus surrounding the vertebral artery for illustrating the deep structures): A = occipital condyle, B = condylar process of atlas, C = vertebral artery, D = C1 nerve, E = dural mater, F = occipital bone, G = posterior condylar canal. H = posterior arch of atlas, I = posterior margin of foramen magnum, J = muscular branches of vertebral artery, K = venous plexus surrounding the vertebral artery.

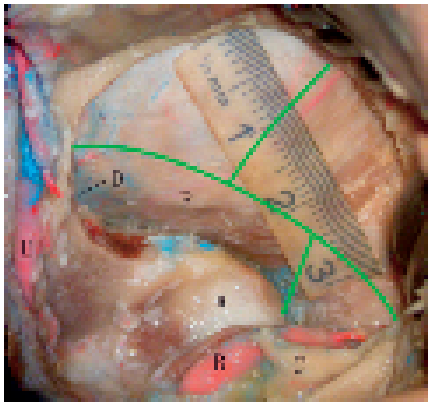

Fig. **8** A small suboccipital craniotomy about 3 cm in diameter was performed, with its lateral border to the sigmoid sinus, opening the lateral rim of foramen magnum: A = occipital condyle, B = vertebral artery, C = C1 nerve, D = sigmoid sinus, E = occipital artery, F = dural mater: the green line shows the shape of the dural incision.

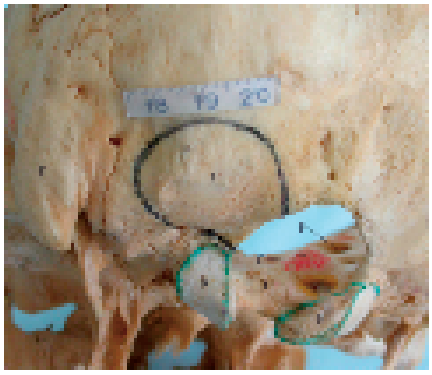

Fig. **9** Illustration of the placement of the bone window: A = bone window, B = occipital condyle, C = right jugular tubercle, D = right hypoglossal canal, E = left mastoid, F = right internal auditory foramen.

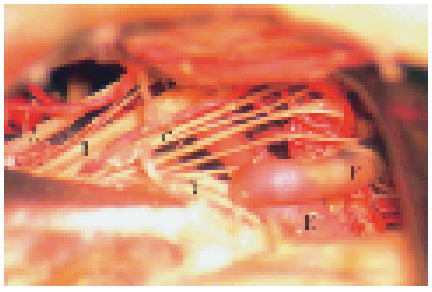

Fig. **10** Structures after retracting the cerebellar hemisphere medially and superiorly: A = glossopharyngeal nerve, B = vagus nerve, C = brain branch of accessory nerve, D = spinal branch of accessory nerve, E = posterior inferior cerebellar artery, F = medulla oblongata branch of the posterior inferior cerebellar artery.

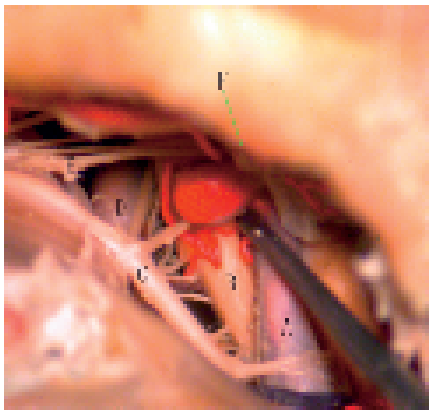

Fig. **11** Manipulation triangle formed by retracting the posterior inferior cerebellar artery: A = the posterior inferior cerebellar artery, B = medulla oblongata, C = spinal branch of accessory nerve, D = vertebral artery, E = brain branch of accessory nerve, F = the margin of bone window.

condylar foramen. A “double Y” shaped dural incision was made with its one base towards to sigmoid sinus (Fig. **8**).

Exposure of intradural anatomic structures: On opening the cisterna magna and retracting the cerebellar hemisphere with a self-retaining retractor medially and superiorly, many anatomic structures could be observed by means of adjusting the head position and the angle of microscope via this keyhole approach (Fig. **10**). When the anteflexed angle of the head was about 15 , the posterior inferior cerebellar artery, IX, X, XI cranial nerves and the ventral lateral aspect of the medulla oblongata were exposed, especially the brain branch of the accessory nerve (upper margin), the lateral aspect of medulla oblongata (medial margin) and the spinal branch of accessory nerve (lateral margin) formed a triangle (Fig. **11**), which could be used as a working space. Through this triangle, the ipsilateral vertebral artery and the XII cranial nerve could be observed. Besides these, the anterior inferior cerebellar artery and the VII, VIII cranial nerves could be exposed when the anteflexed angle of the head was about 30º, and a tetragon was formed by the VIII cranial nerve (upper margin), the lateral aspect of the medulla oblongata (medial margin), the IX cranial nerve (inferior margin) and the branch of the anterior inferior cerebellar artery (lateral margin) (Fig. **12**). In some specimens, the inferior extremity of basilar artery was relatively lower; via this tetragon the inferior segment of the basilar artery could be seen.

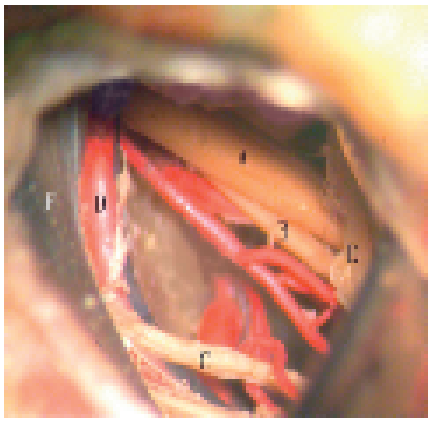

Fig. **12** A tetragon can be seen when the anteflexed angle of the head was about 30 : A = vestibulocochlear nerve; B = facial nerve, C = glossopharyngeal nerve, D = branch of the anterior inferior cerebellar artery, E = flocculus, F = sigmoid sinus.

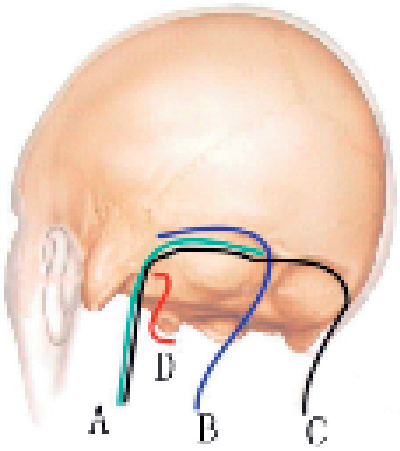

Fig. **13** Illustration of the skin incisions: A, B and C = skin incisions of conventional far lateral approach, D = skin incision of the retrosigmoid-retrocondylar keyhole approach.

Discussion

In 1978 Wolfgang Seegethe first described the far lateral transcondylar approach [18], and later Helmut Bertalanffy applied it in clinical cases as a method of providing surgical access anterior to the medulla without the need for retraction of the brainstem [4]. Since that time, several modifications of the far lateral approach have been developed, turning it into one of the main approaches to the skull base. The terminology used to describe the far lateral approach was not standardized. Based on the position of the bone window, removal of bone structure, and the mode of denomination, there are a variety of terms [19], such as far-lateral approach, extreme-lateral approach, lateral suboccipital approach, dorsolateral-suboccipital-transcondylar approach, extreme-lateral transcondylar and transjugular approach, extreme-lateral transcondylar approach, extreme-lateral inferior transtubercular approach. However, Rhoton [20] has summarized that the basic-far lateral exposure provided access for the following approaches: 1) the transcondylar approach directed through the occipital condyle or the adjoining portions of the occipital and atlantal condyles; 2) the supracondylar approach directed through the area above the occipital condyle; and 3) the paracondylar exposure directed through the area lateral to the occipital condyle.

The skin incisions of the conventional far lateral approach can be described as follows [5]: 1) a "symmetrical inverted L" shaped incision beginning at the mastoid, passing the superior nuchal line to the midline, and downward to the level of C3 or C4. This incision could expose the cervical part. 2) A "inverted L" shaped incision beginning at the external occipital eminence, passing along the superior nuchal line to the mastoid notch, and downward to the level of C3 or C4. 3) A "reverse U" shaped incision is employed when the posterior midline needs to be exposed (Fig. **13**).

The keyhole approach has emerged in recent years as a higher stage in the process of microneurosurgical development. With the exquisite techniques of microsurgery, most lesions could be treated minimally-invasively via the keyhole approaches, without increasing the incidence of postoperative complications [7,9–11,21,22]. According to this study, we come to a conclusion that the retrosigmoid-retrocondylar keyhole approach is feasible and more minimally invasive with many intrinsic advantages:

- The 7-cm skin incision of this keyhole approach was significantly shorter than the traditional ones, but it could fully expose all of important portions such as the retrocondylar occipital bone, the lateral margin of the foramen magnum, and the vertebral artery satisfactorily. The design of this keyhole incision fully followed the principle of keyhole incision "as far as possibly short and sufficiently long".
- The number of suboccipital muscles needing to be dissected was less than that of the traditional approach, which reduces the injuries of operation.
- By reflecting the muscles, the distance between the skin and cranial structures was reduced, but the operation field and surgical freedom were increased.
- The 3-cm small bone window not only avoided extensive brain exposure, but also reduced brain retraction through dissecting the cisterna magna and releasing cerebral spinal fluid.
- Lesions related to this approach were mostly located at the skull base, so the magnification effect of keyhole could reach its maximum.
- Based on our study, anatomic structures exposed in the keyhole approach were not significantly different from those in the conventional far lateral approach [3,5,19,20].

As we all know, there was always controversy about the necessity of condyle removal in the far lateral approach. Especially in recent years, there was even a voice to abandon this approach because of its difficulties of operation and too many complications. Many neurosurgeons would prefer treating lesions in the lower clivus and the anterior portion of the foramen magnum via a posterior or posterolateral approach [23]. All in all, the complications of the transcondylar approach included cranial nerves paralysis (about 17–30%), cerebrospinal fluid leakage (about 22–43%), intracranial infection (12%), post-operative hydrocephalus (22%), occipitocervical instability and injuries of important structures such as the vertebral artery, internal jugular vein, sigmoid sinus and jugular bulb [3,4,17,24]. It was clear that the procedure for removal of the occipital condyle or jugular tubercle is obviously related to the occurrence of the above complications. Therefore if possible the resection of occipital condyle or jugular tubercle should be avoided.

This study preliminarily demonstrates that by means of adjusting the head position and the angle of the microscope, several pathologies, such as an aneurysm situated at the vertebral artery

or posterior inferior cerebellar artery, a small hypoglossal neurinoma, and a tumor located at the ventral lateral aspect of the medulla oblongata, might be operated via this retrosigmoid-retrocondylar keyhole approach without removal of the occipital condyle. In our opinion, the occipital condyle should be considered to be preserved in this retrosigmoid-retrocondylar keyhole approach under the following conditions. First, when lesions are located along the lateral or anterolateral aspect of the foramen magnum [16]. Second, when a small or medial tumor is situated at the ventral lateral aspect of the inferior clivus. Nanda [25] believed that it was unnecessary to drill the occipital condyle when treating ventral clivus tumors since the increased space formed by the tumor was large enough for a surgeon to debulk the tumor. Third, if a patient was preoperatively confirmed as having the type of small occipital condyle by 3D reconstruction after thin slice CT scan, this retrosigmoid-retrocondylar keyhole approach might be performed with little obstruction from the occipital condyle [26].

The paired occipital condyles were situated at the lateral to the anterior half of the foramen magnum and the jugular tubercle, situated above the hypoglossal canal and medial to the jugular foramen, was a rounded prominence found at the junction of the basilar and condylar parts of the occipital bone [1,2,15]. These two structures hinder a clear line of sight to the region anteriorly to the brainstem. On the one hand, the working space at the level of the foramen magnum was extremely limited and afforded only a narrow cleft between the medial medulla oblongata and the lateral occipital condyle. On the other hand, the jugular tubercle was an obstruction to observe the midclivus or vertebrobasilar junction. Therefore, if a tumor is completely situated at the ventral aspect of the medulla oblongata or the anterior portion of the foramen magnum, the mediosuperoposterior $^1/_3$ – $^1/_2$ of the occipital condyle probably need to be removed in order to obtain more sufficient exposure [3 – 5,24]. Likewise, the removal of the jugular tubercle can expand the exposure of the middle clivus [13,27].

In general, the retrosigmoid-retrocondylar keyhole approach in our study really offered several distinct advantages when treating lesions located at the lateral or anterolateral aspect of the foramen magnum or inferior clivus. Chiefly it provided a good view of the dorsolateral inferior skull base in a minimally invasive method. Moreover, based on the magnification effect of keyhole and with exquisite microsurgical techniques, lesions probably could be operated via this keyhole approach without removal of the occipital condyle.

References

[1] Kawashima M, Tanriover N, Rhoton AL, Ulm AJ, Matsushima T. Comparison of the far lateral and extreme lateral variants of the atlantooccipital transarticular approach to anterior extradural lesions of the craniovertebral junction. Neurosurgery 2003; 53: 662 – 675

[2] Rhoton AL. The foramen magnum. Neurosurgery 2000; 47 (3 Suppl): 155 – 193

[3] Babu RP, Sekhar LN, Wright DL. Extreme lateral transcondylar approach: technical improvements and lessons learnt. J Neurosurg 1994; 81: 49 – 59

[4] Bertalanffy H, Sugar W. The dorsolateral, suboccipital, transcondylar approach to the lower clivus and anterior portion of the craniocervical junction. Neursurgery 1991; 29: 815 – 821

[5] Banerji D, Behari S, Jain VK, Pandey T, Chhabra DK. Extreme lateral transcondylar approach to the skull base. Neurol India 1999; 47: 22 – 30

[6] Perneczky A, Fries G. Endoscope-assisted brain surgery: part 1 – evolution, basic concept, and current technique. Neurosurgery 1998; 42: 219 – 224

[7] Lindert E, Perneczky A, Fries G, Pierangeli E. The supraorbital keyhole approach to supratentorial aneurysms: concept and technique. Surg Neurol 1998; 49: 481 – 489

[8] Dare AO, Landi MK, Lopes DK, Grand W. Eyebrow incision for combined orbital osteotomy and supraorbital minicraniotomy: application to aneurysms of the anterior circulation. Technical note. J Neurosurg 2001; 95: 714 – 718

[9] Taniguchi M, Perneczky A. Subtemporal keyhole approach to the suprasellar and petroclival region: microanatomic considerations and clinical application. Neurosurgery 1997; 41: 592 – 601

[10] Grand W, Landi M, Dare AO. Transorbital keyhole approach to anterior communicating artery aneurysms. Neurosurgery 2001; 49: 483 – 484

[11] Magnan J, Barbieri M, Mora R, Murphy S, Meller R, Bruzzo M, Chays A. Retrosigmoid approach for small and medium-sized acoustic neuromas. Otol Neurotol 2002; 23: 141 – 145

[12] Nathal E, Gomez-Amador JL. Anatomic and surgical basis of the sphenoid ridge keyhole approach for cerebral aneurysms. Neurosurgery 2005; 56: 178 – 185

[13] Fossett DT, Caputy AJ. Operative neurosurgical anatomy. New York: Thieme Medical Publishers, 2002: 65 – 77

[14] Arnautovic KI, Al-Mefty O, Pait TG, Krisht AF. The suboccipital cavernous sinus. J Neurosurg 1997; 86: 252 – 262

[15] Wen HT, Rhoton AL, Katsuta T, de Oliveira E. Microsurgical anatomy of the transcondylar, supracondylar, and paracondylar extensions of the far-lateral approach. J Neurosurg 1997; 87: 555 – 585

[16] de Oliveira E, Wen HT, Tedeschi H, Rhoton AL, Rodrigues FC, Bittencourt JC. Far lateral transcondylar approach for lesions of the foramen magnum. Techn Neurosurg 2003; 9: 93 – 105

[17] Salas E, Sekhar LN, Ziyal IM. Variations of the extreme-lateral craniocervical approach: anatomical study and clinical analysis of 69 patients. J Neurosurg 1999; 90 (4 Suppl): 206 – 219

[18] Seeger W. Atlas of Topographical Anatomy of the Brain and Surrounding Structures. Vienna: Spinger Verlag, 1978; 25: 486 – 489

[19] Spektor S, Anderson GJ, McMenomey SO, Horgan MA, Kellogg JX, Delashaw JB. Quantitative description of the far-lateral transcondylar transtubercular approach to the foramen magnum and clivus. J Neurosurg 2000; 92: 824 – 831

[20] Rhoton AL. The far-lateral approach and its transcondylar, supracondylar, and paracondylar extensions. Neurosurgery 2000; 47 (3 Suppl): 195 – 209

[21] Lan Q. The general discussion of microscopic operation of keyhole approach in neurosurgery. Chinese Minim Invas Neurosurg 2003; 8: 1 – 3

[22] Duggal N, Campos M. Surgical approaches and complications. Craniocervical junction. Seminars in Neurosurgery 2002; 13 (2): 179 – 189

[23] Margalit NS, Lesser JB, Singer M, Sen C. Lateral approach to anterolateral tumors at the foramen magnum: Factors determining surgical procedure. Neurosurgery 2005; 56: 324 – 336

[24] Al-Mefty O, Borba LA, Aoki N. The transcondylar approach to extradural non-neoplastic lesions of the craniovertebral junction. J Neurosurg 1996; 84: 1 – 6

[25] Nanda A, Vannemreddy PS, Baskaya MK. Far-lateral approach to intracranial lesions of the foramen magnum without resection of the occipital condyle. J Neurosurg 2002; 96: 302 – 309

[26] Feng DX, Ye FH, Gao H. The quantitative anatomical comparison between suboccipital lateral and far lateral approach to the lower clival lesion. Chinese Minim Invas Neurosurg 2004; 9: 502 – 504

[27] Gilsbach JM, Sure U, Mann W. The supracondylar approach to the jugular tubercle and hypoglossal canal. Surg Neurol 1998; 50: 563 – 570

A. Inui[1]
K. Sairyo[1,3]
S. Katoh[1]
K. Higashino[1]
T. Sakai[1]
M. Shiiba[2]
N. Yasui[1]

Extruded Lumbar Osseous Endplate Causing Long-Term Radiculopathy in an Adult: An Endoscopic Excision

Abstract

In this report, we described an adult case that had a long-term radiculopathy due to an extruded osseous endplate of the lumbar spine at the L5-S1 intervertebral disc level. The osseous material inside the extruded material was not absorbed, and it had continued compressing the nerve root for one year. Endoscopically, the bony fragment was successfully removed. After the surgery, the patient's symptom disappeared, and neurological deficits became normalized. In conclusion, we propose that surgical intervention should be taken into account for the treatment of HNP, when the extruded material contains bony fragment such as osseous endplate.

Key words

Endoscopic surgery · endplate · lumbar disc · radiculopathy

Introduction

Recently, the natural history of the extruded lumbar disc material has been well studied using MRI with high resolution, and it was found that the extruded material would have a natural reduction with time [1–4]. The extruded disc material is mainly nucleus pulposus; however, it sometimes contained annulus fibrosus and osseous endplate [5]. One can assume that it is not easy for osseous endplate to be absorbed unlike herniated nucleus pulposus. Also, presently, there have been no reports of natural absorption of extruded osseous endplate.

In this report, we described an adult case of an extruded osseous endplate causing lumbar radiculopathy for long duration and not showing natural reduction.

Case Report

A 44-year-old woman, a nurse, visited our spine clinic with a one year history of lumbar radiculopathy. When she carried a patient from a stretcher in January, 2002, strong back/right leg pain had appeared; thereby she could not even move. Thus, she visited and was admitted to a local hospital. Herniated nucleus pulposus at right side of L5/S1 was detected on MRI at that time (Fig. **1**). On a T_2-weighted MR image, the herniated material was shown to be of very high signal intensity (Fig. **1**). The right S1 nerve root was shown to be severely compressed by the extruded material.

Conservative treatment including epidural steroid injection, administration of analgesics, and physical therapy was first conducted. Initially, conservative treatment caused the pain to decrease. Thus, she returned to the previous nursing work 4 months after the initial episode. She could work in the morning without pain; however, every afternoon she had been having right leg pain, which hindered her work. She continued working while taking epidural steroid injections as needed. A follow-up MRI (Fig. **1**) was taken one year after the initial MRI examination.

Affiliation
[1] Department of Orthopedics, The University of Tokushima School of Medicine, Tokushima, Japan
[2] Tenseido Hospital, Hyuga, Japan
[3] Spine Research Center, University of Toledo & Medical University of Ohio, Toledo, Ohio, USA

Correspondence
Koichi Sairyo, M. D., Ph. D. · Spine Research Center · Department of Bioengineering · 5040 Nitschke Hall · University of Toledo · Toledo, Ohio 43606–3390 · USA · Tel.: +1/419/530-8030 · Fax: +1/419/530-8076 · E-mail: sairyokun@hotmail.com

Bibliography
Minim Invas Neurosurg 2006; 49: 55–57 © Georg Thieme Verlag KG Stuttgart · New York
DOI 10.1055/s-2005-919165
ISSN 0946-7211

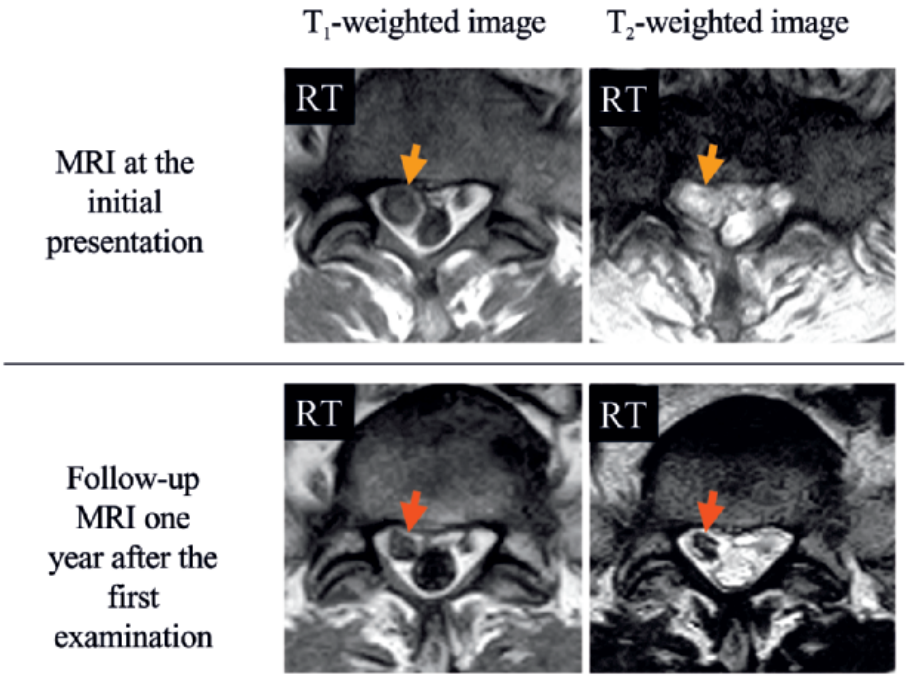

Fig. **1** MRI at the initial presentation and at one year follow-up. The size of the mass has decreased; however, the mass still exists at the follow-up MRI. Note the signal intensity on T_2-weighted image changed from very high to low.

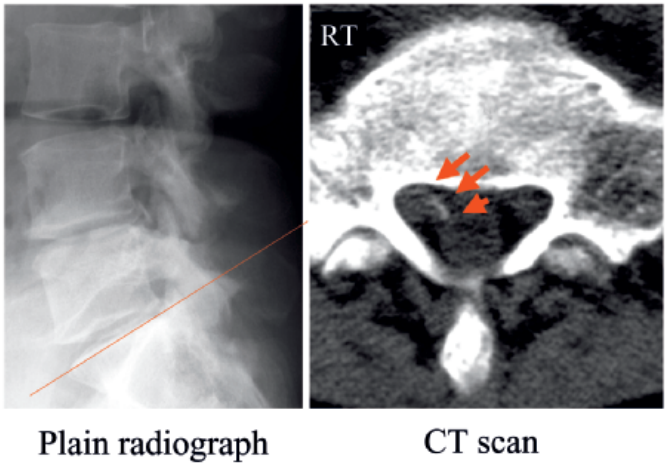

Fig. **2** Plain radiograph and CT. On CT (right), it is noted that a mass with high density (red arrows) is located just ventral of the right S1 nerve root, which is unclear on the plain radiograph (left).

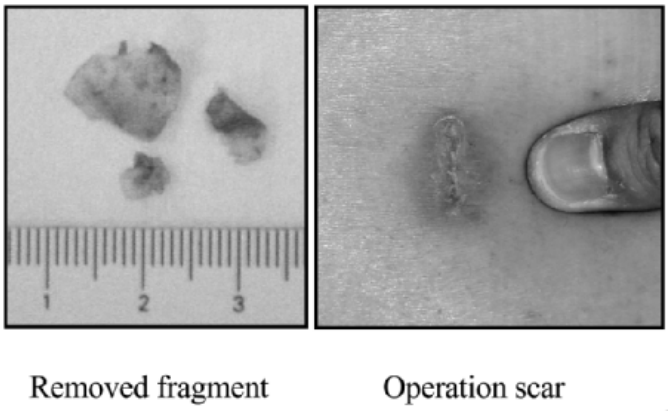

Fig. **3** Left picture indicates the removed osseous endplate which compressed the nerve root. It was minimally invasively removed using a spine endoscope. The right picture shows the operation scar of 16-mm length.

The second MRI demonstrated that the size of the mass of the extruded material had decreased, but it had not disappeared. Also, the signal intensity in the extruded material on a T_2-weighted image showed only a low signal (Fig. **1**). The doctor recommended that the patient undergo a surgical removal of this extruded material, since the extruded material did not disappear within one year and it still compressed the lumbar nerve root. Thus, she was referred to our clinic in January, 2003.

At the initial presentation of our clinic, there were positive straight leg raising test (SLRT) at 80 degree at the right side, weakness of right flexor hallucis longus being 4/5 in manual muscular testing, hypoactive Achilles tendon reflex and hypoesthesia along the dermatome of the right S1 (right 5th toe). Fig. **2** demonstrates a plain lateral radiograph and CT on the initial presentation at our clinic. There is a mass showing high density on the CT scan at the just ventral side of the nerve root, which is unclear on the plain radiograph. Thus, the long-term radiculopathy was diagnosed to occur due to compression of the nerve root by an osseous endplate. Surgical removal was conducted using the endoscope with small skin incision of 16 mm in length (Fig. **3**, right). During the operation, it was found that the osseous endplate, which corresponded to the high density mass on CT, was compressing the S1 nerve root, and it was removed endoscopically (Fig. **3**, left). Following the surgery, the pain disappeared completely, and she returned to the previous full-time nursing work. Also, muscle weakness and hypoethesia were normalized after the surgery.

Discussion

Recently, the natural history of the extruded lumbar disc material has been well studied using high resolution MRI, and it was found that the extruded material would have a natural reduction with time [1–4]. Experimental studies [6–9] have been carried

out to clarify the pathomechanism of the absorption. Thus, most patients with herniated nucleus pulposus (HNP) have been conservatively treated. However, one can assume that it is difficult to get natural absorption when the herniated material includes bony fragments inside.

A larger size mass, migration to the caudal/cranial side, a mass with high signal intensity on T_2-weighted images, and a mass showing enhancement with gadolinium are features of HNP on MRI which signal the natural reduction [1 – 4]. The initial MRI of the present case showed exactly these features. Thus, her family physician proceeded with conservative therapy, and it decreased the back/leg pain. Also, the follow-up MRI one year after the initial picture clearly demonstrated the decreased size of the HNP. However, after one-year of conservative treatment, small disc fragments still remained and compressed the nerve root. From the CT scan, the fragments appeared to be bony tissue, and we diagnosed HNP with an osseous endplate.

In the literature, there are no reports on the natural history of the extruded bony fragment. The similar pathology of the HNP with the osseous endplate is the apophyseal bony rim fracture in the pediatric popuration [10]. Actually, pediatric patients with apophyseal bony ring fractures were recommended to be surgically treated, because the extruded bony fragment, which compresses neural tissue, would not be expected to absorb naturally. Sucato [11] stated that treatment of the apophyseal bony ring is different from that of HNP and surgical removal of the fragment should be considered. Thus, coupled with the present case and the previous reports, we propose that surgical intervention should be taken into account for the treatment of HNP including bony fragments such as an osseous endplate.

Recently, the HNP has been removed endoscopically [12,13]. Also, this technique has been applied to the other kinds of spinal disorders [14,15]. For this case, the extruded osseous endplate was also successfully removed endoscopically with a small 16-mm skin incision. Endoscopic surgery is reported to be minimally invasive on the basis of clinical [12 – 15] as well as biomechanical [16] standpoints. Thus, endoscopic excision of the osseous endplate in the present case is considered to be the best surgical option for facilitating the early return to normal activities of daily living.

Acknowledgements

The authors wish to thank Mr. Ian Cowgill, M.S., Spine Research Center, Department of Bioengineering, University of Toledo, Toledo, Ohio for his help during the editing process.

References

[1] Ahn SH, Ahn MW, Byun WM. Effect of the transligamentous extension of lumbar disc herniations on their regression and the clinical outcome of sciatica. Spine 2000; 25: 475 – 480
[2] Henmi T, Sairyo K, Nakano S et al. Natural history of extruded lumbar intervertebral disc herniation. J Med Invest 2002; 49: 40 – 43
[3] Masui T, Yukawa Y, Nakamura S et al. Natural history of patients with lumbar disc herniation observed by magnetic resonance imaging for minimum 7 years. J Spinal Disord Tech 2005; 18: 121 – 126
[4] Saal JA, Saal JS, Herzog RJ. The natural history of lumbar intervertebral disc extrusions treated nonoperatively. Spine 1990; 15: 683 – 686
[5] Henmi T, Endo H, Nakano S et al. Histological findings of herniated disc materials of lumbar spine in the aged. Jpn J Orthopedics Traumatology 1993; 42: 1148 – 1152 [in Japanese]
[6] Haro H, Kato T, Komori H et al. Vascular endothelial growth factor (VEGF)-induced angiogenesis in herniated disc resorption. J Orthop Res 2002; 20: 409 – 415
[7] Kato T, Haro H, Komori H, Shinomiya K. Sequential dynamics of inflammatory cytokine, angiogenesis inducing factor and matrix degrading enzymes during spontaneous resorption of the herniated disc. J Orthop Res 2004; 22: 895 – 900
[8] Koike Y, Uzuki M, Kokubun S, Sawai T. Angiogenesis and inflammatory cell infiltration in lumbar disc herniation. Spine 2003; 28: 1928 – 1933
[9] Minamide A, Hashizume H, Yoshida M et al. Effects of basic fibrobrast growth factor on spontaneous resorption of herniated intervertebral discs: An experimental study in the rabbit. Spine 1999; 24: 940 – 945
[10] Ikata T, Morita T, Katoh S et al. Lesions of the lumbar posterior end plate in children and adolescents. An MRI study. J Bone Joint Surg [Br] 1995; 77: 951 – 955
[11] Sucato DJ. Back pain in children and adolescent. In: The Adult and Pediatric Spine, 3rd edn, Frymoyer JW, Wiesel SW (eds) Philadelphia: Lippincott Williams & Wilkins, 2004: pp 445 – 461
[12] Hsieh PC, Wang CH. Posterior endoscopic lumbar discectomy using a thoracoport as a tubular retractor. Minim Invas Neurosurg 2004; 47: 319 – 323
[13] Perez-Cruet MJ, Foley KT, Isaacs RE, Rice-Wyllie L, Wellington R, Smith MM, Fessler RG. Microendoscopic lumbar discectomy: technical note. Neurosurgery 2002; 51 (5 Suppl): S129 – 136
[14] Sairyo K, Katoh S, Sakamaki T et al. A new endoscopic technique to decompress lumbar nerve root affected by lumbar spondylolysis. J Neurosurg 2003; 98 (3 Suppl): 290 – 293
[15] Yabuki S, Kikuchi S. Endoscopic partial laminectomy for cervical myelopathy. J Neurosurg Spine. 2005; 2(2): 170 – 174
[16] Sairyo K, Goel VK, Masuda A, Biyani A, Ebraheim N, Mishiro T, Terai T. Biomechanical rationale of endoscopic decompression for lumbar spondylolysis as an effective minimally invasive procedure – A study based on the finite element analysis. Minim Invas Neurosurg 2005; 48: 119 – 122

Utilization of Personal Digital Assistants (PDA) for Intraoperative Naming Tasks in Awake Surgery

S. Sato[1]
H. Oka[1]
S. Utsuki[1]
S. Shimizu[1]
S. Suzuki[1]
K. Fujii[1]
H. Okamoto[2]
S. Hoka[2]
A. Obonai[3]

Abstract

The naming task, one of the most important tasks for screening essential language function, is widely used in awake surgery. We employed personal digital assistants (PDA) for the display of objects in three patients performing the naming task during awake surgery for gliomas adjacent to the language area in the left hemisphere. The compact, light-weight, self-illuminated instrument can easily be held close to the patient's face. None had difficulty seeing the screen despite the presence of the surgical drape around the face. The examiner could easily change the displayed objects with a click. However, the PDA screen is too small for use in auditory comprehension tasks such as the Token Test.

Key words

Personal digital assistants (PDA) · naming task · language area · awake surgery

Introduction

Intraoperative mapping of the language area is important in patients undergoing resection of glial tumors or epileptic foci in the dominant hemisphere [1–4]. Tasks for the assessment of language function include object naming, counting, repetition and auditory comprehension [3]. Of these, the naming task, one of the most important for screening essential language function, is widely used in awake surgery [1–4].

Few reports detail the practical methods used in the operating room when surgically draped patients are asked to perform naming tasks [1,2,4]. Here we propose the utilization of personal digital assistants (PDA), small instruments that are convenient for the performance of intraoperative naming tasks in the spatially confined operating room setting.

Materials and Methods

A handy PDA (SONY® Clie PEG-TJ25) was used by three patients performing naming tasks during surgery for gliomas adjacent to the language area in the left cerebral hemisphere. The instrument featured a square (55 × 55 mm), back-lighted liquid crystal display (LCD) for the display of objects to be named and a switch that facilitated the easy changing of the displayed objects (Fig. **1**).

We prepared collections of objects with common names using Microsoft® Power Point and a personal computer. The file was then converted into PDA format with software (Documents To Go Premium 6) from XLSOFT Co. and loaded onto the PDA. During awake surgery, a speech therapist held the PDA screen in front of the patient's face and asked for the identification of serially displayed objects (Fig. **2**).

When the patients were sufficiently awake to assess their language function during awake surgery, they were asked to perform the naming task during awake surgery. All could easily see and name the displayed objects and none had difficulty seeing

Affiliation
[1] Department of Neurosurgery, Kitasato University School of Medicine, Kanagawa, Japan
[2] Department of Anesthesiology, Kitasato University School of Medicine, Kanagawa, Japan
[3] Department of Otorhinolaryngology, Kitasato University School of Medicine, Kanagawa, Japan

Correspondence
Sumito Sato · Department of Neurosurgery · Kitasato University School of Medicine · Kitasato 1-15-1 · Sagamihara-city · Kanagawa #228-8555 · Japan · Tel.: +81/42/778-9337 · Fax: +81/42/778-7788 · E-mail: sumitosatou-nsu@umin.ac.jp

Bibliography
Minim Invas Neurosurg 2006; 49: 58–59 © Georg Thieme Verlag KG Stuttgart · New York
DOI 10.1055/s-2005-919166
ISSN 0946-7211

Fig. **1** A handy PDA with a square (55 × 55 mm), back-lighted LCD is used to display the objects during the naming task.

Fig. **2** A speech therapist shows the PDA display to the patient during awake surgery. Although the surgical drape around the patient's face leaves only a small, badly lit area available for the display of the objects, they can be seen on the back-lighted screen of the small instrument.

the PDA screen in spite of the darkness due to the presence of the surgical drape. The speech therapist encountered no problems with holding the PDA close to the patient's face or with changing the displayed objects with a click. Use of the PDA circumvented visualization problems due to the patient's position and inadequate illumination under the surgical draping.

Discussion

In our experience, the use of note-type PCs or sheets of paper to display objects to be named in the course of awake surgery is suboptimal because of the darkness and limited space to work under the draping. We found that the PDA, a compact, lightweight, self-illuminated instrument that allows changing the displayed objects with a click, circumvents visualization problems due to the patient's position and inadequate illumination under the draping.

On the other hand, the PDA screen is too small for use in the also important auditory comprehension task [3]. Therefore, to administer the Token Test [5], in which the patient identifies objects on command, we continue to use A3-size cards.

References

[1] Berger M, Ojemann G. Techniques of functional localization during removal of tumors involving the cerebral hemisphere. In: Loftus CM, Traynelis VC (eds), Intraoperative monitoring techniques in neurosurgery. New York: McGraw-Hill Inc, 1994: pp 113 – 127
[2] Kayama T, Sato S. Definition of individual language related area by awake surgery. Brain and Nerve 2001; 53: 151 – 160 [in Japanese]
[3] Lesser R, Gordon B, Uematsu S. Electrical stimulation and language. J Clin Neurophysiol 1994; 11: 191 – 204
[4] Ojemann G, Ojemann J, Lettich E, Berger M. Cortical language localization in left, dominant hemisphere: an electrical stimulation mapping investigation in 117 patients. J Neurosurg 1989; 71: 316 – 326
[5] DeRenzi E, Vignolo LA. The Token Test: a sensitive test to detect receptive disturbance in aphasics. Brain 1962; 85: 665 – 678

Endoscopic Third Ventriculostomy in Post-Tubercular Meningitic Hydrocephalus

A. A. Figaji[1]
A. G. Fieggen[1]
J. F. Schoeman[2]
J. C. Peter[1]

Sir,

It is with interest that we note the paper by Singh et al. reporting on endoscopic third ventriculostomy (ETV) in post-tubercular meningitic hydrocephalus [1]. They report on a prospective study of 35 patients, 54.3% of whom are described as having obstructive hydrocephalus and 45.7% with communicating hydrocephalus. These are defined by the authors using certain criteria. The discrepancy between large supratentorial ventricles and a smaller fourth ventricle is used to identify aqueduct stenosis and a large fourth ventricle identifies obstruction of the foramina of Luschka and Magendie. However, we have had hydrocephalic patients with a relatively small fourth ventricle on computed tomography (CT) scans in whom magnetic resonance imaging (MRI) revealed patency of the aqueduct (Fig. **1**). Also, we have investigated patients with a dilated fourth ventricle with air studies and found no obstruction to the outlet foramina.

Communicating hydrocephalus is defined in this paper by the presence of cerebrospinal fluid (CSF) in the subarachnoid spaces. However, Bruwer et al. [2] convincingly demonstrated that CT findings are not reliable in the prediction of the level of block in

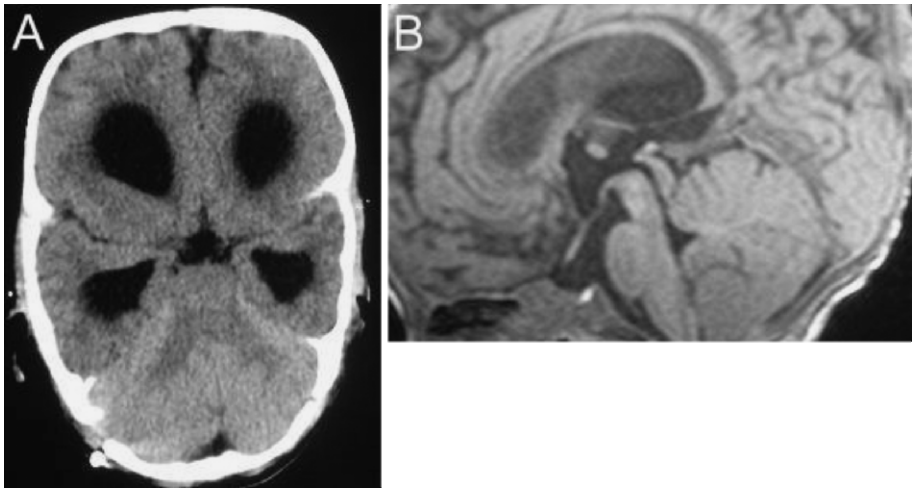

Fig. **1** **A** CT scan showing triventricular hydrocephalus. **B** Sagittal MRI scan showing the same patient with a patent cerebral aqueduct. ETV was attempted because of shunt dysfunction but also failed.

Affiliation
[1] Division of Paediatric Neuroscience (Neurosurgery), School of Child and Adolescent Health, University of Cape Town, Cape Town, South Africa
[2] Department of Paediatrics and Child Health, University of Stellenbosch, Cape Town, South Africa

Correspondence
A. A. Figaji · Division of Paediatric Neuroscience (Neurosurgery) · School of Child and Adolescent Health · University of Cape Town and Red Cross Children's Hospital · Klipfontein Road · 7700 Rondebosch · Cape Town · South Africa · E-mail: afigaji@ich.uct.ac.za

Bibliography
Minim Invas Neurosurg 2006; 49: 60–61 © Georg Thieme Verlag KG Stuttgart · New York
DOI 10.1055/s-2006-932148
ISSN 0946-7211

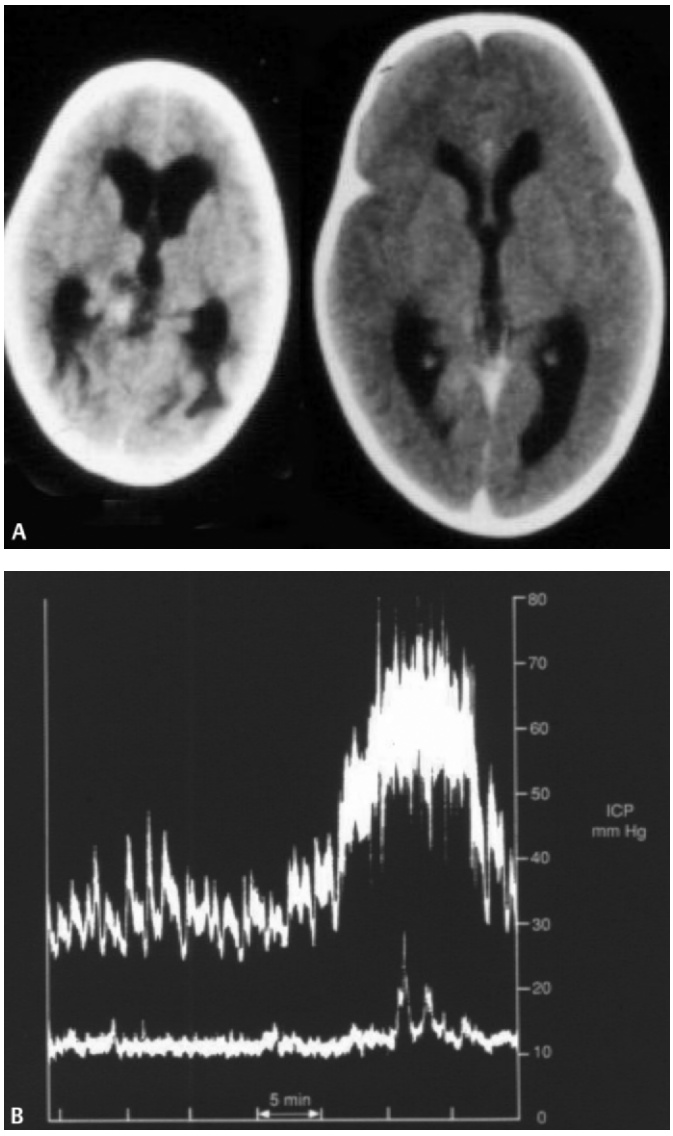

Fig. **2** **A** CT scan appearance before (left) and after (right) one month of medical treatment as described. **B** The accompanying decrease in pressure on lumbar pressure monitoring before (above) and one month after (below) commencement of medical treatment.

tuberculous hydrocephalus. This was supported by a report from our institution [3]. CSF in the subarachnoid space is not a reliable predictor of communicating hydrocephalus.

In a separate report by Lamprecht et al. the incidence of non-communicating hydrocephalus was 17% [4]. This is in keeping with the older reports of this condition that demonstrate the CSF block to be predominantly at the level of the basal cisterns. The series by Lamprecht et al. is of particular interest because patients with communicating hydrocephalus were treated medically in the first instance with a combination of anti-tuberculous medication, steroids, acetazolamide and furosemide, with regular pressure monitoring. Medical treatment of the hydrocephalus was successful in 75% of the cases, i.e., these patients required *no* surgical treatment for hydrocephalus. Response can be assessed by the improvement in the appearance of the CT scan and confirmed by lumbar pressure monitoring, an example of which is shown in Fig. **2**.

Visudiphan et al. [5] also confirm a very high rate of success with a medical strategy that avoids surgical treatment. This is worth keeping in mind when one considers the ETV success rate reported in this paper of 84.2% for obstructed hydrocephalus and 68.7% for communicating hydrocephalus. From the authors' description we are unsure that there was the same targeted approach to the medical treatment of hydrocephalus in the early and intermediate group.

As we have added to our original experience with endoscopy in tuberculous hydrocephalus we have progressively refined our approach. We agree with the authors that TBM is a challenge for the endoscopist because of the technical difficulty, which we initially reported [6]. This is precisely why we believe that a more selective approach should be taken to the management of these patients. We do not believe that ETV is appropriate if one can demonstrate with the use of air encephalography or MRI scans an unimpeded passage of CSF flow through the ventricle system and to the basal cisterns. Modified air encephalography can be performed safely; however a strict protocol must be adhered to [3]. According to our thinking this is preferable to performing an unnecessary endoscopic procedure, particularly in a group of patients who experience such a high rate of success with adequate medical treatment alone.

References

[1] Singh D, Sachdev V, Singh AK, Sinha S. Endoscopic third ventriculostomy in post-tubercular meningitic hydrocephalus: a preliminary report. Minim Invas Neurosurg 2005; 48: 47 – 52

[2] Bruwer GE, Westhuizen S Van Der, Lombard CJ, Schoeman JF. Can CT predict the level of CSF block in tuberculous hydrocephalus. Childs Nerv Syst 2004; 20: 183 – 187

[3] Figaji AA, Fieggen AG, Peter JC. Air encephalography for hydrocephalus in the era of neuroendoscopy. Childs Nerv Syst 2005; 21: 559 – 565

[4] Lamprecht D, Schoeman J, Donald P, Hartzenberg H. Ventriculoperitoneal shunting in childhood tuberculous meningitis. Brit J Neurosurg 2001; 15: 119 – 125

[5] Visudhiphan P, Chiemchanya S. Hydrocephalus in tuberculous meningitis in children: Treatment with acetazolamide and repeated lumbar puncture. J Pediatr 1979; 95: 657 – 660

[6] Figaji AA, Fieggen AG, Peter JC. Endoscopic third ventriculostomy in tuberculous meningitis. Childs Nerv Syst 2003; 19: 217 – 225